

Transport of spin anisotropy without spin currents

Michael Hell,^{1,2} Sourin Das,^{1,2,3} and Maarten R. Wegewijs^{1,2,4}

¹*Peter Grünberg Institut, Forschungszentrum Jülich, 52425 Jülich, Germany*

²*JARA-Fundamentals of Future Information Technology*

³*Department of Physics and Astrophysics, University of Delhi, Delhi 110 007, India*

⁴*Institute for Theory of Statistical Physics, RWTH Aachen, 52056 Aachen, Germany*

(Received 9 May 2013; published 27 September 2013)

We revisit the transport of spin-degrees of freedom across an electrically and thermally biased tunnel junction between two ferromagnets with noncollinear magnetizations. Besides the well-known charge current and spin current we show that a nonzero *spin-quadrupole current* flows between the ferromagnets. This tensor-valued current describes the nonequilibrium transport of spin anisotropy relating to both local and nonlocal multiparticle spin correlations of the circuit. This quadratic spin anisotropy, quantified in terms of the spin-quadrupole moment, is fundamentally a two-electron quantity. In spin valves with an embedded quantum dot such currents have been shown to result in a quadrupole accumulation that affects the measurable quantum dot spin and charge dynamics. The spin-valve model studied here allows fundamental questions about spin-quadrupole *storage* and *transport* to be worked out in detail, while ignoring the detection by a quantum dot. The physical understanding of this particular device is of importance for more complex devices where spin-quadrupole transport can be detected. We demonstrate that, as far as storage and transport are concerned, the spin anisotropy is only partly determined by the spin polarization. In fact, for a thermally biased spin valve the charge current and spin current may vanish, while a pure *exchange* spin-quadrupole current remains, which appears as a fundamental consequence of Pauli's principle. We extend the real-time diagrammatic approach to efficiently calculate the average of multiparticle spin observables, in particular the spin-quadrupole current. Although the paper addresses only leading-order and spin-conserving tunneling, we formulate the technique for arbitrary order in an arbitrary, spin-dependent tunnel coupling in a way that lends itself to extension to quantum-dot spin-valve structures.

DOI: [10.1103/PhysRevB.88.115435](https://doi.org/10.1103/PhysRevB.88.115435)

PACS number(s): 85.75.-d, 73.63.-b, 75.30.Gw

I. INTRODUCTION

Spintronics combines the concepts of electronic transport and spin physics. One of the earliest examples in solid-state physics was the tunnel magnetoresistance effect, discovered by Julliere in 1975:¹ The charge current through two tunnel-coupled ferromagnets decreases when their magnetizations are changed from a parallel to an antiparallel configuration. The simple explanation of Julliere,¹ based on the *spin*-dependence of the density of states for spin- \uparrow and $-\downarrow$, has been refined and extended by later works. Slonczewski calculated the spin current through the FM-I-FM junction,² which can be detected by a second tunnel junction.³ The spin current is responsible for an exchange coupling between magnetizations of the two ferromagnets.^{2,4} An important early application of spin currents is spin injection from ferromagnets into nonmagnetic systems (for a review, see Ref. 5).

Since then, the frontiers of spintronics have been pushed more and more towards the nanoscale, in particular by attaching macroscopic leads to small quantum dots. To name only a few interesting effects in which the transport relies heavily on the spin physics, we mention the Kondo effect,^{6,7} Pauli blockade,⁸ and various types of spin-blockade effects.⁹ The spintronic features mentioned for the mesoscopic systems also have a counterpart in microscopic quantum dot physics. For instance, spin injection into quantum dots and spin currents have been measured.¹⁰ Moreover, for noncollinearly magnetized ferromagnets, the above-mentioned exchange effect translates into a dipolar exchange field,¹¹ which can even lift the spin-valve effect.

Besides these analogies, there are, however, profound differences when microscopic systems such as quantum dots are involved. Due to the spatial confinement of electrons, Coulomb electron-electron interaction becomes all important and correlations between electrons play a prominent role. Spin correlations are built up due to the exchange spin-spin interaction, which results from the concerted action of charging effects and the Pauli principle. This couples the spin-dipole moments of the individual electrons to high-spin states ($S \geq 1$). Such high-spin quantum systems have nontrivial higher spin moments beyond the average spin, such as the *spin-quadrupole moment* (SQM), which is usually the dominant part. In the physical language of atomic and molecular magnetism, the SQM characterizes the quadratic *spin anisotropy*. It quantifies the preference of pairs of spins that make up the large moment $S \geq 1$ to be *aligned* along a specific *axis* irrespective of their *orientation* along this axis (up, down). Spin-quadrupole moment is also relevant to transport: For example, a spin anisotropy barrier can completely determine the signatures of the conductance through molecule magnets¹² and magnetic adatoms.¹³ However, in these devices the spin anisotropy appears rather as a property “fixed” to the atoms/molecule and not something that could be moved around. This latter idea has been introduced by recent publications,^{14–16} which point out that SQM, like spin-dipole moment, can be *injected* and accumulated in a high-spin quantum dot attached to ferromagnets. Thus, spin anisotropy has turned out to be a true *transport* quantity in some ways similar to spin-dipole moment. As a consequence, the transport picture of spin degrees of freedom needs to be

extended beyond that offered by charge and spin currents. This is at the heart of this paper, which studies the *storage* and *transport* of SQM in spintronic devices, merging concepts of spintronics and electron-spin *correlations* (for example present in single-molecule magnets). The aim of this paper is to answer the following three fundamental questions raised by the above-cited studies.

(i) How is SQM *stored* in *macroscopic* system, i.e., ferromagnets?

(ii) How is SQM *transported macroscopically* between such reservoirs?

(iii) How can one define an SQM *current operator* and what is the physical interpretation of its average?

The answers are by no means obvious since SQM, unlike charge and spin, is a *two*-electron quantity. We therefore resort to the simplest possible setting: the Julliere model of two tunnel-coupled ferromagnets *without* an embedded quantum dot. The idea is to take one step “back” relative to the references^{14–17} and to learn as much as possible from this simple spin-valve model about the concepts essential to multispin transport.

We emphasize from the start that we thereby completely ignore the complications of the measurable effects of SQM currents, which seem to occur only when SQM can accumulate in a quantum dot. In the tunnel-junction spin valve the charge current as in Refs. 14–16 does not measure the spin current, although it displays spin-dependent effects. Similarly, this study shows that the charge current and spin current do not measure the SQM current. Thus, our results in no way invalidate results of previous studies of the charge current and spin current; in this *simple* setup they simply coexist with the SQM currents. As long as one is only interested in the charge current, one can ignore SQM currents in this setup. We therefore do not suggest any concrete “meters” of SQM effects in this paper. These were addressed elsewhere,^{14–16} where, for instance, in Ref. 16 the Kondo effect was shown to be sensitive to the quadrupolar analog of the spin torque.

Still, the physical insights gained by this study provide a sound foundation for the discussion of their counterparts in more complex, interacting nanoscale devices, which allow for SQM detection. For this reason, we also address how SQM transport through the spin valve may be controlled by various nonlinear driving parameters such as voltage, temperature gradients, and magnetic parameters. Finally, we note that all our results are obtained within a modern version of the real-time transport formalism, which we have extended to deal efficiently with multiparticle spin-degrees of freedom.

The paper is structured as follows. In Sec. II we formulate the spin-valve model and discuss the physical situations to which it applies. We define the one- and *two*-particle densities of states that enter into the results. In Sec. III we show that simple Stoner ferromagnets provide reservoirs of uniaxial spin anisotropy in addition to spin polarization. We introduce a spin-multipole network picture extending the idea of a charge and spin transport network. For multielectron quantities, such as spin anisotropy, this picture is radically different since they describe local and *nonlocal* correlations. In Sec. IV we see how this naturally suggests the general definition of spin quadrupole current operators. In Sec. V the nonequilibrium averages of these operators are presented for our spin-valve model. We

discuss the decomposition of the spin-quadrupole currents into a dissipative part (spin-quadrupole injection/emission) and a coherent part (spin-quadrupole torque), similar to the spin dipole current. The appendixes contain—besides details—a systematic account of some important technical developments of the real-time transport theory that we employ.

II. SPIN-VALVE MODEL

We start with an overview of the main concepts and ideas, which are central to our comprehensive analysis, aimed at answering the three guiding questions posed in the introduction. The key to understanding the first question, i.e., how SQM is *stored*, is to investigate the microscopic origin of SQM by considering a system of two coupled spin- $\frac{1}{2}$'s. This provides a natural link to atomic and molecular physics, which is discussed in Sec. II A. Note that we deal here with the *spin*-quadrupole moment of a system consisting of *electrons* and not with the *electric nuclear* quadrupole moment, which has been investigated in great detail.¹⁸

We moreover introduce the Hamiltonian for the spin-valve structure (see Sec. II B) consisting of two tunnel-coupled ferromagnets, allowing for noncollinear magnetization directions. The ferromagnets are described using a Stoner model. Importantly, the spin-dependent one-particle density of states is *not* sufficient to quantify spin-multipole properties of ferromagnets. In Sec. II C, we introduce a *two-particle density of states* [see Eq. (16)], which is required for the calculation of the average SQM and its current (Secs. III A 2 a and V). It can be calculated only if the explicit spin-dependence of the dispersion relation is available. For all concrete results presented in this paper, we employ a single wide, flat-band approximation, whose validity is discussed in Sec. II D. Throughout the paper we set $\hbar = e = c = k_B = 1$.

A. Spin-quadrupole moment: From atomic physics to spintronics

To address the storage of SQM, we consider two electrons occupying two different orbitals with the combined system being in a spin-triplet state. The single-particle spin vector operators of these electrons, s_i^1 and s_i^2 , add up the total spin operator $S_i = s_i^1 + s_i^2$ ($i = x, y, z$). From the operator components of the latter, the SQM *tensor* operator $\mathcal{Q} = \sum_{ij} Q_{ij} \mathbf{e}_i \mathbf{e}_j$ can be constructed,

$$Q_{ij} = \frac{1}{2} \{S_i, S_j\} - \frac{1}{3} S^2 \delta_{ij}, \quad (1)$$

where $i, j = x, y, z$. In the triplet states $|T+\rangle = |\uparrow\uparrow\rangle$ or $|T-\rangle = |\downarrow\downarrow\rangle$, the average spin dipole moment is nonzero: $\langle Tm|S|Tm\rangle = m\mathbf{e}_z$, for $m = \pm$. The average SQM has nonzero components as well (see Appendix A 3):

$$\langle T\pm|\mathcal{Q}|T\pm\rangle = \frac{1}{3} \mathbf{e}_z \mathbf{e}_z - \frac{1}{6} \sum_{l \neq z} \mathbf{e}_l \mathbf{e}_l. \quad (2)$$

Since the largest element of this tensor, given by the component $\langle T\pm|\mathcal{Q}_{zz}|T\pm\rangle$, is positive, the spins are likely to be *aligned* with the z th axes in state $|T\pm\rangle$, irrespective of their *orientation*. Thus, besides spin polarization, SQM is “*stored*” in this two-electron system. One may object and ask whether the SQM is not completely determined by the spin-dipole

moment since the tensor (2) could be entirely expressed in terms of $\langle T \pm | \mathbf{S} | T \pm \rangle$. However, in a *quantum* system, even without two-particle interactions, we have $\langle S_i S_j \rangle \neq \langle S_i \rangle \langle S_j \rangle$ due to exchange processes. As a result, a system may be purely “quadrupolarized”; i.e., $\langle \mathcal{Q} \rangle \neq 0$, while $\langle \mathbf{S} \rangle = 0$. An example of this is the triplet state $|T0\rangle = \frac{1}{\sqrt{2}}(|\uparrow\downarrow\rangle + |\downarrow\uparrow\rangle)$, for which the expectation values of all spin components vanish, $\langle T0 | \mathbf{S} | T0 \rangle = 0$, but

$$\langle T0 | \mathcal{Q} | T0 \rangle = -\frac{2}{3} \mathbf{e}_z \mathbf{e}_z + \frac{1}{3} \sum_{l \neq z} \mathbf{e}_l \mathbf{e}_l, \quad (3)$$

indicating that this is a “planar” spin state, in contrast to the axial spin state (2). In the context of quantum information, this state is one of the triplet Bell states $|B_z\rangle = |T0\rangle$. The other two Bell states $|B_x\rangle = \frac{1}{\sqrt{2}}(|\uparrow\uparrow\rangle - |\downarrow\downarrow\rangle)$, $|B_y\rangle = \frac{1}{\sqrt{2}}(|\uparrow\uparrow\rangle + |\downarrow\downarrow\rangle)$ further illustrate that states of zero spin polarization ($\langle B_k | \mathbf{S} | B_k \rangle = 0$ for each $k = x, y, z$) can be distinguished by their *spin anisotropy*: The latter is quantified by the average of the spin-quadrupole tensor (see Appendix A 3), which reads

$$\langle B_k | \mathcal{Q} | B_k \rangle = -\frac{2}{3} \mathbf{e}_k \mathbf{e}_k + \frac{1}{3} \sum_{l \neq k} \mathbf{e}_l \mathbf{e}_l. \quad (4)$$

Since the largest element of this tensor, $\langle B_k | \mathcal{Q}_{kk} | B_k \rangle$, is negative in state $|B_k\rangle$, the spins lie in the plane perpendicular to the k th axes without any definite orientation. Such states appear as eigenstates of *biaxial* spin Hamiltonians of type $H = -DS_z^2 + E(S_x^2 - S_y^2)$, which are also well known in molecular magnetism. In general, the average of \mathcal{Q} in any triplet superposition state is a symmetric tensor, whose principal values lie in the interval $[-2/3, +1/3]$. In fact, a triplet quantum state is completely specified by giving the average of *both* the spin-dipole and the SQM: Formally, one can show that an arbitrary mixed-state density operator in the triplet subspace can be decomposed into a bases of spin dipole and quadrupole operators.^{14,15} In this sense, the SQM is thus a degree of freedom independent of the spin-dipole moment in any system of more than at least two spins. Quadrupole moments are not limited to the spin degree of freedom only. One may define *pseudospin* dipole and -quadrupole operators whenever one deals with a system of at least three levels. Such systems arise, for instance, when combining spin and orbital degrees of freedom. Such pseudoquadrupole moments then express other types of correlations, which are inevitably needed to fully characterize the state of such systems. In this paper we are, however, concerned only with the SQM, which is most relevant for spintronics.

The above ideas can be extended to one of the basic circuit element of spintronics: a ferromagnetic many-electron system (see Sec. III A 2 a). The average of the macroscopic spin operator $S_i = \sum_a s_i^a$, where s_i^a is the i th component of the spin of electron a , quantifies the magnetization of the ferromagnet. Similar to the spin, the macroscopic SQM can also be decomposed into a sum of microscopic contributions coming from electron pairs. By inserting $S_i = \sum_a s_i^a$ into Eq. (1), we obtain

$$Q_{ij} = \sum_{a < b} q_{ij}^{ab}, \quad (5)$$

$$q_{ij}^{ab} = s_i^a s_j^b - \frac{2}{3} (\mathbf{s}^a \cdot \mathbf{s}^b) \delta_{ij}. \quad (6)$$

The average SQM thus quantifies spin *correlations* between all possible *electron pairs*. It can be shown that \mathcal{Q} captures the *triplet* correlations between the spins (see Appendix A 3). Other types of spin correlations become important if spin singlet states are additionally considered. This does not only concern spin-singlet correlations, but also correlations of Dzyaloshinskii-Moriya type, related to antisymmetric tensors quadratic in the spin, as found in Ref. 14. Furthermore, observables expressed by higher powers in the spin operators describe spin-multipole correlations of higher rank (e.g., spin octupoles, etc.). Although all of these are of interest, we focus in this paper only on two-electron spin-triplet correlations, which are exclusively determined by the SQM and were found in the simplest possible situation¹⁵ to be the dominant spin-multipole moment coupling to the spin-dipole dynamics.

For a ferromagnet, we see later that the spin dipolarization induces a spin-quadrupolarization similar to the simple example of two-electron triplet states $|T\pm\rangle$, see the discussion of Eq. (2). This will become evident when we identify a classical or *direct* contribution, which is completely determined by the spin polarization. In addition, there is a quantum or *exchange* contribution to spin anisotropy, which is independent of spin. The latter reveals the two-electron nature of SQM and comes as a consequence of the Pauli principle. We will see that this pure quantum anisotropy can be understood as a tensor-valued “Pauli-exclusion hole” in the triplet spin correlations, accounting for correlations that are forbidden by the Pauli principle (see Sec. III B 4). This in particular makes the SQM an independent degree of freedom that is “stored” in a ferromagnet in addition to the charge and the spin-dipole moment. The studies^{14,15} indicate that it is a quantity that must be reckoned with in nanoscale spintronic systems with high spin polarizations.

We now turn to the second, central question announced in the Introduction: How can one *transport* SQM (see Secs. IV B and V)? If we tunnel-couple two ferromagnets and apply a finite voltage bias, it is well known that besides a charge current a spin current will flow² since electrons carry both charge and spin as an intrinsic degree of freedom. However, can there also be a *flow* of spin anisotropy? At first sight, one may answer “no” because single electrons do not have an intrinsic SQM. However, as an electron spin tunnels from one ferromagnet to the other, it retains its correlations with other electrons. By this, triplet correlations initially stored locally in one of the ferromagnets turn into *nonlocal* triplet correlations between electrons in different ferromagnets. This leads, even by tunneling of single electrons, to a nonzero *spin-anisotropy current*. The aspect of nonlocality of SQM is another essential aspect of its two-particle nature. Even on a macroscopic level, spin-anisotropy transport can therefore only be understood in a network picture accounting for both local and *nonlocal* sources of SQM. Such a spin-multipole network picture—radically different from that for charge and spin—is developed here. It illustrates that storage and transport of SQM cannot be understood independently from each other.

These general considerations bring us to the third main question of our paper, namely how to define the SQM current operator (see Sec. IV B). It can then be identified with the rate of change in SQM stored in these local and nonlocal sources. To develop a further understanding of SQM transport,

we need to calculate the average currents for the simple spin valve. We discuss how to decompose the result into various physically meaningful contributions. Besides a direct and an exchange part we find in analogy to the spin-current dissipative and coherent contributions. The interplay of these contributions causes the SQM current to generate a *biaxial spin anisotropy* for noncollinear ferromagnets. This transport of spin anisotropy opens up the interesting possibility to generate anisotropic magnetic systems starting with isotropic ones, in a way similar to creating spin-polarized systems by spin transport. To our knowledge, this has not been discussed so far, even though the effects of “static” spin anisotropy on transport have been studied extensively in atomic/molecular magnetism¹² and spintronics. Based on this it is expected that spin-quadrupole currents play a role in many nanoscale spintronics devices with significant quantum spin correlations.

In our comprehensive study of the dependence of the SQM current on physical parameters we find a striking result, highlighting the above-mentioned different nature of SQM transport as compared to spin transport. We predict the possibility of a *pure spin-quadrupole current*, i.e., a quadrupole current not accompanied by charge current and spin current. This SQM current is entirely due to quantum exchange processes and is driven by a density gradient of “Pauli exclusion holes” across the junction. A clear notion of the Pauli exclusion holes will be defined in Sec. III B4. We find that the spin-anisotropy flow direction can be controlled by the direction of the thermal bias, a nontrivial result as a deeper analysis of SQM storage will reveal. Transport of spin correlations is thus possible and controllable without affecting net spin polarization or charge distribution. This remarkable conclusion illustrates most clearly that the SQM is really an independent *transport quantity* that should be incorporated into spintronics theories. It also indicates possible, promising applications: Injection of such an SQM current may, for instance, modify or even generate spin anisotropy in an embedded system without changing its spin polarization. This may perhaps allow for novel ways of performing operation in multispin systems.

B. Spin-valve Hamiltonian

We start from a quite general model Hamiltonian,

$$H = H_0^L + H_0^R + H_T, \quad (7)$$

with the noninteracting Hamiltonians of subsystem $r = L, R$,

$$H_0^r = \sum_{nk\sigma} \varepsilon_{nk\sigma}^r c_{rnk\sigma}^\dagger c_{rnk\sigma}, \quad (8)$$

and the tunneling Hamiltonian with $T_{\sigma\sigma'}^{LR} = (T_{\sigma'\sigma}^{RL})^*$:

$$H_T = \sum_{nn'kk'\sigma\sigma'} T_{\sigma\sigma'}^{LR} c_{Lnk\sigma}^\dagger c_{Rn'k'\sigma'} + \text{H.c.} \quad (9)$$

Here the field operators $c_{rnk\sigma}$ act on the single-particle level k of band n in subsystem $r = L, R$ with spin $\sigma = \uparrow, \downarrow$. We assume that the single-electron spin \mathbf{s} for every orbital (n, k) in the same ferromagnet can be quantized along a common physical direction $\hat{\mathbf{J}}^r$ (with $|\hat{\mathbf{J}}^r| = 1$), i.e.,

$$(\hat{\mathbf{J}}^r \cdot \mathbf{s})|\sigma\rangle_r = \sigma|\sigma\rangle_r, \quad (10)$$

with $|\sigma\rangle_r = e^{-i\theta^r \hat{\mathbf{m}}^r \cdot \mathbf{s}}|\sigma\rangle_{\mathbf{e}_z}$, where we rotate by the angle θ^r between $\hat{\mathbf{J}}^r$ and \mathbf{e}_z about the axis perpendicular to both these vectors, defined by $\hat{\mathbf{m}}^r = \mathbf{e}_z \times \hat{\mathbf{J}}^r / |\mathbf{e}_z \times \hat{\mathbf{J}}^r|$. For simplicity, we assume the tunneling amplitudes to be band (n) and energy (k) independent; moreover, the spin is conserved by the tunneling, $[H_T, \mathbf{S}] = 0$. Nevertheless, the tunneling amplitudes in Eq. (9),

$$T_{\sigma\sigma'}^{LR} = t_L \langle \sigma | \sigma' \rangle_R, \quad (11)$$

are, in general, spin-dependent because the field operators $c_{Lnk\sigma}$ and $c_{Rnk\sigma}$ annihilate electrons with spins quantized along noncollinear directions $\hat{\mathbf{J}}^L \nparallel \hat{\mathbf{J}}^R$. The spin conservation in the tunneling is reflected by a *spin-independence* of the “bare” tunneling amplitude t . More on this can be found in Appendix E, where we include spin-symmetry breaking tunneling processes in our extension of the real-time transport theory.

We model the two subsystems as reservoirs, each kept in a thermal equilibrium state $\rho^r = e^{-(H_0^r - \mu^r N^r)/T^r} / Z_r$, where $Z^r = \text{Tr} e^{-(H_0^r - \mu^r N^r)/T^r}$ is the grand-canonical partition function and N^r is the particle number operator of electrode r . Both electrodes are held at fixed electrochemical potentials μ^r and temperatures T^r , whose gradients drive the stationary state currents of interest. Note that even if the tunneling is present, each electrode is held in equilibrium at each instant of time.

C. Two-particle density of states

In Sec. III we calculate the expectation values of the charge and the spin multipoles involving sums over the mode index k . We now indicate which quantities parametrize the spin information from the ferromagnetic electrodes. As usual, we take the continuum limit and replace sums over k by a frequency integral. For one-particle quantities such as charge and spin, one can express the results in terms of the spin-dependent one-particle density of states (1DOS),

$$v_\sigma^r(\omega) = \sum_{n,k} \delta(\varepsilon_{nk\sigma}^r - \omega) \quad (12)$$

$$= \bar{v}^r(\omega)[1 + \sigma n^r(\omega)], \quad (13)$$

where $\bar{v}^r(\omega)$ is the *spin-averaged* DOS,

$$\bar{v}^r(\omega) = \frac{v_\uparrow^r(\omega) + v_\downarrow^r(\omega)}{2}. \quad (14)$$

All the spin dependence of the 1DOS is contained in the *spin polarization* (of the 1DOS),

$$n^r(\omega) = \frac{v_\uparrow^r(\omega) - v_\downarrow^r(\omega)}{v_\uparrow^r(\omega) + v_\downarrow^r(\omega)}. \quad (15)$$

Importantly, we find that the 1DOS (13), although formulated for a general one-particle energy spectrum $\varepsilon_{nk\sigma}^r$, is not sufficient to quantify quantum transport of spin completely, in particular the spin-spin correlations described by the SQM. We will see that the latter requires an additional, spin-dependent *two-particle exchange DOS* (2DOS):

$$v_{\sigma\sigma'}^r(\omega, \omega') = \sum_{n,k} \delta(\varepsilon_{nk\sigma}^r - \omega) \delta(\varepsilon_{nk\sigma'}^r - \omega'). \quad (16)$$

The physical meaning of the 2DOS can be understood most easily by considering two identical *copies* of the same

ferromagnet. The 2DOS is nonzero if there is a pair of states for an electron with spin σ at energy ω in the first copy and an electron of spin σ' at energy ω' in the second copy, but within the *same* k mode in the *same* band n . We emphasize that the latter restriction requires additional modeling: One cannot make independent approximations for the 1DOS and the 2DOS since they are not completely independent of each other. For example, the spin-diagonal components of the 2DOS must satisfy the relation $v_{\sigma\sigma}^r(\omega, \omega') = \delta(\omega - \omega')v_{\sigma}^r(\omega)$. Yet, the remaining components of the 2DOS, $v_{\sigma\bar{\sigma}}(\omega, \omega')$, where $\bar{\sigma} = -\sigma$ denotes the opposite of σ , can *not* be constructed from 1DOS. If the energies of electrons with spin σ and $\bar{\sigma}$ are related by a function $\varepsilon_{nk\bar{\sigma}}^r = g_{n\sigma\bar{\sigma}}^r(\varepsilon_{nk\sigma}^r)$ (for example, if the dispersion relation can be solved for k), then

$$v_{\sigma\sigma'}^r(\omega, \omega') = v_{\sigma}^r(\omega)\delta[g_{n\sigma\sigma'}^r(\omega) - \omega'], \quad (17)$$

with $g_{n\sigma\sigma}^r(\omega) = \omega$ trivially. Clearly, more than the 1DOS is needed here. As a consequence, in general, one has to start from the spin-dependent dispersion relation and calculate all required components of the 1DOS and 2DOS consistently. Transport of two-particle transport properties therefore probes more of the electronic structure of the ferromagnets than the one-particle currents of charge and spin.

D. Stoner model and flat-band approximation

The central results of this paper, Eqs. (89)–(91), are valid for the general case of the above 1DOS and 2DOS. However, since we focus on physically understanding spin-anisotropy transport, rather than making material-specific predictions, we keep all complications by band structure/dispersion relation features to a minimum.

Stoner model/external magnetic field. As explained above, we must specify the spin dependence of the dispersion relation for a consistent treatment of the 1DOS and 2DOS. We model this by a rigid (i.e., energy-independent) splitting of absolute value J_n^r between the spin- \uparrow and spin- \downarrow states,

$$\varepsilon_{nk\sigma}^r = \varepsilon_{nk}^r - \sigma J_n^r/2, \quad (18)$$

which may be different in each band n . This model can be used to discuss several situations, sketched in Figs. 1(a) and 1(b). In case (a) macroscopic ferromagnets are treated within the Stoner model. In this case J_n^r can differ depending on the strength of the electron-electron interaction in each band. In this case the restriction $J_n^r \gtrsim T^r$ must be imposed to avoid the breakdown of ferromagnetism [which is not modeled by Eq. (8)]. In case (b) we consider mesoscopic magnetic islands, each in equilibrium with a reservoir. One may now let the J_n^r model an external magnetic field, which may be different locally in each electrode; i.e., we identify $J_n^r = B^r$. The main difference between cases (a) and (b) is the relative importance of quantum exchange contributions in two-particle spin quantities due to the smaller magnetic moment of the reservoirs (see below). When considering nanoscopic islands charging and nonequilibrium effects on the transport will, of course, be important, which are neglected here. The main motivation for considering case (b) is that it provides an interesting comparison with results for quantum dot spin valves where the latter effects are fully taken into account.^{14,15} For readability we discuss the results throughout

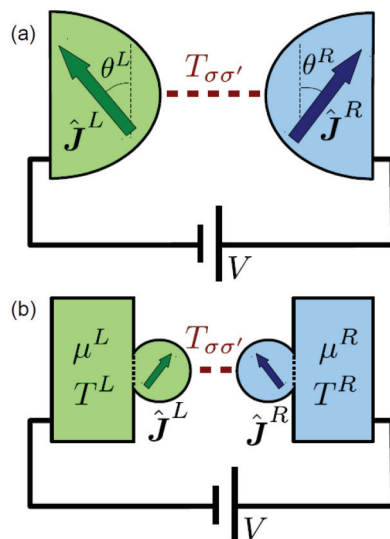


FIG. 1. (Color online) Spin-valve setup: a tunnel junction between (a) macroscopic ferromagnets with Stoner fields $\mathbf{J}^r = J^r \hat{\mathbf{J}}^r$. (b) Mesoscopic islands with local magnetic fields $B^r = J^r \hat{\mathbf{J}}^r$, each in equilibrium with energy and particle reservoirs. A combination of (a) and (b) is another possibility (not shown).

the paper in the language of case (a), ferromagnets with Stoner splittings, unless explicitly stated otherwise.

Flat-band approximation. Second, we restrict ourselves to a single flat band (sketched in Fig. 2) in each ferromagnet in the limit of large bandwidth $2D^r = 2D$. The latter limit assumes that all other energy scales (T^r, J^r, μ^r) are much smaller than the distance W of the band edge closest to all electrochemical potentials, given by

$$W := \min_{r,r',\sigma,p=\pm} \left(pD - \sigma \frac{J^r}{2} - \mu^{r'} \right), \quad (19)$$

which is positive since we assume all μ^r to lie inside the bands. We refer to this in the following shortly as the *flat-band approximation*, keeping in mind that we actually refer

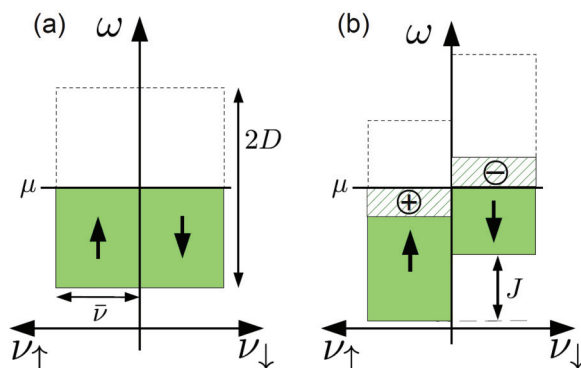


FIG. 2. (Color online) Spin-dependent density of states of a single flat band for a nonmagnetic system (left) and a Stoner ferromagnet (right). The Stoner splitting redistributes a fraction of $J/4D$ of the N_0 particles from spin-down to the spin-up states relative to the nonmagnetic case, as indicated by the + and -. We omit the electrode and band index for simplicity.

to a set of assumptions. For all frequencies $\omega < W$, the spin-dependent DOS is given by

$$v_{\uparrow}^r = v_{\downarrow}^r = \frac{N_o}{2D}, \quad (20)$$

where N_o is the total number of orbitals in each subsystem and

$$v_{\sigma\sigma'}^r(\omega, \omega') = v_{\sigma}^r(\omega) \delta\left(\omega + \frac{\sigma - \sigma'}{2} J - \omega'\right), \quad (21)$$

where we used Eq. (18) to rewrite Eq. (17). One may criticize the simplicity of this approximation in that it does not account for spin polarization near the Fermi energy, but only for a Stoner shift, which is noticeable only at the band edges. We see in Sec. V A, however, that this already captures plenty of important aspects in SQM transport.

Clearly, the results for the average particle number, spin, SQM, and their currents have to be independent of the choice of both the coordinate system and the spin-quantization axis (spin Hilbert space basis); they may only depend on the physical vectors \hat{J}^r and the scalar parameters μ^r , T^r , and J_n^r and t (below). A key technical result of the paper is that we reformulate real-time diagrammatic transport theory such that the calculation explicitly shows this covariance at *every stage*, which also makes it much more efficient (see Appendix E).

Moreover, the usual modification that implements a spin-dependent DOS as $v_{\sigma} = \bar{v}(1 + \sigma n)$ with constant \bar{v} and n is valid only as long one deals with single-particle *observables* such as the spin (even when accounting for many-body effects). For these calculations, all results can usually be expressed using the 1DOS. However, when dealing with *two-particle observables* relying on the 2DOS, it is crucial to specify the dispersion relation as we discussed in Sec. II C. The above spin-dependent but constant DOS physically arises from mixing of different types orbitals in a tight-binding picture, resulting in more than one band. These additional bands can often be ignored, but this is no longer true for the 2DOS which is sensitive to these details. To make this clear, we merely mention two possible valid alternative models accounting consistently for a spin-polarization at the Fermi energy: (i) a single curved band [see Fig. 3(a)] and (ii) two

bands with different bandwidths and a large Stoner splitting so that *different* bands overlap at the Fermi energy [see Fig. 3(b)]. Since our single-band model in the wide-band approximation is already sufficient to illustrate essential effects of spin-quadrupole storage and transport we do not pursue these band-structure details further here.

III. SPIN-MULTIPOLE STORAGE

In this section, we show that a system of ferromagnets, each kept at equilibrium, does not only store charge and spin polarization, but also *stores spin anisotropy*, quantified by the expectation value of the SQM operator (1).

In Sec. III A we will first investigate the simplest case of a single ferromagnet at zero temperature. We discuss how the average SQM tensor relates to fluctuations in a macrospin picture and relate this to the microscopic triplet spin-spin correlations. We identify an *exchange* contribution, which accounts for a ‘‘hole’’ in the quantum two-particle correlations of the spins due to the Pauli principle, giving rise to negative or Pauli-forbidden anisotropy.

In Sec. III B we extend these considerations to finite temperatures and multiple electrodes (without coupling them, i.e., $H_T = 0$), both of which introduce new aspects. The case of two electrodes needs to be carefully addressed in order to define an SQM current later on: We must understand *from where* and *to where* SQM flows. It turns out that the ferromagnetic electrodes *cannot* simply be identified with the sources of SQM and we formalize our considerations in a convenient general spin-multipole network theory in Sec. III B2.

A. Single electrode at $T = 0$

We first calculate and analyze the average particle number, spin-dipole moment, and SQM of an isolated electrode in the simple limit of zero temperature in the approximation of a Stoner-shifted flat band (see Sec. II D). In this section we omit the electrode index r and band index n and denote by $\langle \cdot \rangle = \langle \psi_0 | \cdot | \psi_0 \rangle$ the $T = 0$ ground-state average.

1. Average charge and spin

We first review the average charge and spin-dipole moment for later comparison of these one-particle quantities with the SQM, a two-particle quantity. For zero temperature, all states with energy $\varepsilon_{k\sigma} \leq \mu$ below the electrochemical potential μ are occupied and all levels with $\varepsilon_{k\sigma} > \mu$ are empty (cf. Fig. 2). Thus, the ground-state average of particle number operator,

$$N = \sum_{k,\sigma} c_{k\sigma}^{\dagger} c_{k\sigma}, \quad (22)$$

corresponds to the sum of the green areas below the electrochemical potential in Fig. 2: With $v_{\sigma} = \bar{v}$ we find

$$\langle N \rangle = \sum_{\sigma} \bar{v} \left(\mu + D + \frac{\sigma}{2} J \right) \quad (23)$$

$$= N_o \left(1 + \frac{\mu}{D} \right). \quad (24)$$

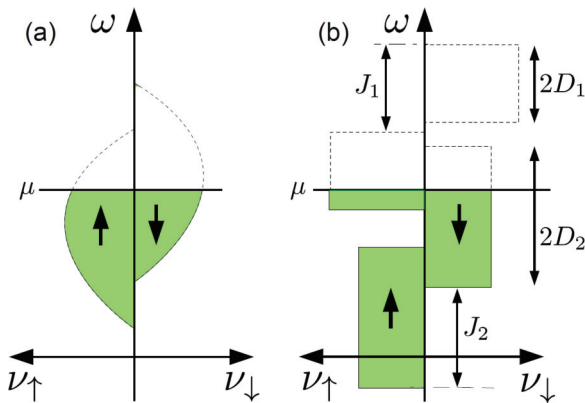


FIG. 3. (Color online) (a) Spin- and energy-dependent density of states for a *one-band* Stoner ferromagnet. (b) Spin-dependent, *constant* density of states for a *two-band* Stoner ferromagnet with different bandwidths $2D_n$ and Stoner splittings J_n for band $n = 1, 2$.

Here $N_o = 2D\bar{v}$ is the number of orbitals in the bandwidth $2D$. The particle number is independent of the Stoner splitting J in this simple approximation.

The average of the spin operator,

$$\mathbf{S} = \sum_{k,\sigma} \mathbf{s}_{\sigma\sigma'} c_{k\sigma}^\dagger c_{k\sigma'}, \quad (25)$$

measures the spin *dipolarization* of the system, where $(s_i)_{\sigma\sigma'} = (\sigma_i)_{\sigma\sigma'}/2$ and σ_i , $i = x, y, z$ are the Pauli matrices. Choosing the coordinate system such that $\mathbf{e}_z = \hat{\mathbf{J}}$, we obtain for $T = 0$: $\langle S_x \rangle = \langle S_y \rangle = 0$ and

$$\langle S_z \rangle = \frac{1}{2} \sum_{\sigma} \sigma \bar{v} \left[\mu - \left(-D - \frac{\sigma}{2} J \right) \right] = \frac{1}{2} N_s. \quad (26)$$

This equals the difference of the number of spin-up and -down electrons, i.e., the number of half-filled orbitals with polarized spins,

$$N_s = \bar{v} J = \frac{J}{2D} N_o, \quad (27)$$

and corresponds to the difference of the areas under two DOS curves below μ in Fig. 2.

2. Average SQM and spin anisotropy

The average SQM $\langle \mathbf{Q} \rangle = \sum_{ij} \langle Q_{ij} \rangle \mathbf{e}_i \mathbf{e}_j$ is a real and symmetric tensor, which can therefore always be diagonalized. With the above choice of the coordinate system with $\mathbf{e}_z = \hat{\mathbf{J}}$, $\langle Q_{ij} \rangle$ is already diagonal by symmetry with respect to rotations about $\hat{\mathbf{J}}$. The average of the nonzero tensor operator component

$$Q_{zz} = \frac{2}{3} S_z^2 - \frac{1}{3} (S_x^2 + S_y^2) \quad (28)$$

now measures the *spin anisotropy* with respect to the z axis in the ground state: $\langle Q_{zz} \rangle > 0$ indicates that the spin is aligned (but not necessarily oriented) with the easy z axis, while $\langle Q_{zz} \rangle < 0$ indicates an easy-plane configuration where the spin preferably lies in the perpendicular xy plane. If $\langle Q_{zz} \rangle$ vanishes, neither alignment longitudinal or transverse to the z direction is favored. This is the case, e.g., for a spin-isotropic state for which $\langle S_x^2 \rangle = \langle S_y^2 \rangle = \langle S_z^2 \rangle$; however, it can also be realized by states that are *anisotropic* in the xy plane, for which $\langle S_x^2 \rangle \neq \langle S_y^2 \rangle$, while $\langle S_z^2 \rangle = \frac{1}{2} (\langle S_x^2 \rangle + \langle S_y^2 \rangle)$. These two situations are thus distinguished by the average of one other nonzero SQM tensor components $\langle Q_{xx} \rangle$ or $\langle Q_{yy} \rangle$ (since $\sum_i \langle Q_{ii} \rangle = 0$ these are not independent).

We now investigate to what extent the average spin polarization in a Stoner ferromagnet implies a uniaxial anisotropy. Classically, one expects spin polarization to always imply some nonzero spin anisotropy, but the converse need not be true, as our example in Sec. I shows. We now calculate the average SQM in two ways, first focusing on a collective macrospin picture, common in atomic and molecular magnetism, and then disentangling it into its microscopic contributions from electron pairs relevant to spintronics.

a. Average macrospin SQM. The ground state of the ferromagnet is a maximally polarized pure spin state, $|\psi_0\rangle = |S, m = S\rangle$ (as sketched in Fig. 4).

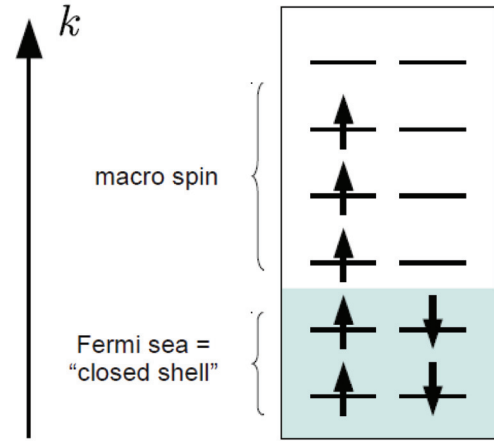


FIG. 4. (Color online) Schematics of the occupation of the orbitals for an electrode at zero temperature. Doubly occupied orbitals form a zero spin state (Pauli principle) while all spins in the singly occupied orbitals are parallel, maximizing the total spin (cf. text)

The value of the spin S is determined from the half-filled orbitals with N_s polarized spins:

$$S \approx \langle S_z \rangle = \frac{1}{2} N_s. \quad (29)$$

Since $|\psi_0\rangle$ is a maximal spin eigenstate there are no quantum fluctuations in the first, longitudinal part of Eq. (28): $\langle S_z^2 \rangle = \langle S_z \rangle^2$. The second, transverse contribution, however, can be written as $S_x^2 + S_y^2 = S_- S_+ - i[S_x, S_y] = S_- S_+ + S_z$ using $S_{\pm} = S_x \pm iS_y$. It has a nonvanishing part due to the quantum spin commutation relations: Since $S_+ |\psi_0\rangle = 0$, $\langle S_x^2 + S_y^2 \rangle = \langle S_z \rangle$. The $T = 0$ average Eq. (28) is found to be

$$\langle Q_{zz} \rangle = \frac{2}{3} \langle S_z^2 \rangle - \frac{1}{3} \langle S_x^2 + S_y^2 \rangle \quad (30)$$

$$= \frac{2}{3} S^2 - \frac{1}{3} S. \quad (31)$$

The spin anisotropy, quantified by the average SQM, thus has competing contributions: Spin polarization induces anisotropy in the z direction ($\propto S^2$), but transverse spin fluctuations tend to suppress it ($\propto S$). The quantum fluctuations of the spin in the ground state “resist” perfect alignment of the spin, despite the maximal spin alignment. In fact, Eq. (31) also holds with $N_s = 1$, $S = 1/2$, in which case the longitudinal term is completely canceled by the transverse fluctuations: A spin- $\frac{1}{2}$ is “so quantum” that it always has zero spin anisotropy due to spin fluctuations, in fact, in *any* state. Since the filled shells do not contribute to the value of S , this suggests that $\langle Q_{zz} \rangle$ at $T = 0$ accounts for only triplet correlations between the open-shell electrons with parallel spin. However, a full understanding of the transverse fluctuations needs a further refinement of that picture.

b. Microscopic SQM storage. Above we linked the zero-temperature average SQM to the spin anisotropy stored in a ferromagnet and related it to its average collective spin and its transverse quantum fluctuations. We investigate now how these quantum fluctuations tend to smear out the spin, reducing the uniaxial anisotropy. For this, we decompose the spin anisotropy into its microscopic contributions from all particles: We start with the longitudinal contribution to Q_{zz} in Eq. (28) and express the total spin operator $S_z = \sum_a s_z^a$ as the

sum of the single-electron spins:

$$S_z^2 = \sum_a (s_z^a)^2 + 2 \sum_{a < b} s_z^a s_z^b \quad (32)$$

$$= \sum_{k\sigma} \frac{1}{4} c_{k\sigma}^\dagger c_{k\sigma} + \sum_{kk'\sigma\sigma'} \frac{\sigma\sigma'}{4} c_{k\sigma}^\dagger c_{k'\sigma'}^\dagger c_{k'\sigma'} c_{k\sigma}. \quad (33)$$

Thus, S_z^2 has both a *one*- and a *two*-electron part. When averaging, the first term gives $\sum_\sigma \frac{1}{4} N_\sigma$, where $N_\sigma = (D + \sigma J)/2$ is the number of orbitals occupied with spin σ . For the two-particle part, we can first treat the electrons as if they were classically distinguishable, yielding a contribution whenever the states (k, σ) and (k', σ') are occupied. This allows us to factorize the resulting expression $(\sum_\sigma \frac{\sigma}{2} N_\sigma)(\sum_{\sigma'} \frac{\sigma'}{2} N_{\sigma'}) = \frac{1}{4} N_s^2$ into the product of averages, i.e., $\langle S_z \rangle^2$. We therefore call this a *direct (two-particle) contribution*. However, if $(k, \sigma) = (k', \sigma')$, we have to be careful: Due to Pauli's principle, it is forbidden to annihilate electrons in the same state twice; hence we have to *exclude* this possibility by a correction term $-\sum_\sigma \frac{\sigma\sigma}{4} N_\sigma = -N_o$. We call this the *exchange (two-particle) contribution*, a denotation that will become more clear in Sec. III B3. This yields altogether

$$\langle S_z^2 \rangle = \frac{1}{4} (N_o + N_s^2 - N_o) = \langle S_z \rangle^2, \quad (34)$$

confirming the result trivially obtained in the macrospin picture (since $|\psi_0\rangle$ is an eigenstate of S_z). The classical intuition is correct only because of a nontrivial cancellation of a one-particle and “quantum” Pauli exclusion term on a microscopic level. The importance of this subtlety becomes clear later (cf. Sec. III B4).

We proceed with decomposing the transverse fluctuations into a one-particle term and a two-particle term,

$$\begin{aligned} S_x^2 + S_y^2 &= \sum_{i=x,y} \left[\sum_a (s_i^a)^2 + 2 \sum_{a < b} s_i^a s_i^b \right] \quad (35) \\ &= \sum_{k\sigma} \frac{1}{2} c_{k\sigma}^\dagger c_{k\sigma} + \sum_{kk'\sigma\sigma'} \frac{1 - \sigma\sigma'}{4} c_{k\sigma}^\dagger c_{k'\sigma'}^\dagger c_{k'\sigma'} c_{k\sigma}, \quad (36) \end{aligned}$$

and averaging over the ground state yields a nonvanishing one-particle term $\frac{1}{2} \sum_\sigma N_\sigma$, describing transverse *single*-spin fluctuations. For the two-particle part, the direct term vanishes as the individual spins are flipped in the modes k and k' so that the ground state is not reproduced any more. This agrees with the fact that the averages $\langle S_x \rangle = \langle S_y \rangle = 0$. However, we must again treat the case $k = k'$ separately: When this mode is doubly occupied and we have $\sigma' = \bar{\sigma}$, the sequence of the four field operators together *exchanges* the spins, reproducing the ground state. This gives a correction $-N_\downarrow$, which is again due to Pauli's principle: A configuration of two indistinguishable spins and the same configuration with both spin exchanged cannot be told apart. This two-electron exchange fluctuations together with the single-spin fluctuations make up for the total transverse fluctuations of the macrospin,

$$\langle S_x^2 + S_y^2 \rangle = \frac{1}{2} N_o - N_\downarrow = \langle S_z \rangle. \quad (37)$$

If we next combine the longitudinal and the transverse term to obtain $\langle Q_{zz} \rangle$, we see that the one-particle contributions drop out:

$$\langle Q_{zz} \rangle = \frac{1}{6} N_s^2 - \left(\frac{1}{6} N_o - \frac{1}{3} N_\downarrow \right). \quad (38)$$

As the SQM of a spin- $\frac{1}{2}$ vanishes (cf. the end of Sec. III A2 a), the SQM exclusively measures true *two*-spin correlations and does not contain any single-spin information: The second bracket in Eq. (38) is a pure *two-spin exchange* correction that accounts for a kind of “hole” in the triplet correlations. The notion of this “Pauli exclusion hole” will be explained precisely in Sec. III B4. It physically arises from exchange contributions in *both* $\langle S_z^2 \rangle$ and $\langle S_x^2 + S_y^2 \rangle$.¹⁹ Equation (38) can be expressed as

$$\langle Q_{zz} \rangle = \frac{1}{3} \times \frac{1}{2} N_s (N_s - 1). \quad (39)$$

Thus, in the present case, the SQM counts the number of pairs of parallel spins in different half-filled orbitals. In accordance with the macrospin picture, the doubly occupied orbitals can be simply ignored. However, at finite temperatures, the Fermi edge becomes unsharp and modes below the electrochemical potential μ also contribute to SQM. In contrast to the macrospin picture, the present microscopic description already included the entire Fermi sea into the description and can therefore be extended to finite temperatures (see Sec. III B4). For $T > 0$ we also start directly from \mathcal{Q} in second-quantized form, which provides a clear way to demonstrate why SQM only senses spin-*triplet* correlations.

Importantly, these direct and exchange contributions to Eq. (38) scale differently with the number of polarized spins, $N_s = \frac{J}{2D} N_o$. For a macroscopic ferromagnet, the exchange contribution to the SQM can be neglected due to the relative unimportance of excluding a single orbital among many. In this case, SQM is entirely induced by spin dipolarization. For $N_s \rightarrow \infty$ the SQM per pair of polarized spins has only a finite direct contribution of 1/3 by Eq. (39), or alternatively, per orbital $(J/2D)^2/3$. For mesoscopic ferromagnetic systems with $N_s \sim 10$ –100 polarized spins the exchange corrections start to become relevant, and for magnetic molecular quantum dots in magnetic field $N_s \sim 1$ –10 and both terms can even be of comparable size. In both these cases, the exclusion principle for a few quantum levels becomes relatively important.

B. Two electrodes at $T > 0$

We now extend the above analysis to two electrodes, which are, moreover, at finite temperatures T^L and T^R . This brings in two new aspects. First, in Sec. III B1, we find that for finite temperatures the average SQM cannot be expressed anymore in the average spin as for $T = 0$. The exchange-SQM contribution is responsible for this difference, quantifying pure quantum contributions to the anisotropy, as we see in Sec. III B3. This contribution involves a two-particle exchange DOS, which is evaluated and discussed in Sec. III B4. This new quantity is used to explain the notion of a “Pauli exclusion hole” in the triplet spin correlations, which are encoded in the SQM. This provides the key to understanding how quantum two-particle exchange processes allow for an SQM current in the absence of spin-dipole current, the central result of the paper in Sec. V C.

The second new aspect, the subdivision of the system into smaller units, touches upon the seemingly naive question of how to define an SQM current. Clearly, an SQM current cannot quantify the “amount” of spin anisotropy that flows *through* a tunnel barrier as single tunneling electrons have zero SQM:

This idea only makes sense for a one-particle quantity such as charge or spin. In contrast, SQM is a two-particle quantity, i.e., built up by *pairs* of electrons. As the electrons of a pair can stay at different sides of the tunnel junction, SQM is not only stored *locally* in each ferromagnet, but also *nonlocally* between the ferromagnets. The concept of storage of SQM thus needs to include *nonlocal* sources of SQM in addition to the local ones discussed so far. In Sec. III B2 we develop a spin-multipole network theory to aid the physical intuition and which will prove to be very helpful for the discussion of SQM *transport* later on and which has a wider range of application than the model studied in this paper.

1. Average charge and spin

In the following we calculate the average charge and spin-dipole moment in a more technical way and in some more detail. We illustrate how to rewrite the spin-dependent part of expectation values most elegantly in terms of expressions independent of the choice of the coordinate system and the spin quantization axis. This serves as a good example of the manipulations we present in Appendix E, where we reformulate the real-time diagrammatic transport theory in an explicitly *covariant* way. First, the one-particle operators (22) for the charge and (25) for the spin (now including the reservoir index r) are jointly described by the four-component operator

$$R_{\mu}^r = \sum_{k, \sigma, \sigma'} (r_{\mu}^r)_{\sigma\sigma'} c_{rk\sigma}^{\dagger} c_{rk\sigma'}. \quad (40)$$

Here $(r_{\mu}^r)_{\sigma\sigma'} = {}_r \langle \sigma | r_{\mu} | \sigma' \rangle_r$ denotes the matrix elements of the single-particle operator r_{μ} for spin states quantized along $\hat{\mathbf{J}}^r$. Using $r_0 = \mathbb{1}$ and $r_i = s_i$ ensures that $R_0 = N$ and $R_i = S_i$ for $i = 1, 2, 3$. We from hereon distinguish whether the 0 component is included or not by using Greek or Latin indices, respectively. Taking the average of Eq. (40) involves

$$\langle c_{rk\sigma}^{\dagger} c_{rk'\sigma'} \rangle = f_{+}^r (\varepsilon_{k\sigma}^r) \delta_{rr'} \delta_{kk'} \delta_{\sigma\sigma'}, \quad (41)$$

with the Fermi function,

$$f_{+}^r(\omega) = \frac{1}{e^{(\omega - \mu^r)/T^r} + 1}. \quad (42)$$

Recasting the sum over all k modes as an integral over all energies by inserting the DOS [see Eq. (13)] yields

$$\langle R_{\mu}^r \rangle = \sum_{\sigma, \sigma'} (r_{\mu}^r)_{\sigma\sigma'} \int d\omega \delta_{\sigma\sigma'} v_{\sigma} f_{+}^r, \quad (43)$$

where we suppressed the ω dependence for brevity. Using Eq. (10), i.e., $(\hat{\mathbf{J}}^r \cdot \mathbf{s})|\sigma\rangle_r = \sigma|\sigma\rangle_r$, we may rewrite

$$v_{\sigma}^r(\omega) \delta_{\sigma\sigma'} = \bar{v}^r(\omega)_r \langle \sigma | \hat{\mathbf{n}}^r(\omega) \cdot \hat{\mathbf{r}} | \sigma' \rangle_r, \quad (44)$$

introducing $\check{r}_0 = \mathbb{1}/\sqrt{2}$ and $\check{\mathbf{r}} = \sqrt{2}\mathbf{s}$ and the four-component vector $\check{\mathbf{n}}^r = \sqrt{2}(\mathbb{1}, \hat{\mathbf{J}}^r n^r)$. The spin-dependent part of Eq. (43) can be recast as a trace in spin space:

$$\langle \mathbf{R}^r \rangle = \int d\omega \bar{v}^r f_{+}^r \text{Tr}[\mathbf{r}(\check{\mathbf{n}}^r \cdot \check{\mathbf{r}})]. \quad (45)$$

The trace is clearly *covariant* in the general sense, i.e., form-invariant under changes of either the coordinate system and/or quantization axis (it is not related to concepts from relativity;

vectors with four elements are just convenient). We obtain

$$\langle N^r \rangle = \int d\omega 2\bar{v}^r(\omega) f_{+}^r(\omega), \quad (46)$$

$$\langle \mathbf{S}^r \rangle = \int d\omega 2\bar{v}^r(\omega) s^r(\omega) \hat{\mathbf{J}}^r. \quad (47)$$

Analogous to the *average occupation number* of a single level at energy ω in Eq. (46), $f_{+}^r(\omega)$, we denote

$$s^r(\omega) = f_{+}^r(\omega) \frac{1}{2} n^r(\omega) \quad (48)$$

in Eq. (47) as the *average spin-polarization function* of electrons at frequency ω , where $n^r(\omega)$ is the spin polarization (15). Note that we only need to use spin- $\frac{1}{2}$ operator algebra to calculate the average in Eq. (45) in coordinate-free form and the same can be done for all the less transport calculations; see Appendix E.

2. Network picture: Nonlocality

Equations (46) and (47) show that each physical electrode corresponds to a single source of charge and spin. We now formalize the concept of particle and spin-dipole storage in terms of a *network theory*, which at first sight may seem superfluous. In fact, it will prove to be helpful to compare this with the storage and transport of SQM.

The following considerations are formulated more compactly and hold more generally for a composite system of number of subsystems labeled by an index r . Such a system may comprise just two electrodes, each at equilibrium, as discussed in this paper (then $r = L, R$), but it may also include, e.g., strongly interacting quantum dots out of equilibrium as discussed in Refs. 14–16 and in forthcoming works. We first ask how the total charge and spin-dipole moment is distributed over the subsystems. The answer is fairly intuitive for these one-particle quantities: The total charge (spin) is the sum of the charge (spin) stored in each electrode, i.e.,

$$R_{\mu}^{\text{tot}} = \sum_r R_{\mu}^r. \quad (49)$$

We can simply associate each subsystem shown in Fig. 5(a) with a *node* of charge (spin) as depicted in Fig. 5(b). Note that decomposition (49) is even possible if R_{μ}^{tot} is *not* conserved. (We postpone the discussion of the *links* in the network until

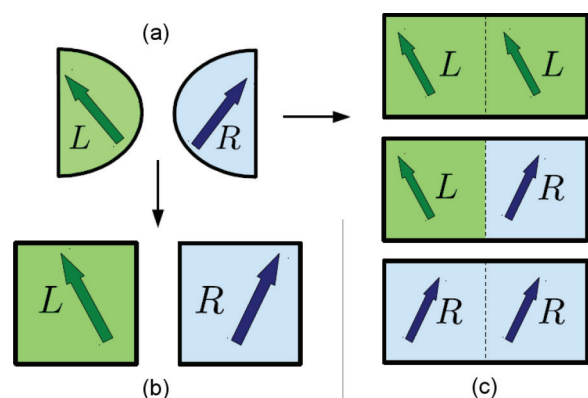


FIG. 5. (Color online) (a) Physical setup of two ferromagnets and network picture for (b) the spin-dipole moment, a one-particle quantity (like the charge), and for (c) the SQM, a two-particle quantity.

we defined current operators in Sec. IV, where we complete the network theory.)

This simple correspondence breaks down for SQM. When we ask how this *two-particle* quantity is distributed over composite system, the answer is radically different. We start from the total SQM of the system, written as

$$\mathcal{Q}^{\text{tot}} = \mathbf{S}^{\text{tot}} \odot \mathbf{S}^{\text{tot}}, \quad (50)$$

abbreviating the symmetric, traceless dyadic product of two vector operators \mathbf{a} and \mathbf{b} as

$$(\mathbf{a} \odot \mathbf{b})_{ij} = \frac{1}{2}(a_i b_j + b_i a_j) - \frac{1}{3} \delta_{ij} \mathbf{a} \cdot \mathbf{b}. \quad (51)$$

We decompose \mathcal{Q}^{tot} by inserting $\mathbf{S}^{\text{tot}} = \sum_r \mathbf{S}^r$,

$$\mathcal{Q}^{\text{tot}} = \sum_{\langle rr' \rangle} \mathcal{Q}^{rr'}, \quad (52)$$

where $\langle rr' \rangle$ indicates that we sum only over all *pairs*

$$\mathcal{Q}^{rr'} = \mathcal{Q}^{r'r} = g^{rr'} \mathbf{S}^r \odot \mathbf{S}^{r'}, \quad (53)$$

and the factor $g^{rr} = 1$ and $g^{rr'} = 2$ ($r \neq r'$) accounts for the double occurrence of each pair r, r' with $r \neq r'$ in the expansion (50). Equation (53) is symmetric in r and r' since $\mathbf{S}^r \odot \mathbf{S}^{r'} = \mathbf{S}^{r'} \odot \mathbf{S}^r$ and we can write

$$\mathcal{Q}^{rr'} = \frac{1}{2} g^{rr'} (\mathbf{S}^r \odot \mathbf{S}^{r'} + \mathbf{S}^{r'} \odot \mathbf{S}^r). \quad (54)$$

Note that $\mathcal{Q}^{rr'}$ is a Hermitian operator and therefore an observable because spin operators of different subsystems commute: $(\mathbf{S}^r \odot \mathbf{S}^{r'})^\dagger = \mathbf{S}^{r'} \odot \mathbf{S}^r = \mathbf{S}^r \odot \mathbf{S}^{r'}$.

We now develop a network picture for the SQM by associating to each *pair* of subsystems $\langle rr' \rangle$ a single effective source or node. For the *two-terminal* spin valve in Fig. 5(a) that we study, *three* SQM nodes appear in the corresponding network picture of Fig. 5(c). The total SQM is stored in two *local* nodes (\mathcal{Q}^{LL} , \mathcal{Q}^{RR}) and in one *nonlocal* node ($\mathcal{Q}^{LR} = \mathcal{Q}^{RL}$). The (non)local nodes describe spin-triplet correlations between pairs of electrons of the same (different) subsystem(s). This nonlocality of SQM storage is very important for the physical understanding and definition of a SQM current operator. It is the injection of SQM currents from these nonlocal nodes that drive the measurable local SQM dynamics in embedded quantum dots, as found in Ref. 15. For the spin-valve considered here it now becomes clear how single-electron tunneling can transport SQM. First, local correlations, e.g., in the $\langle LL \rangle$ node are turned into nonlocal correlations in the $\langle LR \rangle$ node. The transfer of SQM is then completed by another single-electron tunneling event that relocalizes the pair, but now in the right electrode, contributing then to the $\langle RR \rangle$ node. This picture will be refined once we defined SQM current operators in Sec. IV B.

3. Direct and exchange contribution to average SQM

We next inquire to which extent the stored SQM is independent of the average spin-dipole moment, extending the discussion of Sec. III A2 b. The average of the SQM operator for node $\langle rr' \rangle$ given by Eq. (53), can be decomposed it into a direct and an exchange part using Wick's theorem for the averages of products of field operators (see Appendix A3 for details):

$$\langle \mathcal{Q}^{rr'} \rangle = \langle \mathcal{Q}^{rr'} \rangle_{\text{dir}} + \langle \mathcal{Q}^{rr'} \rangle_{\text{ex}}. \quad (55)$$

Direct SQM. The first possible *direct* contraction combines field operators from the same spin operator in Eq. (30). It can therefore be factorized into the expectation values of the spin operators given by Eq. (47),

$$\langle \mathcal{Q}^{rr'} \rangle_{\text{dir}} = \sum_{kk'\sigma\sigma'} \mathbf{s}_{\sigma\sigma}^r \odot \mathbf{s}_{\sigma'\sigma'}^{r'} f_+^r(\varepsilon_{k\sigma}^r) f_+^{r'}(\varepsilon_{k'\sigma'}^{r'}) \quad (56)$$

$$= \langle \mathbf{S}^r \rangle \odot \langle \mathbf{S}^{r'} \rangle = q_{\text{dir}}^{rr'} \widehat{\mathbf{J}}^r \odot \widehat{\mathbf{J}}^{r'}, \quad (57)$$

with

$$q_{\text{dir}}^{rr'} = |\langle \mathbf{S}^r \rangle| |\langle \mathbf{S}^{r'} \rangle|. \quad (58)$$

This direct SQM incorporates the cumulative effect of the energy-resolved spin polarization $s^r(\omega)$. It quantifies the uncorrelated contribution of the quantum spins to the spin anisotropy: As intuitively expected, an electrode with a favored spin *direction* (polarization) possesses a favored spin *alignment* (anisotropy). For a macroscopic system in equilibrium, the average SQM is dominated by the direct part, which is completely determined by the average spin-dipole moment.

Exchange SQM. For meso- and nanoscopic systems the last statement ceases to be true due to the neglect of Pauli's principle in the spin-spin correlations. In the second *exchange* contraction field operators of different spin operators are contracted, giving a term

$$\langle \mathcal{Q}^{rr'} \rangle_{\text{ex}} = \delta^{rr'} \sum_{k\sigma\sigma'} \mathbf{s}_{\sigma\sigma'}^r \odot \mathbf{s}_{\sigma'\sigma}^{r'} f_+^r(\varepsilon_{k\sigma}^r) f_+^{r'}(\varepsilon_{k\sigma'}^{r'}), \quad (59)$$

which accounts for true *correlations* in the sense of Spearman's rank correlation coefficient.²⁰ This becomes clear when rewriting Eq. (59) using Eq. (57):

$$\langle \mathcal{Q}^{rr'} \rangle_{\text{ex}} = \langle (\mathbf{S}^r - \langle \mathbf{S}^r \rangle) \odot (\mathbf{S}^{r'} - \langle \mathbf{S}^{r'} \rangle) \rangle. \quad (60)$$

Note that Eq. (59) involves only *one* sum over k . Thus, the exchange term indeed scales linearly with the system size in contrast to the direct term [see Eq. (57)] and can be neglected for macroscopic systems (cf. last paragraph in Sec. III A2 b). Here it is interesting to consider our Hamiltonian as a model for a mesoscopic ferromagnet or a metallic island in a strong external magnetic field [Fig. 1(b)]. In this case the exchange contribution may even become the dominant part in transport when the spin current vanishes: Then the spin polarization $\langle \mathbf{S}^r \rangle$ and therefore also $\langle \mathcal{Q}^{rr'} \rangle_{\text{dir}}$ do not change, while $\langle \mathcal{Q}^{rr'} \rangle_{\text{ex}}$ does. When including a tunnel-coupling between the ferromagnets the transport through the junction correlates spins of both systems and nonlocal exchange-SQM currents *can* indeed arise. For this reason, we keep the exchange term here and study it in some more detail.

Tensorial structure. Equation (60) can be expressed as

$$\langle \mathcal{Q} \rangle_{\text{ex}} = -\delta^{rr'} q_{\text{ex}}^{rr'} \widehat{\mathbf{J}}^r \odot \widehat{\mathbf{J}}^{r'}, \quad (61)$$

with the positive quantity

$$q_{\text{ex}}^{rr} = \frac{1}{4} \sum_k [f_+^r(\varepsilon_{k\uparrow}^r) - f_+^r(\varepsilon_{k\downarrow}^r)]^2 > 0 \quad (62)$$

(see Appendix A2). Clearly, only if $\varepsilon_{k\uparrow}^r - \varepsilon_{k\downarrow}^r \ll T^r$ for all k , the exchange contribution vanishes, i.e., for the Stoner model if $J^r \ll T^r$. However, if $J^r > T^r$, each spin-polarized orbital k gives a negative correction to the direct spin anisotropy. We refer to this as the *Pauli exclusion hole*, located in orbital

k with a “distribution function” $[f(\varepsilon_{k\uparrow}) - f(\varepsilon_{k\downarrow})]^2$. We give a microscopic interpretation of this below in Sec. III B4. A gradient of these Pauli exclusion holes across the junction drives an exchange-SQM current, which may even flow in the absence of a spin current; see Sec. V C.

We moreover note that the tensor $\langle \mathcal{Q} \rangle_{\text{ex}}$ has the same principal axes as $\langle \mathcal{Q} \rangle_{\text{dir}}$ (the reason for this is discussed in the following section). Thus, the local SQM $\langle \mathcal{Q}^{rr} \rangle \propto \hat{\mathbf{J}}^r \odot \hat{\mathbf{J}}^r$, has a diagonal representation in any coordinate system that includes the Stoner field direction, e.g., $\mathbf{e}_z = \hat{\mathbf{J}}^r$, with nonzero elements $\langle \mathcal{Q}_{xx}^{rr} \rangle = \langle \mathcal{Q}_{yy}^{rr} \rangle = -\langle \mathcal{Q}_{zz}^{rr} \rangle/2$. This shows that the local SQM sources are *uniaxially* anisotropic, and different alignments in the plane perpendicular to $\hat{\mathbf{J}}^r$ are not preferred. Since the direct contribution exceeds the exchange contributions, we find, as expected, $\langle \mathcal{Q}_{zz}^{rr} \rangle > 0$, i.e., an easy-axis anisotropy favoring the collinear orientation of the spins into the z direction over any orientation in the xy plane, $\langle \mathcal{Q}_{xx}^{rr} \rangle = \langle \mathcal{Q}_{yy}^{rr} \rangle < 0$.

The nonlocal SQM $\langle \mathcal{Q}^{rr'} \rangle$, $r \neq r'$, has three nondegenerate principal values: It describes *biaxial anisotropy*. It has unique principal axes in which $\langle \mathcal{Q}_{zz}^{rr'} \rangle > \langle \mathcal{Q}_{yy}^{rr'} \rangle > \langle \mathcal{Q}_{xx}^{rr'} \rangle$; i.e., directions perpendicular to the dominant easy axis (z) are distinguished; see Appendix B.

4. Microscopic picture of SQM storage

The physical meaning of the exchange SQM becomes transparent when revisiting the microscopic picture of SQM storage. When calculating the direct SQM by Eq. (56) one pretends to have two distinct ferromagnets r and r' and “counts” triplet correlations by adding all cross-correlations between electrons occupying these distinguishable ferromagnets. This procedure gives the full result for the nonlocal SQM [cf. Eq. (59)]: For $r \neq r'$

$$\langle \mathcal{Q}^{rr'} \rangle = \langle \mathcal{Q}^{rr'} \rangle_{\text{dir}}. \quad (63)$$

This is correct as we treat the two ferromagnets as distinguishable objects by assumption (the total density operator is a direct product).

The direct, *local* SQM ($r = r'$) also correctly counts the local spin anisotropy as long as it concerns correlations of electrons from different modes $k \neq k'$, which are also distinguishable (green lines in Fig. 6). However, this procedure fails for electrons occupying the *same* mode $k' = k$: A single mode (irrespective of whether being singly or doubly occupied) does not contribute to the total SQM (see Appendix A3). Thus, the local exchange SQM has to cancel the contribution that the direct SQM (56) incorrectly ascribes to single modes (indicated by the red line in Fig. 6).

For establishing an “uncounting” procedure to exclude the single-mode SQM, one may again simply think of two identical, but distinguishable copies of the same mode k and calculate the direct SQM generated from all these modes (see Fig. 6). In this picture, exchange SQM represents a “spin-anisotropy hole” ascribed to each mode and therefore shows a formal analogy to a *one-particle quantity*. This analogy will reemerge when we consider the transport of SQM in Sec. III B5. To emphasize this multiparticle exchange aspect, we refer to this as a *Pauli exclusion hole* in the spin-triplet correlations.

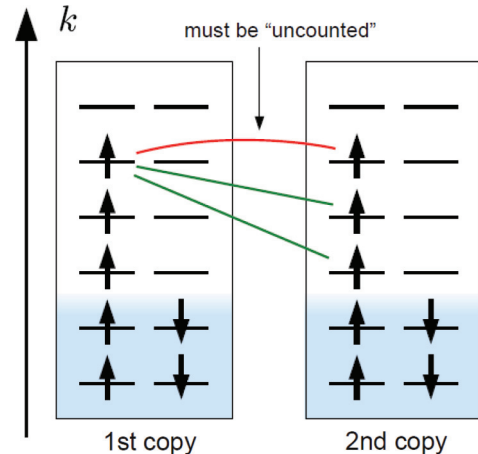


FIG. 6. (Color online) Microscopic contributions to the local SQM $\langle \mathcal{Q}^{rr} \rangle$. Two copies of the same ferromagnet are considered and green lines indicate correlations between pairs of distinguishable electrons in different orbitals (counted by the direct SQM). The red line indicates the correlations between indistinguishable electrons in the same orbital that the direct SQM counts *too much*: According to Pauli’s principle two electrons cannot form a triplet state in the same orbital. The exchange-SQM contribution takes care of this and thus represents a Pauli hole in the correlations, corresponding to the red line. When considering only the first copy at finite temperature, the macrospin picture discussed in Sec. III A2a is recovered. For finite temperature, the occupation probabilities are thermally smeared at the Fermi edge.

As a consequence, local exchange SQM must have the same tensorial structure as the direct SQM, but with opposite magnitude, which is explicitly conveyed by the negative sign in Eq. (61). Since $q_{\text{dir}}^{rr} > 0$ [by Eq. (58)], it follows also that $q_{\text{ex}}^{rr} > 0$ must hold. This is confirmed explicitly by Eq. (62), which shows that the exchange SQM senses the spin alignment, a non-negative quantity that accumulates when summing over all energies or k modes, respectively. This prohibits cancellations of signed contributions as they occur in the spin-dipole moment. This means that spin-dipole moment may cancel whence SQMs do *not*. Equation (62) also shows explicitly that exchange corrections become negligible at high temperatures, i.e., if $T^r \gg \varepsilon_{k\uparrow}^r - \varepsilon_{k\downarrow}^r$ for all k , as expected.

5. Energy-resolved exchange-SQM storage

So far, it was helpful to discuss the microscopic picture of SQM storage in terms of contributions from *orbitals* k . However, to make progress in calculations we replace the k sums with energy integrals. An *energy-resolved* picture of SQM storage will therefore be important for understanding the key features of SQM transport compared to charge and spin; see Sec. V C. For the rest of this chapter, we discuss only the local exchange SQM, i.e., $r' = r$, and therefore drop the electrode index for brevity. Replacing the sum over k in Eq. (62) with integrals over frequencies ω, ω' and inserting the *two-particle density of states* (16), we can recast the exchange SQM into the form of Eq. (59) after carrying out the spin sum (see Appendix A). The SQM exchange *magnitude* then reads

as

$$q_{\text{ex}} = \int d\omega \bar{v}(\omega) q_{\text{ex}}(\omega). \quad (64)$$

The *average exchange spin quadrupolarization* for electrons at frequency ω is,

$$q_{\text{ex}}(\omega) = f_+(\omega) a(\omega), \quad (65)$$

with the *spin-anisotropy function*

$$a(\omega) = \sum_{\sigma} a_{\sigma}(\omega), \quad (66)$$

and

$$\bar{v}(\omega) a_{\sigma}(\omega) = \int d\omega' f_+(\omega') \sum_{\sigma'} \frac{\sigma \sigma'}{4} v_{\sigma \sigma'}(\omega, \omega'), \quad (67)$$

which is valid for general dispersion relations. Note that the integrand in Eq. (64) is *not* a positive function, in contrast to each term in Eq. (62). For the discussion of the SQM currents, it is important to understand the meaning of the function $q_{\text{ex}}(\omega)$: It quantifies the cumulative exchange triplet correlation for electrons occupying the same orbital. It is the formal analog to the average spin-polarization function $s(\omega)$. To link the above result further to the microscopic picture developed in Sec. III B 4 and to simplify the interpretation of the exchange-SQM current in Sec. V A, we decomposed the spin-anisotropy function $a(\omega)$ into its spin-dependent contributions $a_{\sigma}(\omega)$: They give the direct single-mode SQM, provided that an electron with spin σ is present at frequency ω in the first copy while summing over the contributions from the second copy in Fig. 6 (cf. Appendix A 4). This reveals the formal analogy between $a(\omega)$ and average spin-polarization function in Eq. (48), given by $n(\omega)/2$. The latter quantifies the average spin at frequency ω , provided we have full occupation at this frequency. However, in stark contrast to the latter, $a(\omega)$ is not solely a band structure property as it depends on a Fermi function due to its two-particle origin. Note that the exchange SQM is entirely described by $q_{\text{ex}}(\omega)$ and that the spin polarization $s(\omega)$ does not enter, in contrast to the direct SQM. These two functions have very different temperature and energy dependence, again making explicit that the SQM is independent of the spin-polarization due to the presence of exchange terms.

The functions $q_{\text{ex}}(\omega)$ and $a(\omega)$ are of key importance for the results of this paper and we therefore explain their basic physical meaning using the simple Stoner model $\varepsilon_{k\sigma} = \varepsilon_k - \sigma J/2$ and the flat-band approximation (cf. Sec. II D). Then the spin-anisotropy function $a(\omega)$ has the spin-resolved contributions

$$a_{\sigma}(\omega) = \frac{1}{4} [f_+(\omega) - f_+(\omega + \sigma J)]. \quad (68)$$

In Fig. 7 we plot these two contributions and their sum together with the average spin quadrupolarization q_{ex} .

We first discuss the shape of $a_{\sigma}(\omega)$ for $\sigma = \uparrow, \downarrow$ for low temperature $4T/J < 1$ translating the arguments of the microscopic picture of Fig. 6 into energy space in Fig. 8. As mentioned, the function $a_{\sigma}(\omega)$ characterizes the single-orbital SQM for a spin σ occupying a mode at energy ω and displays four regimes (in the following \sim means “up to thermal smearing T ”). These are marked (a)–(d) in Fig. 7(a) and

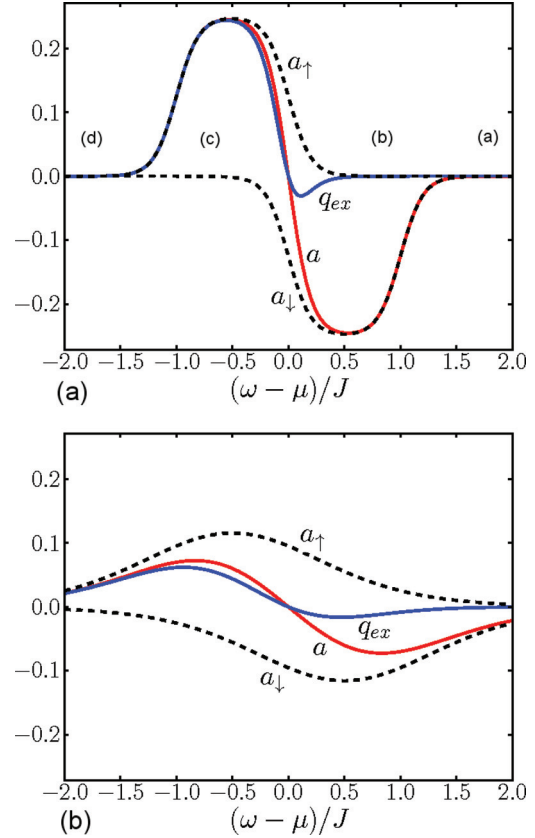


FIG. 7. (Color online) Average local exchange quadrupolarization $q_{\text{ex}}(\omega)$ (blue), spin anisotropy $a(\omega)$ (red), and its two contributions $a_{\uparrow}(\omega) > 0$ (broken line) and $a_{\downarrow}(\omega) < 0$ (broken line) as function of $(\omega - \mu)/J$ for two temperatures $T/J = 0.1$ in (a) and $T/J = 0.5$ in (b). As T approaches J from below, the weight of $a_{\uparrow}(\omega)$ ($a_{\downarrow}(\omega)$) considerably shrinks (rises) and $q_{\text{ex}}(\omega)$ is strongly suppressed. See also Sec. III B 6.

correspond to the regimes in Fig. 8. We discuss them now in detail.

(a) $\omega \gtrsim \mu + J \Rightarrow a_{\uparrow}(\omega) = a_{\downarrow}(\omega) = 0$: There are no occupied states at energy ω , so no exchange correction is needed.

(b) $\mu \lesssim \omega \lesssim \mu + J \Rightarrow a_{\downarrow}(\omega) < 0, a_{\uparrow}(\omega) = 0$: If a spin- \uparrow is in the first copy, the corresponding mode in the second copy has vanishing probability to be occupied with electrons of *any* spin since both $\varepsilon_{k\uparrow} = \omega \gtrsim \mu$ and $\varepsilon_{k\downarrow} = \omega + J \gtrsim \mu$.

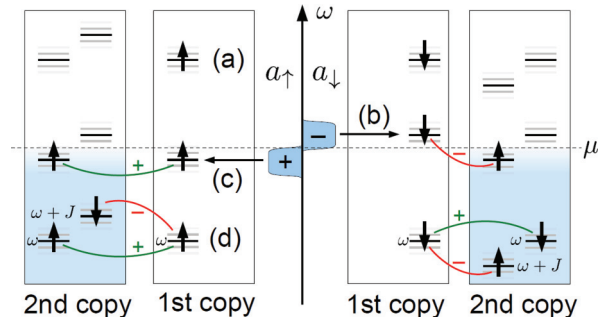


FIG. 8. (Color online) Microscopic picture of the spin-quadrupolarization function $a_{\sigma}(\omega)$, $\sigma = \uparrow, \downarrow$ characterizing the energy-resolved spin-anisotropy content of a ferromagnet (cf. Fig. 6); see text.

Thus, similar to regime (a), no exchange correction for spin- \uparrow electrons is needed and we obtain $a_{\uparrow}(\omega) = 0$. In contrast, if a spin- \downarrow is in the first copy, the corresponding mode in the second copy is predominantly occupied with spin- \uparrow because $\varepsilon_{k\downarrow} = \omega \gtrsim \mu$, but $\varepsilon_{k\uparrow} = \omega - J \lesssim \mu$. This contributes *negatively* to direct SQM, resulting in $a_{\downarrow}(\omega) < 0$.

(c) $\mu - J \lesssim \omega \lesssim \mu \Rightarrow a_{\uparrow}(\omega) > 0, a_{\downarrow}(\omega) = 0$: If in this case a spin- \uparrow is in the first copy, the corresponding mode in the second copy is also mostly occupied with spin- \uparrow since $\varepsilon_{k\uparrow} = \omega \lesssim \mu$, but $\varepsilon_{k\downarrow} = \omega + J \gtrsim \mu$. This gives a *positive* correction to the direct SQM. In contrast, $a_{\downarrow}(\omega) = 0$ as $\varepsilon_{k\downarrow} = \omega$ and $\varepsilon_{k\uparrow} = \omega - J$ refers to a mostly *doubly* occupied mode in the second copy, which has a vanishing direct-SQM contribution [cf. case (d)].

(d) $\omega \lesssim \mu - J \Rightarrow a_{\uparrow}(\omega) = a_{\downarrow}(\omega) = 0$: The corresponding orbital deep inside the Fermi sea is doubly occupied: $f(\varepsilon_{k\uparrow}) = f(\varepsilon_{k\downarrow}) = 1$. By Eq. (62) the direct SQM contributions due to both spin- \uparrow and spin- \downarrow electrons cancel each other.

Altogether, the anisotropy function $a(\omega) = \sum_{\sigma} a_{\sigma}(\omega)$ is exactly *antisymmetric* with respect to the electrochemical potential (see Fig. 7 and Appendix A 3)

$$a(\mu + \omega) = -a(\mu - \omega). \quad (69)$$

As mentioned at the outset, the average exchange quadrupolarization $q_{\text{ex}}(\omega) = f_{+}(\omega)[a_{\uparrow}(\omega) + a_{\downarrow}(\omega)]$ has both positive and negative contributions; however, $q_{\text{ex}} > 0$ as the integrated $q_{\text{ex}}(\omega)$ in Eq. (64) is always positive by Eq. (62). At $T = 0$ only positive correlations at $\omega < \mu$ count, and we recover the result (37). For $T > 0$, thermally excited spins \downarrow negatively correlate with spins \uparrow in the same orbital, thus reducing q_{ex} (see Fig. 7). Eventually, at $T \gg J$ this cancellation reduces q_{ex} exactly to zero without ever becoming negative. We now see explicitly that the exchange SQM only becomes *thermally* suppressed for $T \gg J$.

The average exchange quadrupolarization makes explicit that Pauli-forbidden triplet correlations are stored by electrons in an energy window $\sim 2J$ with opposite signs above and below the Fermi energy. Thus, the integrated exchange quadrupolarization is *thermally* suppressed for $T \gg J$ when the occupation probability is nearly constant across the energy scale J .

6. Parameter dependence of average exchange SQM

In the flat-band approximation (cf. Sec. IID), the integral (64) can be carried out, yielding (see Appendix A 4)

$$q_{\text{ex}} = \frac{\bar{v}T}{2} \left[\frac{J}{2T} \coth\left(\frac{J}{2T}\right) - 1 \right], \quad (70)$$

which is positive since $x \coth(x) > 1$, in agreement with the above discussion. In the limit $J/T \rightarrow 0$, q_{ex} vanishes as it should (see above) and in the opposite limit of $T/J \rightarrow 0$, q_{ex} scales linearly with N_s , the number of free spins in the ferromagnet [cf. Eq. (27)],

$$q_{\text{ex}}|_{T=0} = \frac{1}{4}\bar{v}J = \frac{1}{4}N_s, \quad (71)$$

in accordance with the $T = 0$ result (31) (Ref. 21). The average one-particle spin-dipole moment $\langle S_z \rangle_{T=0} = \frac{1}{2}N_s$ thus basically serves as a reference scale for two-particle q_{ex} (when multiplied by $\hbar = 1$ in our units). The low $T < J$

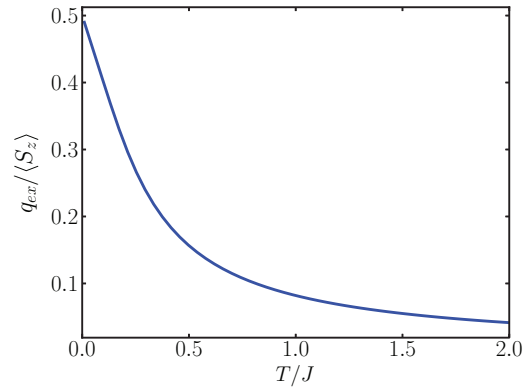


FIG. 9. (Color online) Magnitude of the local exchange SQM, q_{ex} , normalized to $\langle S_z \rangle = N_s/2$ as a function of temperature T/J for $\bar{v} = N_o/2D$, $D = 25J$, $\mu = 0$.

behavior is most interesting because in the regime $J < T$ the results do not apply to a Stoner ferromagnet, for which the self-consistent magnetization J would break down [our model Fig. 1(a) assumes fixed J]. However, considering our model as a description of mesoscopic islands in an external magnetic field of strength $B = J$ [Fig. 1(b)], this range may also be relevant. With this in mind we show in Fig. 9 the pronounced temperature dependence of the exchange SQM (normalized to the spin polarization) over the entire range for fixed J . This should be contrasted with the average spin for which all T dependence completely cancels out due to the constancy of the assumed DOS. As already anticipated in Sec. IIC, a two-particle quantity, the SQM, probes more of the electronic structure of the ferromagnets than the one-particle charge and spin-dipole moment do.

In Fig. 10, we plot the dependence of the exchange SQM (70) on the Stoner splitting J , illustrating that while $|\langle S \rangle|$ scales linearly with J , $\langle Q \rangle_{\text{ex}}$ initially increases quadratically and then approaches a linear asymptote:

$$q_{\text{ex}} = \frac{\bar{v}T}{4} \begin{cases} (J/T)^2/6 & J/T \ll 1, \\ (J/T) - 2 & J/T \gg 1. \end{cases} \quad (72)$$

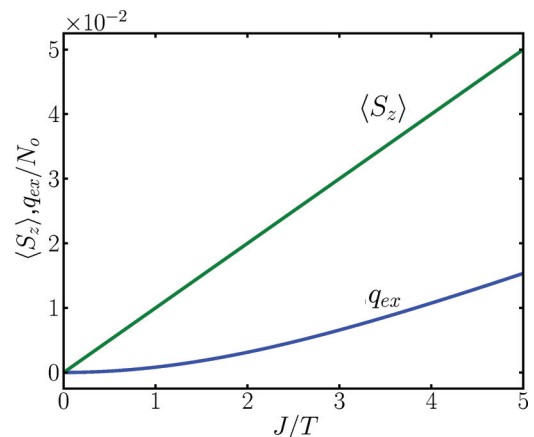


FIG. 10. (Color online) Magnitude of the spin $\langle S_z \rangle \approx N_s/2 = N_o J/2D$ (green) [Eq. (26)] and the exchange SQM q_{ex} [Eq. (70)] (blue) as a function of Stoner splitting J/T for $\bar{v} = N_o/(2D)$, $D = 25T$, $\mu = 0$.

IV. SPIN-MULTIPOLE CURRENT OPERATORS

We now turn to the third central question posed in the introduction: the proper definition of the SQM current operator. In the previous section, we answered the important question *from* where and *to* where SQM can be transported in terms of *nodes* in a spin-multipole network; cf. Sec. III B2. We now investigate the *links* between the nodes in this network, which correspond to the SQM current operators as noted at the end of Sec. III B. Their definition and physical interpretation requires some care because (i) like the spin, the total SQM is not conserved in a device comprising Stoner ferromagnets and (ii) unlike the spin, this two-particle quantity does not flow directly between local nodes, but is buffered in nonlocal nodes.

To tackle point (i), we first revisit the one-particle charge- and spin-currents operators. The spin-dipole current does not have the intuitive definition similar to the charge current (total outgoing current = rate of loss of charge) since the spin is *not* conserved internally in the ferromagnets. Starting from continuity equations in integral form, the spin currents rather have to be defined as the change in spin induced by the *tunneling*. In close analogy, we derive SQM current operators obeying a continuity equation and current conservation laws.

Due to point (ii), we also consider SQM current operators, accounting for the flow of SQM between local and nonlocal nodes. These turn out to be of central physical importance and reflect that on a microscopic level SQM is carried by pairs of correlated spin dipoles. The flow of spin anisotropy in an electronic system is thus inherently a two-particle process. We see that, as a result, the layout of the physical device and the network for SQM transport are *different*: The two-terminal spin valve requires a serial three-node SQM network. For more complex devices, even the connectivity is different.²²

A. Charge and spin-dipole current

The physical quantities of interest are the rates of change in local quantities in the physical subsystems of the circuit due to transport processes. For one-particle quantities such as charge and spin the physical subsystems are in one-to-one correspondence with the nodes of the charge/spin network; cf. Fig. 5. The time derivative operator $\dot{R}_\mu^r(t)$ giving the rate of change in the combined charge-spin one-particle operator R_μ^r [cf. Eq. (40)], $\frac{d}{dt}\langle R_\mu^r(t) \rangle = \langle \dot{R}_\mu^r(t) \rangle$, is given by

$$\dot{R}_\mu^r(t) := i[H, R_\mu^r], \quad (73)$$

exploiting the von-Neumann equation $\dot{\rho}(t) = -i[H, \rho(t)]$ and the cyclic invariance of the trace $\text{tr}(R_\mu^r \dot{\rho}(t)) = \text{tr}(i[H, R_\mu^r] \rho(t))$. We next decompose the total system Hamiltonian H into the part describing the decoupled subsystems, H_0 , and the tunneling $H_T = \sum_{(r,s)} H_T^{rs}$ with H_T^{rs} only accounting for tunneling processes between a pair of nodes r and s . This yields a continuity equation in integral form for operators,

$$\dot{R}_\mu^r(t) = \dot{R}_\mu^r(t)|_0 + \sum_{s \neq r} I_{R_\mu}^{rs}, \quad (74)$$

which decomposes the total rate of change in the charge (spin) operator in node r into two physically meaningful

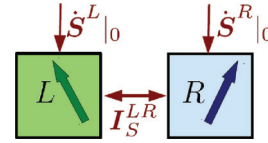


FIG. 11. (Color online) Network picture for the spin with current operators represented by links. The network picture for charge is similar, but without external arrows pointing to the nodes (indicated by $\dot{S}^r|_0$). The latter must be introduced due to the internal violation of spin conservation in each spin node.

contributions: The first contribution to Eq. (74) is given by

$$R_\mu^r|_0 = i[H_0, R_\mu^r] \quad (75)$$

and accounts for the time-evolution due to internal processes in node r . We depict this contribution in the network picture in Fig. 11 by an external arrow attached to node r . The second part $I_{R_\mu}^r = \sum_{s \neq r} I_{R_\mu}^{rs} = i[H_T, R_\mu^r]$ quantifies the rate of change induced by tunneling; i.e., this *defines the current* of observable R_μ^r *into* node r . In the form of Eq. (74), it has already decomposed into its various contributions emanating from all other subsystems s :

$$I_{R_\mu}^r = \sum_{s \neq r} I_{R_\mu}^{rs}. \quad (76)$$

Whenever the *operator* $I_{R_\mu}^{rs} \neq 0$, we depict this in the network picture by an arrow linking the two nodes r and s . Note that still the *average* current $\langle I_{R_\mu}^{rs} \rangle$ that flows between the nodes may vanish, e.g., for a some special set of parameters. So far, our considerations are quite general and also apply to systems including quantum dots.

In our model [Eqs. (7)–(9)], the particle number $R_0^r = N^r$ is conserved internally in each electrode individually and, therefore,

$$N^r|_0 = [H_0, N^r] = 0, \quad (77)$$

which is the 0 component of Eq. (75) and $\dot{N} = \sum_r \dot{N}^r$. These make up for the total change in charge. The spin $R_i^r = S_i^r$ ($i \neq 0$), however, is *not* conserved internally in the ferromagnets:

$$\dot{S}^r = \dot{S}^r|_0 + \mathbf{I}_S^r, \quad (78)$$

where \mathbf{I}_S^r is the operator for spin current into node r . Using Eq. (8), one finds

$$\dot{S}^r|_0 = \sum_n J_n^r \hat{\mathbf{J}}^r \times \mathbf{S}_n^r \neq 0 \quad (79)$$

for $\mathbf{S}_n^r = \sum_{k\sigma\sigma'} \mathbf{S}_{\sigma\sigma'}^r c_{rnk\sigma}^\dagger c_{rnk\sigma'}$ being the contribution from band n to the spin of electrode r . This describes a precession of \mathbf{S}_n^r about the Stoner field of electrode r .

To obtain an explicit starting point for the real-time calculation of the average charge current and spin current (see Appendix E), we use Eqs. (75) and (9) and recover the familiar form of the charge- and spin-current operators,

$$I_{R_\mu}^{rs} = \sum_{nn'kk'\sigma\sigma'} (-ir_\mu T)_{\sigma\sigma'}^{rs} c_{rnk\sigma}^\dagger c_{sn'k'\sigma'} - \text{H.c.}, \quad (80)$$

abbreviating the matrix product in spin -space $(r_\mu T)_{\sigma\sigma'}^{rs} = \sum_\tau (r_\mu)_{\sigma\tau} T_{\tau\sigma'}^{rs}$. The operator (80) describes the net current

injected from node s into node r , accounting for tunneling processes from node s to node r [the first contribution in Eq. (80)] and the reverse process (the second). Only the sum of both terms is a Hermitian operator and therefore a physical observable. Since both processes contribute with an opposite sign to the current (80), we obtain the antisymmetry relation $I_{R_\mu}^{rs} = -I_{R_\mu}^{sr}$. This has an important physical consequence: summing up all charge (spin) currents in the system yields the zero operator:

$$\sum_r \sum_{s \neq r} I_{R_\mu}^{rs} = 0. \quad (81)$$

This charge (spin) *current* conservation law expresses that charge (spin) is conserved by *tunneling*, that is $[H_T, R_\mu^{\text{tot}}] = 0$. Since the total spin is not conserved under the full time evolution (due to the *internal* evolution $\dot{\mathbf{S}}^{\text{tot}}|_0 \neq 0$), there is no analog of Eq. (81) for the total time derivative $\dot{\mathbf{S}}^r$. We emphasize furthermore that this conservation law holds on an *operator* level and not only for expectation values.

B. Spin-quadrupole current

We now try to proceed analogously for the SQM network in Fig. 5 of Sec. III B. Generally, we are interested in finding the rate of change in the spin anisotropy stored in local nodes. To this end, we need to consider the change in SQM, $\dot{\mathcal{Q}}^{rr'}$, in both the local nodes ($r = r'$) and the nonlocal nodes ($r \neq r'$). Taking the time derivative of Eq. (54) and using Eq. (74) we obtain

$$\dot{\mathcal{Q}}^{rr'} = \dot{\mathcal{Q}}^{rr'}|_0 + \sum_{\langle ss' \rangle \neq \langle rr' \rangle} \mathcal{I}_{\mathcal{Q}}^{rr',ss'}, \quad (82)$$

where $\langle ss' \rangle$ denotes the sum over *pairs* of indices ss' (i.e., ignoring their order). This is the continuity equation in integral form for the change in SQM in node $\langle rr' \rangle$. The first term is the change in SQM due to the internal time evolution,

$$\dot{\mathcal{Q}}^{rr'}|_0 = \frac{g^{rr'}}{2} [\dot{\mathbf{S}}^r|_0 \odot \mathbf{S}^{r'} + \mathbf{S}^r \odot \dot{\mathbf{S}}^{r'}|_0 + (r \leftrightarrow r')], \quad (83)$$

which involves the nonzero internal time evolution $\dot{\mathbf{S}}^r|_0$ given by Eq. (79). Like the spin, the SQM is thus *not* conserved in any of the nodes in our model. The responsible Stoner fields also effectively exert a “torque” on the SQM, thereby rotating the principal axes of this tensor. Similar to the spin, we depict this in the network picture (Fig. 12) by one-sided arrows pointing at this node.

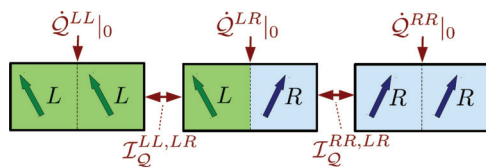


FIG. 12. (Color online) Network picture for SQM including the links representing SQM current *operators*. Similar to spin, SQM is not conserved internally in the nodes, giving rise to external SQM currents.

The SQM current $\mathcal{I}_{\mathcal{Q}}^{rr'} = \sum_{\langle ss' \rangle \neq \langle rr' \rangle} \mathcal{I}_{\mathcal{Q}}^{rr',ss'}$ is given by the Hermitian tensor operator

$$\mathcal{I}_{\mathcal{Q}}^{rr'} = \frac{g^{rr'}}{2} [\mathbf{I}_{\mathbf{S}}^r \odot \mathbf{S}^{r'} + \mathbf{S}^r \odot \mathbf{I}_{\mathbf{S}}^{r'} + (r \leftrightarrow r')]. \quad (84)$$

This is a central result of the paper. Since the spin and the spin current do, in general, not commute as operators on Fock space,²³ the individual terms in this expression are not Hermitian and therefore not observables. The operator (84) reflects that, in general, the average SQM current is not simply the product of spin and spin current since $\langle \mathbf{I}_{\mathbf{S}_i}^r \mathbf{S}_j^{r'} \rangle \neq \langle \mathbf{I}_{\mathbf{S}_i}^r \rangle \langle \mathbf{S}_j^{r'} \rangle$ due to quantum mechanical exchange correlations, interactions, etc. Therefore, SQM is not determined by spin-dipole moment: It requires a separate description in spintronics transport theory. For the bilinear tunnel coupling (9), the contribution to the net current from node $\langle ss' \rangle$ into in node $\langle rr' \rangle$ is

$$\mathcal{I}_{\mathcal{Q}}^{rr',ss'} = \frac{g^{rr'}}{2} [[\mathbf{I}_{\mathbf{S}}^r \odot \mathbf{S}^{r'} \delta^{r's'} + \mathbf{S}^r \delta^{rs} \odot \mathbf{I}_{\mathbf{S}}^{r's'}] + (r \leftrightarrow r')]. \quad (85)$$

Notably, this SQM current is zero unless one of the indices s, s' matches the indices r, r' . This puts an important restriction on the network connectivity: The local SQM nodes are linked *only* to nonlocal nodes and not to other local nodes. Changes of local spin-anisotropy,

$$\dot{\mathcal{Q}}^{rr} = \dot{\mathcal{Q}}^{rr}|_0 + \mathcal{I}_{\mathcal{Q}}^{rr}, \quad (86)$$

which are due to transport thus occur only through changes in nonlocal spin correlations:

$$\mathcal{I}_{\mathcal{Q}}^{rr} = \sum_{s \neq r} (\mathbf{I}_{\mathbf{S}}^s \odot \mathbf{S}^r + \mathbf{S}^r \odot \mathbf{I}_{\mathbf{S}}^s), \quad (87)$$

where $\mathbf{I}_{\mathbf{S}}^s$ is the spin-current operator from node s into r .

All the considerations so far in this section were general. For the simple spin valve we consider in this paper the general theory above implies that SQM cannot be directly transferred from the local node $\langle LL \rangle$ to the local node $\langle RR \rangle$; it is rather first “buffered” in the intermediate, nonlocal node $\langle LR \rangle$. This restriction on the SQM network connectivity is related to the real-space picture of SQM transport sketched in Fig. 13. This picture unveils why SQM transport is possible even in the single-electron transport limit (leading order in H_T),

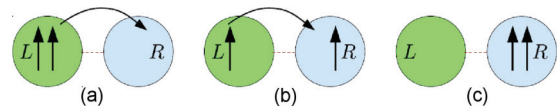


FIG. 13. (Color online) Illustration of the microscopic picture of SQM transport. (a) Consider two electrons in electrode L that contribute to the SQM of the local node $\langle LL \rangle$. (b) By transferring one of these electrons to subsystem R , the local spin-spin correlation is lost but new nonlocal correlations are established, increasing the SQM of node $\langle LR \rangle$. Thus, by emitting spin-polarized electrons nonlocal correlations are set up in the circuit. (c) When the second electron follows the first, local SQM correlations are created, but now in subsystem R (node $\langle RR \rangle$). Note that this picture is meant only to illustrate the *nonlocality* aspect of SQM, but incorrectly portrays the spins as distinguishable objects.

as discussed for spin valves with embedded spin-*isotropic* quantum dots.^{14–16} In this case we have on the right-hand side of Eq. (86) $\hat{\mathcal{Q}}^{rr}|_0 = 0$, where r now labels the quantum dot embedded in this spin valve. Then SQM currents are responsible for the change in the local QD spin anisotropy of subsystem r , i.e., $\hat{\mathcal{Q}}^{rr} = \mathcal{I}_{\mathcal{Q}}^{rr}$, where $\mathcal{I}_{\mathcal{Q}}^{rr}$ of Eq. (87) was already obtained in Ref. 15 for a spin valve with an embedded quantum dot, however, without using the new network picture. The calculations in Ref. 15 demonstrate that in such more complicated devices the SQM current $\mathcal{I}_{\mathcal{Q}}^{rr}$, averaged over the nonequilibrium state, depends nontrivially on the average accumulated charge and spin of the dot. The SQM current thus couples to the measurable charge current and spin current and should, in general, be considered for the description of spin and charge dynamics.

Analogous to the charge current and spin current the SQM current (85) is antisymmetric with respect to the node indices, i.e., when the two pairs of subsystem indices rr' and ss' are interchanged: $\mathcal{I}_{\mathcal{Q}}^{rr',ss'} = -\mathcal{I}_{\mathcal{Q}}^{ss',rr'}$. (Note that the order of indices denoting a pair does not matter; i.e., $rr' = r'r$). As a consequence, the SQM currents sum to the zero tensor operator:

$$\sum_{(rr')} \mathcal{I}_{\mathcal{Q}}^{rr'} = \sum_{(rr')} \sum_{(ss') \neq (rr')} \mathcal{I}_{\mathcal{Q}}^{rr',ss'} = 0. \quad (88)$$

Similar to spin, this *SQM current conservation law* expresses the conservation of total circuit SQM (50) in the *tunneling*. This is a direct consequence of the total spin-dipole conservation by tunneling: $[H_T, \mathcal{Q}^{\text{tot}}] = \mathbf{S}^{\text{tot}} \odot [H_T, \mathbf{S}^{\text{tot}}] + [H_T, \mathbf{S}^{\text{tot}}] \odot \mathbf{S}^{\text{tot}} = 0$.

Finally, we note that the restriction on the network connectivity found above derives from the particular form of our tunneling Hamiltonian (9), which is bilinear in the field operators. The network thus describes the connectivity on the *operator* level. The topology of this network is different when H_T is, e.g., an effective exchange coupling that is quartic in the fields. Since such a coupling is usually derived from the bilinear tunneling model (9) studied here, we do not dwell on this further.²⁴

V. AVERAGE SPIN-MULTIPOLE CURRENTS

In this section we complete the discussion of the third main question posed in the Introduction: We present explicit results for the average spin-quadrupole current calculated to first order in the tunnel coupling Γ of the two ferromagnets and compare it to the average charge current and spin current. The calculations of these are compactly presented in Appendix D, applying a covariant reformulation of the real-time diagrammatic technique (for a systematic, self-contained technical presentation, see Appendix E). Covariance is used here in the sense that all expressions are form-invariant under a change of the spatial coordinate system and the spin quantization axis. An advantage of this technique is that it can be extended to spin valves with embedded quantum dots.²²

In Sec. VA we discuss the results for a general multiband dispersion relation $\varepsilon_{nk\sigma}^r$, applying the insights obtained from the spin-multipole network theory developed in Secs. IIIB2 and IV and the microscopic picture explained in Sec. IIIB4. We decompose the SQM current into physically meaningful

contributions: direct vs exchange (Pauli exclusion hole aspects) and dissipative vs coherent (quantum fluctuation aspects). An intimate connection between storage (see Sec. III) and transport of charge, spin, and SQM is then established by comparing their *energy-resolved* contributions (see Sec. IIIB5).

In Sec. VB we specialize to the flat-band approximation (cf. Sec. IID) to obtain tangible analytical and numerical results. Even in this simple limit—where the dissipative spin current vanishes due to the energy-independent DOS—the average SQM current tensor has a nontrivial parameter dependence. This concerns both its magnitude (principal values) and its alignment (principal vectors), which are substantially controllable by magnetic and electric parameters for noncollinear Stoner vectors.

In Sec. VC we demonstrate that a *pure* SQM current, i.e., not accompanied by a spin current, is, in principle, possible. This spin-anisotropy transfer is entirely carried by Pauli exclusion holes, giving rise to a nonvanishing exchange-SQM current. For a *temperature* bias between ferromagnets with collinear Stoner vectors, we even show that a pure SQM current even persists in the absence of a charge current. Electrodes with nontrivial spin structure can thus “talk” to each other in ways not described by charge current and spin current.

A. Charge, spin, and SQM currents

The average charge, spin, and spin-quadrupole currents associated with the left electrode read

$$\langle I_N^L \rangle = I_{N,0}^L + I_{N,F}^L (\hat{\mathbf{J}}^L \cdot \hat{\mathbf{J}}^R), \quad (89)$$

$$\langle \mathbf{I}_S^L \rangle = E_S^L \hat{\mathbf{J}}^L + A_S^L \hat{\mathbf{J}}^R + T_S^L (\hat{\mathbf{J}}^L \times \hat{\mathbf{J}}^R), \quad (90)$$

$$\langle \mathcal{I}_{\mathcal{Q}}^{LL} \rangle = 2(\mathbf{S}^L) \odot \langle \mathbf{I}_S^L \rangle - \hat{\mathbf{J}}^L \odot [E_{\text{ex}}^L \hat{\mathbf{J}}^L + A_{\text{ex}}^L \hat{\mathbf{J}}^R + T_{\text{ex}}^L \hat{\mathbf{J}}^L \times \hat{\mathbf{J}}^R]. \quad (91)$$

These were calculated in Appendix D to the first order in the energy-resolved tunneling rate,

$$\Gamma(\omega) = 2\pi t^2 \bar{v}^L(\omega) \bar{v}^R(\omega), \quad (92)$$

where $\bar{v}^r(\omega)$ is given by Eq. (14). Here \odot denotes the symmetric, traceless tensor product (51). The charge current coefficients are (we do not write the ω dependence unless confusion may arise)

$$I_{N,0} = \int d\omega 2\Gamma \Delta, \quad (93)$$

$$I_{N,F}^L = \int d\omega 2\Gamma \Delta n^L n^R, \quad (94)$$

where the spin-polarization function $n^r(\omega)$ is given by Eq. (15). The well-known bias function,

$$\Delta(\omega) = f_+^R(\omega) - f_+^L(\omega), \quad (95)$$

is only nonzero in the bias window, $\mu^L \gtrsim \omega \gtrsim \mu^R$, up to thermal smearing. The occurrence of the factor $\Delta(\omega)$ signals that a term arises from *dissipative processes* in which the energy of initial and final state have to be the same. The

spin-current coefficients are

$$E_S^L = \int d\omega \Gamma \Delta n^L, \quad (96)$$

$$A_S^L = \int d\omega \Gamma \Delta n^R, \quad (97)$$

$$T_S^L = \int d\omega \Gamma \left(\beta^L \frac{n^R}{\bar{v}^L} + \beta^R \frac{n^L}{\bar{v}^R} \right), \quad (98)$$

the function $\beta^r(\omega)$ incorporates the effect of the spin-polarization of the DOS, $n^r(\omega)$, through the principal value integral,

$$\beta^r(\omega) = \text{Re} \int \frac{d\omega' \bar{v}^r(\omega') n^r(\omega') f_+^r(\omega')}{\pi (\omega - \omega' + i0)}, \quad (99)$$

integrating over all virtual-state energies ω' . Here and below such functions, not limited by energy conservation as they involve virtual intermediate states, appear in contributions from *coherent processes*. Finally, the exchange-SQM emission, absorption, and torque coefficients,

$$E_{\text{ex}}^L = 2 \int d\omega \Gamma \Delta a^L, \quad (100)$$

$$A_{\text{ex}}^L = 2 \int d\omega \Gamma \Delta n^R \tilde{a}^L, \quad (101)$$

$$T_{\text{ex}}^L = 2 \int d\omega \Gamma (\beta^R - \alpha^R f_+^L) \frac{a^L}{\bar{v}^R}, \quad (102)$$

depend on the local spin-anisotropy function a^L [cf. (66)] and an additional *even* spin-anisotropy function,

$$\tilde{a}^L(\omega) = \int d\omega' f_+^r(\omega') \sum_{\sigma, \sigma'} \frac{\sigma'}{4} \frac{v_{\sigma\sigma'}^r(\omega, \omega')}{\bar{v}^r(\omega)} \quad (103)$$

$$= \sum_{\sigma} \sigma a_{\sigma}^r(\omega), \quad (104)$$

where $v_{\sigma\sigma'}^r(\omega, \omega')$ is the 2DOS (16). Finally, the torque coefficient $T_{\mathcal{Q}}^L$ involves an additional function similar to Eq. (99) but without the distribution function $f_+^R(\omega)$ under the principal value integral:

$$\alpha^R(\omega) = \text{Re} \int \frac{d\omega' n^R(\omega') \bar{v}^R(\omega')}{\pi (\omega - \omega' + i0)}. \quad (105)$$

The reader should note that the coefficients of Eqs. (100)–(102) are defined such that a minus sign appears in Eq. (91), which we introduced in agreement with the sign convention for exchange-SQM in Eq. (61), that is, $\langle \mathcal{Q}^{LL} \rangle = -q_{\text{ex}}^L \hat{\mathbf{J}}^L \odot \hat{\mathbf{J}}^L$. Moreover, one obtains the expressions for $\langle \mathcal{I}_{\mathcal{Q}}^{RR} \rangle$ by formally substituting $L \leftrightarrow R$ in Eq. (91), and $\langle \mathcal{I}_{\mathcal{Q}}^{LR} \rangle = -\langle \mathcal{I}_{\mathcal{Q}}^{LL} \rangle - \langle \mathcal{I}_{\mathcal{Q}}^{RR} \rangle$ follows from the SQM current conservation law (88) (see also below). One checks that the results are invariant under scalar gauge transformations (global energy shifts). Finally, we note that since positive currents are defined as entering a node, positive (negative) absorption coefficients correspond to injection (ejection) of particles and vice versa for emission coefficients.

The SQM current Eq. (91) is the central result of this paper. It depends explicitly (but not exclusively) on the spin current (90). Therefore, its physical interpretation is aided by first giving a pertinent review of the different contributions to the charge current (89) and spin current (90), respectively.

1. Charge current

Equation (89) is a well-known and experimentally tested result for the charge current, which accounts for single electron tunneling processes between the left and right electrode. It has only dissipative contributions [i.e., involving $\Delta(\omega)$]: The first part $I_{N,0}$ in Eq. (89) only depends in the average DOS \bar{v}^r , whereas the second, spin-dependent correction depends on the DOS spin polarizations n^r through $I_{N,F}^L$ and on the angle between the Stoner vectors through $\hat{\mathbf{J}}^L \cdot \hat{\mathbf{J}}^R = \cos \theta$. The reduction going from $\theta = 0 \rightarrow \pi$ is the celebrated spin-valve or tunnel magnetoresistance (TMR) effect.²⁵

2. Spin current

The spin current (90) was obtained by Braun *et al.*¹¹ and we review here its two types of contributions.

a. Dissipative spin emission $\sim \hat{\mathbf{J}}^L$ and *absorption* $\sim \hat{\mathbf{J}}^R$. The dissipative spin-dipole current [first two terms in Eq. (90), containing $\Delta(\omega)$] is analogous to the particle current: An electron emitted from the left node transports a spin-dipole moment $\hat{\mathbf{J}}^L/2$ and the electrons absorbed from the right node transport $\hat{\mathbf{J}}^R/2$. The expression for particle current Eq. (93) simply has to be supplemented by a factor $n^r(\omega) \hat{\mathbf{J}}^r/2$ to obtain the terms for spin emission (96) and absorption (97).

b. Coherent spin torque $\sim \hat{\mathbf{J}}^L \times \hat{\mathbf{J}}^R$. The coherent spin current [last term in Eq. (90)] has no such analogy to the particle current and corresponds to a spin torque. This corresponds to spin flips induced by virtual fluctuations between the left and the right electrode restricted by energy conservation only in the final state, but not in the intermediate state. This is reflected by its dependence on the principal value integral $\beta^r(\omega)$ [cf. discussion of Eq. (99)]: An electron with spin σ occupying a level at energy ω in the left electrode can fluctuate to all empty levels with energy ω' in the right electrode with an amplitude $\propto 1/(\omega - \omega')$. While in the right electrode, the electron spin $\propto \hat{\mathbf{J}}^L$ is not collinear to the Stoner field $\propto \hat{\mathbf{J}}^R$ in the right electrode and precesses about it, explaining the factor $\hat{\mathbf{J}}^L \times \hat{\mathbf{J}}^R$ in the coherent spin current (98). Note that a net *spin torque* on the magnetization of the left electrode only occurs if the 1DOS of *both* electrodes are spin polarized.

Finally, we note that at zero bias, the dissipative spin current vanishes, $E_S^L = A_S^L = 0$, but the coherent spin current (torque contribution) remains, $T_S^L \neq 0$: Noncollinear ferromagnets keep interacting by virtual fluctuations, thereby exerting a torque on each other.

3. SQM current

a. SQM current conservation. The most immediate property of the SQM current expression (91) is its formal lack of symmetry with respect to interchanging the electrodes $L \leftrightarrow R$. This differs notably from charge current and spin current, for which the original expression is reproduced with a minus sign when interchanging $L \leftrightarrow R$. This distinction is related to the striking characteristics of the SQM network picture compared to the charge and spin network (see Sec. VA3): The currents of the latter, $\langle I_{R,\mu}^L \rangle$, describe the net flow into the L node coming from the R node (see Fig. 11). Interchanging L and R yields then the opposite current from R to the L node, reflecting the current conservation law (81): $\langle I_{R,\mu}^L \rangle + \langle I_{R,\mu}^R \rangle = 0$. In contrast, $\langle \mathcal{I}_{\mathcal{Q}}^{LL} \rangle$ describes the net flow of

SQM from the local $\langle LL \rangle$ node to the nonlocal $\langle LR \rangle$ node (see Fig. 12). If we interchange $L \leftrightarrow R$ in Eq. (91), we obtain the current $\langle \mathcal{I}_{\mathcal{Q}}^{RR} \rangle$ emanating from the $\langle RR \rangle$ node. Importantly, $\langle \mathcal{I}_{\mathcal{Q}}^{LL} \rangle + \langle \mathcal{I}_{\mathcal{Q}}^{RR} \rangle = -\langle \mathcal{I}_{\mathcal{Q}}^{LR} \rangle \neq 0$ in accordance with the SQM current conservation law (88). This again emphasizes the relevance of the nonlocal node $\langle LR \rangle$, which “buffers” the SQM currents from both local nodes.

b. Direct and exchange-SQM current. The SQM current allows for two physically meaningful, different decompositions. The first decomposition is given by Eq. (91), which breaks up the SQM current into different two-particle contributions, the first, *direct*, term Eq. (91) and the second, *exchange*, term. This has no analog in the one-particle charge current and spin current.

The direct current $\langle \mathcal{I}_{\mathcal{Q}}^{LL} \rangle_{\text{dir}}$ quantifies the tunneling-induced change in the direct part of the average SQM (57), $\langle \mathcal{Q}^{LL} \rangle_{\text{dir}} := \langle \mathbf{S}^L \rangle \odot \langle \mathbf{S}^L \rangle$, which ignores the Pauli exclusion hole (cf. Sec. III). Indeed, using Eq. (87), we reproduce the first term in Eq. (91):

$$\langle \mathcal{I}_{\mathcal{Q}}^{LL} \rangle_{\text{dir}} := \langle \dot{\mathcal{Q}}^{LL} - \dot{\mathcal{Q}}^{LL} |_{0} \rangle_{\text{dir}} \quad (106)$$

$$= 2 \langle \mathbf{S}^L \rangle \odot \langle \mathbf{I}_{\mathcal{S}}^L \rangle. \quad (107)$$

Similar to the average SQM, the direct average SQM current is completely determined by a product of average spin-dipole properties, here the spin $\langle \mathbf{S}^L \rangle$ and the spin current $\langle \mathbf{I}_{\mathcal{S}}^L \rangle$, given by Eqs. (47) and (90), respectively. This equation substantiates the classical picture of transport SQM or spin-anisotropy sketched in Fig. 13: When single electrons move, the triplet correlations between pairs of electron spins first delocalize and then relocalize, resulting in a change of the local SQM, the part described by $\langle \mathcal{Q}^{LL} \rangle_{\text{dir}}$.

The exchange-SQM current $\langle \mathcal{I}_{\mathcal{Q}}^{LL} \rangle_{\text{ex}}$, the second term in Eq. (91), accounts for the tunnel-induced change in $\langle \mathcal{Q}^{LL} \rangle_{\text{ex}}$, i.e., a negative quantum anisotropy due to the Pauli-exclusion holes in the triplet spin correlations. It *cannot* be expressed in terms of the average spin current. The above classical picture of SQM transport thus needs correction: By reducing SQM transport to “spin times spin current” one overestimates the anisotropy flow, by counting Pauli-forbidden, local triplet correlations (those coming from the same orbital) and accounting for their transformation into nonlocal correlations when one of the two electrons tunnels out. The SQM exchange current compensates for this: It is an effective backflow of nonlocal anisotropy into to the local nodes of the SQM network (Fig. 12). We now reach a central conclusion of the paper: Whenever the average spin current is made to vanish $\langle \mathbf{I}_{\mathcal{S}}^L \rangle = 0$, a nonzero SQM exchange current is generally present since $\langle \mathbf{S}^L \odot \mathbf{I}_{\mathcal{S}}^L \rangle \neq \langle \mathbf{S}^L \rangle \odot \langle \mathbf{I}_{\mathcal{S}}^L \rangle$ due to the Pauli exclusion holes. In Sec. V C we explicitly verify that the cancellations of the single-particle contributions that cause the spin current to cancel have no counterpart for the *two-particle exchange-SQM* current. This indicates the possibility of pure SQM transport, that is, without spin current.

The most prominent distinction between the direct and exchange-SQM currents is that they differ by a relative factor $|\langle \mathbf{S}^L \rangle|$. To see this explicitly, we express the SQM current (91) as a symmetric, traceless tensor product of the unit vector $\hat{\mathbf{J}}^L$ with a linear combination of $\hat{\mathbf{J}}^L$, $\hat{\mathbf{J}}^R$ and $\hat{\mathbf{J}}^L \times \hat{\mathbf{J}}^R$ by inserting

the explicit spin current (90):

$$\langle \mathcal{I}_{\mathcal{Q}}^{LL} \rangle = \hat{\mathbf{J}}^L \odot [E_{\mathcal{Q}}^L \hat{\mathbf{J}}^L + A_{\mathcal{Q}}^L \hat{\mathbf{J}}^R] + T_{\mathcal{Q}}^L \hat{\mathbf{J}}^L \odot (\hat{\mathbf{J}}^L \times \hat{\mathbf{J}}^R). \quad (108)$$

Each of the coefficients has a direct and exchange contribution, respectively:

$$E_{\mathcal{Q}}^L = 2E_{\mathcal{S}}^L(\langle \mathbf{S}^L \rangle \cdot \hat{\mathbf{J}}^L) - E_{\text{ex}}^L, \quad (109)$$

$$A_{\mathcal{Q}}^L = 2A_{\mathcal{S}}^L(\langle \mathbf{S}^L \rangle \cdot \hat{\mathbf{J}}^L) - A_{\text{ex}}^L, \quad (110)$$

$$T_{\mathcal{Q}}^L = 2T_{\mathcal{S}}^L(\langle \mathbf{S}^L \rangle \cdot \hat{\mathbf{J}}^L) - T_{\text{ex}}^L. \quad (111)$$

Since all coefficients, Eqs. (96)–(98) and Eqs. (100)–(102), appearing on the right-hand sides of Eqs. (109)–(111) are, in general, of the same order, the ratio of the direct-SQM current to the exchange SQM scales linearly with the average spin $|\langle \mathbf{S}^L \rangle| \sim N_s = (J/D)N_o$ as expected from our analysis below Eq. (60) in Sec. III B2. Consequently, for a *macroscopic* ferromagnet, the SQM current is dominated by its direct part [Eq. (107)] and is thus *induced* by the spin current. Furthermore, since the SQM current accounts for the change in the correlations between the spin of a transported electron with all *other* spins in the system, only the *SQM current per electron* is expected to be a meaningful quantity in the thermodynamic limit.²⁶ As soon as one of the subsystems is of meso- or nanoscopic dimensions the relative factor $|\langle \mathbf{S}^L \rangle|$ is reduced (cf. Sec. III A2 b) and the exchange-SQM current should be reckoned with. For a nanoscopic system, the full SQM current was already studied in Ref. 15, while also including the relevant charging and nonequilibrium effects, which were neglected here. With this in mind, we in the following always first discuss the direct part, dominating the SQM current for macroscopic ferromagnets [Fig. 1(a)], and then separately consider the exchange correction, relevant for mesoscopic ferromagnets [Fig. 1(b)].

c. Dissipative and coherent SQM current. The second, alternative decomposition of the SQM current is that into a dissipative and coherent part, the first and second term of Eq. (108), respectively, similar to the spin-dipole current. For noncollinear $\hat{\mathbf{J}}^L$ and $\hat{\mathbf{J}}^R$ these terms are linearly independent tensors and their coefficients have very different parameter dependencies. The tensorial structure of the total SQM current is determined by their nontrivial interplay. Its discussion requires explicit results and is therefore postponed to Sec. V B3, where we use the flat-band approximation.

The decomposition of the direct-SQM current follows by Eq. (107) directly from the decomposition of the spin current (90) into dissipative emission, dissipative absorption, and coherent torque parts. Since the exchange-SQM current is a correction to the direct current accounting for Pauli-forbidden triplet correlations [cf. explanation below Eq. (107)], it must have the same decomposition into emission, absorption and torque part with coefficients given by Eqs. (109)–(111), respectively.

Dissipative SQM emission $\sim \hat{\mathbf{J}}^L \odot \hat{\mathbf{J}}^L$ and *absorption* $\sim \hat{\mathbf{J}}^L \odot \hat{\mathbf{J}}^R$. The SQM emission can be microscopically understood as the delocalization of triplet spin correlations from node $\langle LL \rangle$ to node $\langle LR \rangle$ (see Fig. 5). The SQM absorption describes the converse relocalization of such correlations from node $\langle LR \rangle$ to node $\langle LL \rangle$. This is reflected by the tensorial structure of these contributions to the average SQM currents:

They coincide with the average SQM stored in the node, from where they are emitted ($\hat{\mathbf{J}}^L \odot \hat{\mathbf{J}}^L \sim \langle \mathcal{Q}^{LL} \rangle$) or absorbed ($\hat{\mathbf{J}}^L \odot \hat{\mathbf{J}}^R \sim \langle \mathcal{Q}^{LR} \rangle$). Importantly, there is no SQM absorption in $\langle \mathcal{I}_{\mathcal{Q}}^{LL} \rangle$ that originates from the $\langle RR \rangle$ -node ($\hat{\mathbf{J}}^R \odot \hat{\mathbf{J}}^R \sim \langle \mathcal{Q}^{RR} \rangle$) as expected from the connectivity in the SQM network picture of Sec. IV B.

The relation between the storage and transport is also reflected by the integrands of the exchange-SQM current in Eqs. (100) and (101): These resemble the average local spin quadrupolarization $q_{\text{ex}}^L(\omega) = f_+^L(\omega)a^L(\omega)$ in the expression (64) for $\langle \mathcal{Q}^{LL} \rangle_{\text{ex}}$. These can formally be obtained by a replacement $f_+^L(\omega) \rightarrow \Delta(\omega)$, i.e., similar to the relation between the average spin-dipole moment [see Eq. (47)] and the dissipative spin current in Sec. V A2. However, the symmetry of the function $a^L(\omega)$ with respect to ω is very different from that of $n^L(\omega)$ appearing the spin-current emission [Eqs. (96) and (97)]. This fact underlies a key result of the paper in Sec. V C.

The microscopic picture of exchange-SQM storage can be extended to capture a precise physical understanding of the exchange-SQM current as follows: As explained in Sec. III B4, the Pauli exclusion holes can be “counted” as single-mode cross correlations between two identical copies of the same ferromagnet (cf. Fig. 8). For the exchange-SQM current, we have to imagine that the electron in the first copy undergoes a tunneling process [representing to the spin current in Eq. (87)], and the second copy is left unchanged [representing the spin in Eq. (87)].²⁷ For the dissipative exchange-SQM emission, this becomes directly clear from the expression (100): The Fermi function in $\Delta(\omega)$ refers to the electron tunneling at energy ω in the first copy and the local anisotropy function a^L contains the single-mode correlation of that electron with the average (unchanged) second copy. This term therefore describes the flow of Pauli exclusion holes arising from the spin emission $\sim \hat{\mathbf{J}}^L$. The exchange coefficient (101) corresponding to the spin absorption $\sim \hat{\mathbf{J}}^R$, the first factor Δn^R relates to the absorbed spin from the right electrode and the second factor \tilde{a}^L represents the correlations of that absorbed spin with the local spins in the left electrode. Notably, the spin-dependent contributions a_σ^L to $a^L = \sum_\sigma a_\sigma^L$ are added in $\tilde{a}^L = \sum_\sigma \sigma a_\sigma^L > 0$ such that they always count as positive. Here the sign of how to count the Pauli-forbidden anisotropy is related to the sign of n^R : If $n^R > 0$, mostly spin- \uparrow is absorbed and the missing anisotropy generated by this is positive, while for $n^R < 0$ mostly spin- \downarrow is absorbed and the missing anisotropy is negative as explained in Sec. III B4.

Coherent SQM torque $\sim \hat{\mathbf{J}}^L \odot (\hat{\mathbf{J}}^L \times \hat{\mathbf{J}}^R)$. The coherent contribution to the SQM current basically originates from the spin torque. This follows by considering the direct contribution that derives from the spin current; cf. Eq. (107). It accounts for the change of the correlation between of the spin of an electron fixed in the left electrode with the spin of an electron that *virtually fluctuates* into the right electrode (spin-flip scattering). Since during this fluctuation the latter spin precesses about the Stoner field, a net conversion of local into nonlocal correlations results, i.e., there is an associated SQM current. The exchange-SQM torque coefficient T_{ex}^L excludes the single-mode correlations: In the microscopic picture only the electron in the first copy undergoes a virtual fluctuation [indicated by β^R and α^R in Eq. (102)], while the second copy

is left unchanged [indicated by a^L in Eq. (102)].²⁸ This is the effect of the spin torque on the local Pauli exclusion holes.

B. Parameter dependence

Having discussed the general structure and physical meaning of the main results (89)–(91), we now simplify them as far as possible by making the flat-band approximation. Although this is a crude approximation, it reveals a general key feature of the exchange SQM, namely its sensitivity to the spin *alignment*, a non-negative quantity that accumulates when summing over energies/ k modes. This prohibits cancellations in the exchange-SQM current as they occur due to signed contributions in the charge and spin-dipole current. (cf. Sec. III B4). As noted in Sec. II D the 2DOS appearing in the exchange expressions requires modeling of the electrodes that goes beyond the 1DOS. However, in the flat-band approximation we only need Eq. (A44). We furthermore apply the bias voltage symmetrically to the ferromagnets, $\mu^L = +V/2$ and $\mu^R = -V/2$ while considering arbitrary noncollinear Stoner vectors $\hat{\mathbf{J}}^L$ and $\hat{\mathbf{J}}^R$. We assume all further parameters to be symmetric: $J^r = J$, $T^r = T$, $D^r = D$, and $v_\sigma^r = v_\sigma$ for $\sigma = \uparrow, \downarrow$ (except for a temperature gradient discussed in Sec. V C). In this approximation the densities of states are fixed by the bandwidths, $v_\sigma = 1/2D$, and the tunneling rate is set by the spin-conserving tunnel amplitude t : $\Gamma = 2\pi(t/2D)^2$; cf. Eq. (11). Together with the leading order approximation in Γ this limits the applicability of the results to the regime $\Gamma \ll T, J \ll W$ [cf. Eq. (19)]. The central equations (89)–(91) now simplify to

$$\langle I_N^L \rangle = I_{N,0}^L, \quad (112)$$

$$\langle \mathbf{I}_S^L \rangle = T_S^L (\hat{\mathbf{J}}^L \times \hat{\mathbf{J}}^R), \quad (113)$$

$$\langle \mathcal{I}_{\mathcal{Q}}^{LL} \rangle = 2(\langle S^L \rangle \cdot \hat{\mathbf{J}}^L) \hat{\mathbf{J}}^L \odot \langle \mathbf{I}_S^L \rangle - \hat{\mathbf{J}}^L \odot [E_{\mathcal{Q}}^L \hat{\mathbf{J}}^L + T_{\mathcal{Q}}^L (\hat{\mathbf{J}}^L \times \hat{\mathbf{J}}^R)] \quad (114)$$

$$= -E_{\text{ex}}^L \hat{\mathbf{J}}^L \odot \hat{\mathbf{J}}^L + [2(\langle S^L \rangle \cdot \hat{\mathbf{J}}^L) T_S^L - T_{\text{ex}}^L] \hat{\mathbf{J}}^L \odot (\hat{\mathbf{J}}^L \times \hat{\mathbf{J}}^R). \quad (115)$$

In this approximation the DOS (13) is not spin-polarized in the bias window: $n^r(\omega) = 0$ for $\mu^L \lesssim \omega \lesssim \mu^R$. Therefore, the charge current Eq. (112) reduces to its nonmagnetic part; i.e., there is no spin-valve effect. By the same token, the dissipative part of the spin current (113) vanishes due to the cancellation of particle and hole contributions. Thus, only the coherent spin torque part remains, whose coefficient we now estimate as follows: Inserting Eq. (99) into Eq. (98), we obtain

$$T_S^L = 2t^2 \text{Re} \int d\omega \int d\omega' \prod_r (\bar{v}^r(\omega) n^r(\omega)) \times \frac{f_+^R(\omega') - f_+^L(\omega)}{\omega - \omega' + i0}. \quad (116)$$

For our DOS approximation, we have $\bar{v}^L(\omega) n^L(\omega) \bar{v}^R(\omega') n^R(\omega') = \text{sgn}(\omega\omega')/(4D)^2$ if $|\omega| - D \leq J/2$ and $|\omega'| - D \leq J/2$ and zero otherwise. At these energies the Fermi functions are 0 or 1 and if their difference in Eq. (116) is nonzero, we can approximate $1/|\omega - \omega'| \approx 1/(2D)$, yielding

$$T_S^L \approx -\frac{\Gamma}{4\pi} \frac{J^2}{D}. \quad (117)$$

where $\Gamma = 2\pi|t|^2/(2D)^2$. The resulting spin current is equivalent to a spin torque exerted by an magnetic field $\mathbf{B}^R \approx \bar{v}^R J|t|^2/D\hat{\mathbf{J}}^R$ on the spin on \mathbf{S}^L [insert Eq. (26) for $|\mathbf{S}^L|$ into Eq. (113)]. Finally, in the SQM current (114) and (115) the absorption coefficient $A_{\mathcal{Q}}^L$ —and with it, the even anisotropy function \tilde{a}^L —drops out in this approximation because of the vanishing of the spin polarization, $n^r(\omega) = 0$, in the bias window.

1. Dissipative SQM flow direction

We first discuss the direction of the dissipative spin-anisotropy emission, $\langle \mathcal{I}_{\mathcal{Q}}^{LL} \rangle = -2E_{\mathcal{Q}}^{LL}\hat{\mathbf{J}}^L \odot \hat{\mathbf{J}}^L$, which entirely arises from the exchange term in Eq. (114) (the direct part vanishes in absence of dissipative spin current). Remarkably, the emission always results in a *loss* of local exchange spin-anisotropy $\langle \mathcal{Q}^{LL} \rangle_{\text{ex}} = -q_{\text{ex}}^{LL}\hat{\mathbf{J}}^L \odot \hat{\mathbf{J}}^L$ irrespective of the voltage bias direction, because $E_{\mathcal{Q}}^L$ is always *negative* (unless zero). By interchanging the left and right electrode indices in all expressions, we observe that the spin anisotropy of the $\langle RR \rangle$ node decreases as well. We conclude from the SQM current conservation law that nonlocal spin-triplet correlations are built up irrespective of the bias direction. This is in accordance with the physical intuition of SQM *transport* that we have developed using our network picture: The tunneling of electrons across the junction delocalizes spin-triplet correlations. However, such a pure delocalization is special to a voltage-biased tunnel junction. When we discuss the situation of thermal bias later, we see that an effective transfer of spin anisotropy between the local nodes is still possible.

These results can also be clearly understood in terms of the microscopic picture of SQM *storage* introduced in Sec. III B5. To see this, we first note that the exchange-SQM emission (100) is obtained from the average [see Eqs. (64) and (65)] by replacing the Fermi function f_{\pm}^L with the bias function Δ . If $\mu^L > \mu^R$, electrons *leave* the left electrode, which is indicated by $\Delta(\omega) > 0$ at energies $\mu^L \lesssim \omega \lesssim \mu^L$. This destroys the positive local exchange-SQM content at this energy [given by $a^L(\omega) > 0$, see also Fig. 7]. Conversely, for the opposite bias $\mu^L < \mu^R$, we find $\Delta(\omega) < 0$ for $\mu^L \lesssim \omega \lesssim \mu^R$ since the tunneling electrons *enter* the left electrode. Electrons at these frequencies provide *negative* exchange SQM [as $a^L(\omega) < 0$]. In both cases, this results in a *negative* change in q_{ex}^L .

2. Scalar parameter dependence

We next discuss the dependence of the direct and exchange-SQM current on the *scalar* parameters J , $V = \mu^L - \mu^R$, and T . For the direct-SQM current,

$$\langle \mathcal{I}_{\mathcal{Q}}^{LL} \rangle_{\text{dir}} = 2(\langle \mathbf{S}^L \rangle \cdot \hat{\mathbf{J}}^L) T_{\mathcal{S}}^L \hat{\mathbf{J}}^L \odot (\hat{\mathbf{J}}^L \times \hat{\mathbf{J}}^R); \quad (118)$$

this is simple because $T_{\mathcal{S}}^L$ is nearly independent of V and T and the magnitude of $\langle \mathcal{I}_{\mathcal{Q}}^{LL} \rangle_{\text{dir}}$ increases as J^3 [use Eqs. (117) and (26)], as shown in Fig. 14.

The exchange-SQM current, in contrast, shows a stronger dependence on the scalar parameters. To see this, we first roughly estimate how its emission and torque coefficients scale with V and J for low temperatures $T \lesssim V, J$. For $T = 0$ the integrand of Eq. (100) is the product of the anisotropy function $a^L(\omega)$, which has a support of width $2J$, and the bias function

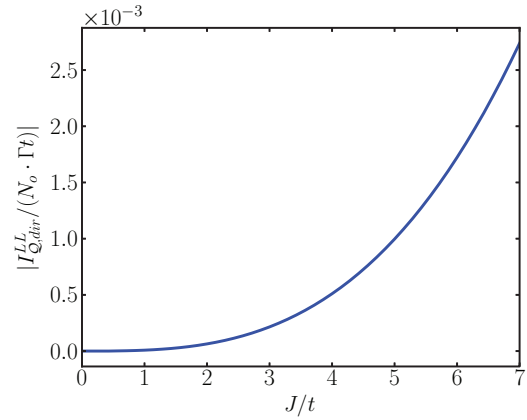


FIG. 14. (Color online) Dependence of $I_{\mathcal{Q},\text{dir}}^{LL} = 2\langle \mathbf{S}^L \rangle \cdot \hat{\mathbf{J}}^L T_{\mathcal{S}}^L$ on the Stoner splitting J/t , where N_o is the fixed number of orbital states of the left subsystem and $J = 5t$, $D = 25t$, $T = t/2$.

$\Delta(\omega)$ with a support of width V , and the smaller one of these energy scales limits the SQM emission,

$$E_{\text{ex}}^L \approx -\frac{\Gamma}{2} \min(|V|, |J|), \quad (119)$$

where $\Gamma = 2\pi|t|^2/(2D)^2$. In contrast, the SQM torque (102) scales in the same way as the spin torque,

$$T_{\text{ex}}^L \approx -\frac{\Gamma J^2}{\pi D}, \quad (120)$$

where we also set $T = 0$ and proceeded analogous to the estimation of the spin torque [cf. Eq. (117)]. The additional suppression factor J/D in Eq. (120) relative to Eq. (119) for $V < J$ reflects that the SQM torque originates from coherent virtual fluctuations to states near the band edges where the spin polarization is nonzero in an energy window proportional to the Stoner splitting J . This gives rise to two regimes, in which the coherent exchange term (120) is larger (smaller) than the dissipative exchange term (119) for $V \lesssim V^*$, where $E_{\text{ex}}^L \sim T_{\text{ex}}^L$ occurs for²⁹

$$V^* = \frac{J^2}{\pi D}. \quad (121)$$

a. Stoner-field dependence. In Fig. 15 we show a numerical calculation of the precise shapes (100) and (102) of the exchange emission coefficient E_{ex}^L and the torque coefficient T_{ex}^L , confirming the estimates (119) and (120): They show that the torque increases quadratically and the emission saturates to a constant on the scale of the bias V [which is smaller than the value predicted by Eq. (119) due to finite temperature].

b. Bias dependence. Figure 16 shows the same crossover, but now as a function of the bias V for fixed J and T . The torque is constant and given approximately by Eq. (120) and the emission saturates at the value set by Eq. (119) when V approaches the scale of J . This voltage dependence allows for magnetic and electric control over the orientation of the exchange-SQM current *tensor*, discussed in the next Sec. V B3. The saturation at $V \sim J$ is an interesting, new feature of the dissipative exchange-SQM current, not present in the charge or spin current. It provides access to the Stoner *shift* of the DOS (cf. Fig. 7), even without spin-polarization of the DOS in the bias window. Similar to the spin current a finite coherent

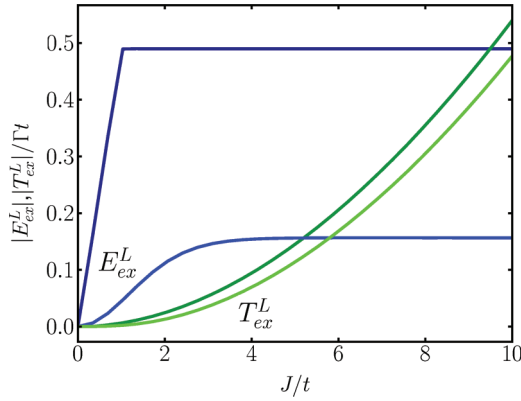


FIG. 15. (Color online) Dependence of the magnitude of SQM emission $|E_{\text{ex}}^L|/\Gamma t$ (blue) and torque $|T_{\text{ex}}^L|/\Gamma t$ (green) on the Stoner splitting J/t for $T = 0$ (dark colors) and $T = 0.5t$ (light colors). The residual parameters are $V = t$, $D = 25t$. For $T = 0$, the crossover occurs at $J \sim J^* = \sqrt{\pi DV} \approx 9t$. The initial nonlinearity of the SQM emission coefficient for the finite temperature (preceded by a linear regime) and the smaller saturation value compared to the $T = 0$ case are due to the thermal smearing.

SQM term remains at zero bias, even though the dissipative SQM current vanishes.

c. Temperature dependence. In Fig. 17 we show the temperature dependence of the exchange-SQM emission and torque coefficients, keeping V and J fixed. Both coefficients decrease monotonously with temperature, but with very different characteristic dependencies on T . The reason is that the emission integral (100) incorporates Fermi functions, which have a much stronger exponential dependence with T^{-1} , whereas torque integral (102) comprises the renormalization function β^R , which depends much more weakly, namely algebraically, on T^{-1} . Moreover, Fig. 17 shows that exchange-

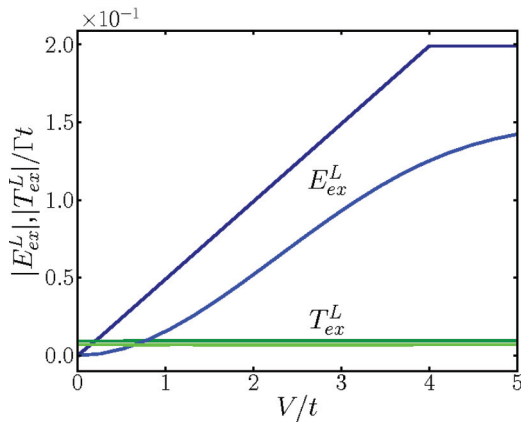


FIG. 16. (Color online) Dependence of the magnitude of SQM emission $|E_{\text{ex}}^L|/\Gamma t$ (blue) and torque $|T_{\text{ex}}^L|/\Gamma t$ (green) on the bias voltage V/t for $T = 0$ (dark colors) and $T = 0.5t$ (light colors). The residual parameters are $J = 5t$, $D = 25t$. For both temperatures, the torque is constant at $|T_{\text{ex}}^L|/\Gamma t \approx 0.15$ according to estimation (120). The small deviation of this value and the saturation level of $|E_{\text{ex}}^L|/\Gamma t$ for finite temperature compared to $T = 0$ is due to the thermal smearing. Therefore, the rough estimate $V^* \approx J^2/\pi D \approx 1/3$ for the crossing point at $E_{\text{ex}}^L = T_{\text{ex}}^L$ is exactly fulfilled only for $T = 0$.

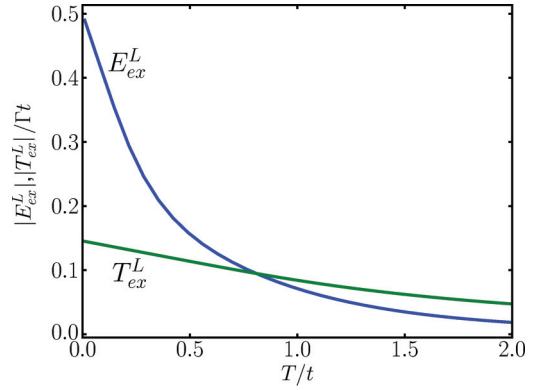


FIG. 17. (Color online) Dependence of the magnitude of exchange SQM emission $|E_{\text{ex}}^L|/\Gamma t$ (blue) and torque $|T_{\text{ex}}^L|/\Gamma t$ (green) on temperature T/t for $V = t$, $J = 5t$, $D = 25t$.

SQM emission is strongly suppressed when T approaches the voltage $V (< J)$ when the bias function $\Delta = f_+^R - f_+^L$ is largely broadened over an energy range of $\sim 4T \sim J$ (for the parameters of Fig. 17), so that positive and negative contributions of the spin-anisotropy function a^L cancel each other. This is similar to the discussion of the exchange-SQM storage in Sec. III B5.

3. Angle dependence

The exchange-SQM current, in contrast to the direct part, has a nontrivial dependence on the angle between the two Stoner vectors $\hat{\mathbf{J}}^L$ and $\hat{\mathbf{J}}^R$ due to the interplay of its dissipative and coherent contributions (see Sec. VB3). This requires a more extensive analysis since we are dealing with a *tensor-valued* current. There are two relevant questions relating to the orientation of the SQM tensors. The first question is whether the orientation of the local SQM $\langle \mathcal{Q}^{LL} \rangle$ is changed by the injected SQM current $\langle \mathcal{I}_{\mathcal{Q}}^{LL} \rangle$. One can show that if these *tensors* commute, $[\langle \mathcal{I}_{\mathcal{Q}}^{LL} \rangle, \langle \mathcal{Q}^{LL} \rangle] = 0$, then the SQM current corresponds only to a change in the principal values of the local SQM *without* changing its principal axes (see Appendix C). Now Eq. (91) shows that for noncollinear $\hat{\mathbf{J}}^L$ and $\hat{\mathbf{J}}^R$ the average SQM current $\langle \mathcal{I}_{\mathcal{Q}}^{LL} \rangle$ is a superposition of three linearly independent, symmetric, and traceless tensors, $\hat{\mathbf{J}}^L \odot \hat{\mathbf{J}}^L$ [emission (100)], $\hat{\mathbf{J}}^L \odot \hat{\mathbf{J}}^R$ [absorption (101)], and $\hat{\mathbf{J}}^L \odot (\hat{\mathbf{J}}^L \times \hat{\mathbf{J}}^R)$ [torque (102)]. The latter two tensors do not commute with $\langle \mathcal{Q}^{LL} \rangle \propto \hat{\mathbf{J}}^L \odot \hat{\mathbf{J}}^L$ for noncollinear $\hat{\mathbf{J}}^L$ and $\hat{\mathbf{J}}^R$ and vanish only for collinear $\hat{\mathbf{J}}^L$ and $\hat{\mathbf{J}}^R$. This holds for both the direct and the exchange contributions. Therefore, the injected average SQM current $\langle \mathcal{I}_{\mathcal{Q}}^{LL} \rangle$ will tend to change the principal axes of the average local SQM $\langle \mathcal{Q}^{LL} \rangle$, besides changing its principal values.

The second question is whether the direct and exchange-SQM currents tend to induce the same rotation of the principal axis of the SQM, which is equivalent to these tensors commuting, $[\langle \mathcal{I}_{\mathcal{Q}}^{LL} \rangle_{\text{dir}}, \langle \mathcal{I}_{\mathcal{Q}}^{LL} \rangle_{\text{ex}}] = 0$. To show that this is not the case, we now first explicitly find the (different) principal axes and values of $\langle \mathcal{I}_{\mathcal{Q}}^{LL} \rangle_{\text{dir}}$ and $\langle \mathcal{I}_{\mathcal{Q}}^{LL} \rangle_{\text{ex}}$. This furthermore allows us to plot and discuss these average SQM currents in a clear way.

a. Principal axes and values. The following analysis holds for any dispersion $\varepsilon_{nk\sigma}^r$. We first diagonalize the full average SQM current tensor Eq. (91) and then show how the direct and

exchange part can be obtained from the result, respectively. Since the former is a real and symmetric tensor it can always be diagonalized:

$$\langle \mathcal{I}_{\mathcal{Q}}^{LL} \rangle = \sum_{\lambda=\pm,0} I_{\lambda} \hat{v}_{\lambda} \hat{v}_{\lambda}. \quad (122)$$

Here the \hat{v}_{λ} denote the orthonormal *principal axes* (the hat indicating normalization) and the I_{λ} denote *principal SQM currents*, which quantify the magnitude of the SQM current. (We dropped the superscripts “LL” on I_{λ} and \hat{v}_{λ} for brevity.) In Appendix B we show that for noncollinear Stoner vectors [$\cos(\theta) = \hat{\mathbf{J}}^L \cdot \hat{\mathbf{J}}^R \neq \pm 1$] the principal SQM currents are

$$I_0 = -\frac{1}{3} D_{\theta}, \quad (123)$$

$$I_{\pm} = \frac{1}{6} D_{\theta} \pm \frac{1}{2} S_{\theta}, \quad (124)$$

which add up to 0 as they should (traceless tensor). The unnormalized principal axes read

$$\mathbf{v}_0 = \hat{\mathbf{J}}^L \times (A_{\mathcal{Q}}^L \hat{\mathbf{J}}^R + T_{\mathcal{Q}}^L \hat{\mathbf{J}}^L \times \hat{\mathbf{J}}^R), \quad (125)$$

$$\mathbf{v}_{\pm} = (D_{\theta} \pm S_{\theta}) \hat{\mathbf{J}}^L + A_{\mathcal{Q}}^L \hat{\mathbf{J}}^R + T_{\mathcal{Q}}^L \hat{\mathbf{J}}^L \times \hat{\mathbf{J}}^R. \quad (126)$$

In Eqs. (123)–(126), we used the abbreviations

$$D_{\theta} := (E_{\mathcal{Q}}^L + A_{\mathcal{Q}}^L \cos \theta), \quad (127)$$

$$S_{\theta} := \sqrt{D_{\theta}^2 + [(T_{\mathcal{Q}}^L)^2 + (A_{\mathcal{Q}}^L)^2] \sin^2 \theta}. \quad (128)$$

The principal SQM currents obey the inequalities

$$I_- \leq I_0 \leq I_+, \quad (129)$$

since $S_{\theta} \geq D_{\theta}$. For collinear Stoner vectors ($\theta = 0, \pi$), two principal values are degenerate,

$$I_+ = \left(\frac{p}{6} + \frac{1}{2} \right) |E_{\mathcal{Q}}^L + A_{\mathcal{Q}}^L|, \quad (130)$$

$$I_- = \left(\frac{p}{6} - \frac{1}{2} \right) |E_{\mathcal{Q}}^L + A_{\mathcal{Q}}^L|, \quad (131)$$

$$I_0 = \frac{p}{3} |E_{\mathcal{Q}}^L + A_{\mathcal{Q}}^L|, \quad (132)$$

with $p = \text{sgn}(D_0)$, $\hat{v}_+ = \hat{\mathbf{J}}^L$, and any two vectors in the plane perpendicular to $\hat{\mathbf{J}}^L$ are principal axes of the SQM current. We thus see that, in general, the principal SQM currents take three different values; i.e., a *biaxial spin anisotropy* is transported whenever the Stoner vectors are noncollinear. We emphasize that *by itself* the average spin-current *vector* provides no information about the noncollinearity of the spin valve. The SQM current tensor, in contrast, does: The transported anisotropy only becomes uniaxial for collinear Stoner vectors ($\theta = 0, \pi$), in which case $\hat{\mathbf{J}}^L$ is the hard axis.³⁰ The possibility of injecting biaxial anisotropy into molecular-scale systems is of interest since this type of anisotropy it is associated with interesting quantum-spin tunneling effects.³¹

We obtain the diagonal form of the direct and exchange SQM individually by replacing the coefficients Eqs. (109)–(111) in the above formulas by $E_{\mathcal{Q}}^L \rightarrow E_{\text{dir}}^L = (\mathbf{S}^L \cdot \hat{\mathbf{J}}^L) E_S^L$ and $E_{\mathcal{Q}}^L \rightarrow -E_{\text{ex}}^L$, respectively, etc. Since these two sets of coefficients are, in general, different functions of the various parameters, we conclude that the direct and exchange-SQM tensors have different principal axes and do not commute,

$[\langle \mathcal{I}_{\mathcal{Q}}^{LL} \rangle_{\text{dir}}, \langle \mathcal{I}_{\mathcal{Q}}^{LL} \rangle_{\text{ex}}] \neq 0$. They therefore tend to induce the different rotations of the principal axis of the local SQM. As a result the total principal SQM currents are *not* the sum of the direct and exchange principal SQM currents.

b. Flat-band approximation. So far the considerations were general. We now investigate the magnetic tuning of the exchange-SQM orientation by the Stoner vectors. For the flat-band approximation, Eq. (112)–(114), the principal SQM currents and the principal axes are symmetric with respect to $\theta = \pi/2$, i.e.,

$$I_{\lambda} \left(\frac{\pi}{2} - \alpha \right) = I_{\lambda} \left(\frac{\pi}{2} + \alpha \right), \quad (133)$$

$$\hat{v}_{\lambda} \left(\frac{\pi}{2} - \alpha \right) = \hat{v}_{\lambda} \left(\frac{\pi}{2} + \alpha \right). \quad (134)$$

This is due to the vanishing SQM absorption coefficient, $A_{\mathcal{Q}}^L$, in this limit. In Fig. 18 we plot both the direct and the exchange principal SQM currents as a function of the angle $\theta \in [0, \pi/2]$. We observe that both I_0^{dir} and I_0^{ex} are constant. In both cases, the repulsion of both $I_{\pm}^{\text{dir/ex}}$ is caused by the respective torque coefficient [see Eq. (127)], which increases with J and decreases with D [cf. Eq. (117)–(120)].

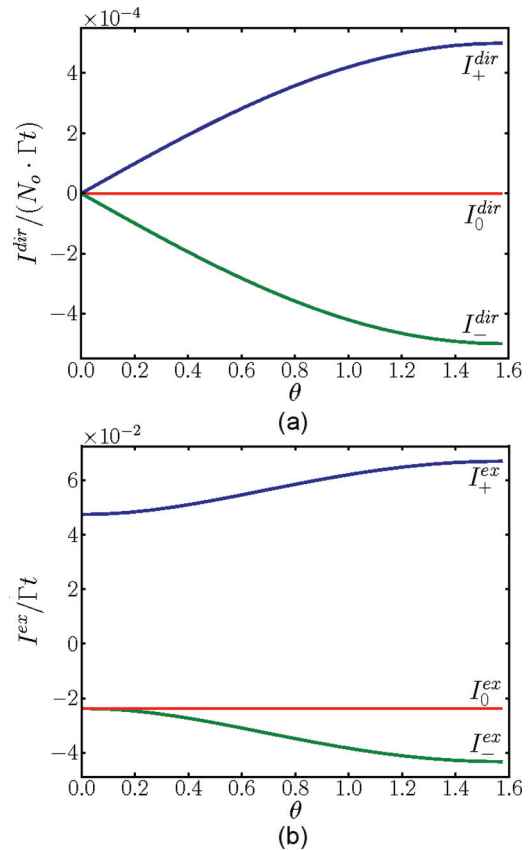


FIG. 18. (Color online) Angle dependence of the principal SQM currents (a) $I_{\lambda}^{\text{dir}} / (t \cdot N_s)$ and (b) $I_{\lambda}^{\text{ex}} / t$ (red, I_0 ; green, I_- ; blue, I_+). The principal direct-SQM currents depend only on the nonzero spin torque $I_{\lambda}^{\text{dir}} = \lambda 2 |\mathbf{S}^L| |T_S^L \sin \theta|$ ($\lambda = 0, \pm$), whence the principal exchange-SQM currents depend both the nonzero exchange-SQM emission and torque. Parameters: $J = 5T$, $D = 25t$, $V = T = t$, $\Gamma = 2\pi/2500$. Note that the inequalities Eq. (129) and $\sum_{\lambda} I_{\lambda}^{\text{dir}} = \sum_{\lambda} I_{\lambda}^{\text{ex}} = 0$ are fulfilled.

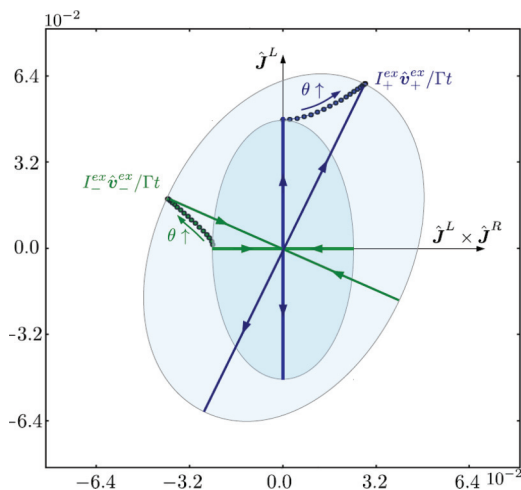


FIG. 19. (Color online) Angle dependence of the exchange-SQM tensor $\langle \mathcal{I}_{\mathcal{Q}}^{LL} \rangle_{\text{ex}}$. Each point corresponds to a principal vector $I_{\pm}^{\text{ex}} \hat{v}_{\pm}^{\text{ex}}/t$ (blue) and $I_{\pm}^{\text{ex}} \hat{v}_{\pm}^{\text{ex}}/t$ (green) of $\langle \mathcal{I}_{\mathcal{Q}}^{LL} \rangle_{\text{ex}}$ for increasing angle θ in steps of $\pi/36$ from 0 to $\pi/2$. Each pair of vectors $I_{\pm}^{\text{ex}} \hat{v}_{\pm}^{\text{ex}}/t$ for one angle defines the semi-axes of an ellipse, drawn for the extremal values $\theta = 0$ and $\theta = \pi/2$. The axes of this ellipse indicate the principal axes of $\langle \mathcal{I}_{\mathcal{Q}}^{LL} \rangle_{\text{ex}}$ and the diameter $2|I_{\pm}/t|$ gives the principal SQM currents. The arrows of the semi-axes indicate the sign of the principal SQM current: It is positive (negative) if the arrow points away from (towards) the origin. The full tensor can be visualized by including the principal vector $I_0^{\text{ex}} \hat{v}_0^{\text{ex}}/t \propto \mathbf{e}_y$ (pointing into the plane), completing the ellipse to an ellipsoid. $\hat{\mathbf{J}}^R$ is rotated from $\hat{\mathbf{J}}^L$ ($\theta = 0$) out of the plane when θ increases. The residual parameters are $D = 25T$, $J = 5T$, $V = T = t$, $\Gamma = 2\pi/2500$.

To analyze the angle dependence of the principal axes $\hat{\mathbf{v}}_{\lambda}$, we construct a right-handed coordinate system from the noncollinear, nonorthogonal Stoner vectors: Let $\mathbf{e}_z = \hat{\mathbf{J}}^L$, $\mathbf{e}_x = \hat{\mathbf{J}}^L \times \hat{\mathbf{J}}^R / \sin \theta$, $\mathbf{e}_y = \mathbf{e}_z \times \mathbf{e}_x$. In Fig. 19 we show the trajectories of the exchange principal axes as we rotate $\hat{\mathbf{J}}^R = -\sin \theta \mathbf{e}_y + \cos \theta \mathbf{e}_z$ through $\theta \in [0, \pi/2]$. Then both $\hat{\mathbf{v}}_0^{\text{dir}} = \hat{\mathbf{v}}_0^{\text{ex}} = \mathbf{e}_y$ are a fixed directions in this coordinate system, i.e., independent of the angle θ . The other principal axes $\hat{\mathbf{v}}_{\pm}^{\text{dir/ex}}$ lie in the xz plane perpendicular to $\hat{\mathbf{v}}_0^{\text{dir/ex}}$ and are different for the direct and exchange contribution.

The direct SQM current consists only of a torque contribution and therefore its principal axes are independent of θ in the above coordinate system fixed by $\hat{\mathbf{J}}^L$ and $\hat{\mathbf{J}}^R$. With $A_{\text{dir}}^L = E_{\text{dir}}^L = 0$ and $T_{\text{dir}}^L = 2(\mathbf{S}^L \cdot \hat{\mathbf{J}}^L)T_S^L$, Eqs. (125) and (126) give $\hat{\mathbf{v}}_{\pm}^{\text{dir}} = (\pm \mathbf{e}_z - \mathbf{e}_x)/\sqrt{2}$ for $\theta \neq 0, \pi$ (when the direct SQM current is nonzero). In contrast, the exchange-SQM current shows a nontrivial competition of the torque and emission contributions: In Fig. 19 we plot the trajectories of its principal axes in the plane perpendicular to $\hat{\mathbf{v}}_0^{\text{ex}} = \mathbf{e}_y$ as θ is increased to from 0 to $\pi/2$.

We emphasize that already in this simple model of flat-band ferromagnets the spin-anisotropy flow has nontrivial tensorial structure: In general, the principal axes of the exchange-SQM tensor are neither collinear to $\hat{\mathbf{J}}^L$, $\hat{\mathbf{J}}^R$ nor collinear to $\hat{\mathbf{J}}^L \times \hat{\mathbf{J}}^R$. Only for nearly collinear configurations ($\theta \approx 0, \pi$), when the torque contribution is negligible, do we have such a simple result: $\hat{\mathbf{v}}_{+}^{\text{ex}} \approx \mathbf{e}_x = \hat{\mathbf{J}}^L$ and $\hat{\mathbf{v}}_{-}^{\text{ex}} \approx \mathbf{e}_z = \hat{\mathbf{J}}^L \times \hat{\mathbf{J}}^R / \sin(\theta)$.

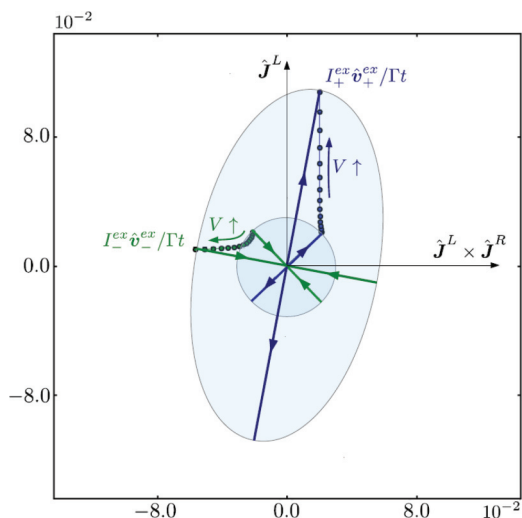


FIG. 20. (Color online) Voltage dependence of the exchange-SQM tensor. For an explanation see Fig. 19, where each point corresponds to a different voltage V/t , increasing in steps of $1/10$ from 0 to 1.5. The remaining parameters are $\theta = \pi/4$, $D = 25T$, $J^L = J^R = 5t$, $T = t$, $\Gamma = 2\pi/2500$.

A further striking property of the exchange principal axes is that they cannot only be tuned magnetically by the Stoner vectors but also to a large extent *electrically* (see Fig. 20). As discussed in Sec. VB2 there is a crossover, shown in Fig. 16, from a torque-dominated (low bias) to an emission-dominated exchange SQM (large bias). As a result, increasing the voltage results in a change of the principal axes of the SQM current, an effect that is comparable to that resulting from tuning the angle θ between the magnetizations in Fig. 19.

The voltage scale at which the direct and exchange-SQM current compete, i.e., $|E_{\text{ex}}^L| \sim |T_{\text{dir}}^L| = 2|\mathbf{S}^L|T_S^L$, can be estimated³² using $|\mathbf{S}^L| \sim JN_o/D \sim N_s$ [cf. Eq. (27)] to

$$V \sim (J^2/D)N_s. \quad (135)$$

Since by Eq. (119) E_{ex}^L has a voltage dependence only for $V \lesssim J$, the electric tunability is feasible only when the crossover scale (135) $\lesssim J$: This is the case when the number of polarized spin $N_s \lesssim D/J$; i.e., the number of orbitals is limited to $N_o \lesssim (D/J)^2$, which can still be a fairly large number. This is a first indication that for mesoscopic ferromagnets this electrical tunability of the SQM orientation may be possible and may be an interesting topic for future analysis. We emphasize the crudeness of our model here and the importance of investigating charging and nonequilibrium effects; see Ref. 22.

C. Transport of spin anisotropy without spin current

Finally, we explore the possibility of a *pure spin-anisotropy current*, i.e., a nonvanishing SQM current in the absence of a spin current, which was anticipated in Sec. VA3.

1. Conditions for zero charge current and spin current

We first discuss the conditions for a vanishing spin current for a general band structure $\varepsilon_{nk\sigma}^r$. We expect zero spin current only for *collinear* magnetizations. If the magnetizations are noncollinear, the spin current has three noncollinear

contributions [cf. Eq. (90)] and demanding that all these vanish requires $E_S^L = A_S^L = T_S^L = 0$. This might be possible, but only for special band structures and parameter values (T^r, μ^r), but this is beyond the scope of this paper. For collinear magnetizations, the spin torque automatically vanishes and the spin current reads $\langle \mathbf{I}_S \rangle = \int d\omega \Gamma \Delta(n^L \hat{\mathbf{J}}^L + n^R \hat{\mathbf{J}}^R)$ with $\hat{\mathbf{J}}^L \parallel \hat{\mathbf{J}}^R$. A generic situation with canceling spin current is then given for antiparallel magnetized ($\hat{\mathbf{J}}^L = -\hat{\mathbf{J}}^R$) ferromagnets with identical spin polarization of the 1DOS in the bias window, that is, $n^L(\omega) = n^R(\omega)$, so that the bracket in the above integrand is zero. This defines a parameter *regime* for which $\langle \mathbf{I}_S \rangle = 0$, as one may still apply any voltage or temperature bias. Again, there might be exotic material combinations, for which the spin current even vanishes for $\hat{\mathbf{J}}^L = +\hat{\mathbf{J}}^R$. For our crude flat-band approximation (cf. Sec. II D), the dissipative spin current is zero in any case, so that collinearity $\hat{\mathbf{J}} = \hat{\mathbf{J}}^L = \pm \hat{\mathbf{J}}^R$ of the Stoner vectors is already sufficient for canceling spin current.

We can even go one step further and envisage a situation for which the charge current vanishes as well: Note that it still has a nonmagnetic contribution (93) $\propto \int d\omega \Delta$ (Γ is constant in the bias window and we consider $T^r \ll D$). For pure voltage bias $\mu^L \neq \mu^R$, but $T^L = T^R$, the bias function $\Delta(\omega)$ is symmetric and positive and we will always have a charge current. However, for a pure *temperature* bias, $T^L \neq T^R$ and $\mu^L = \mu^R$, the bias function $\Delta = f_+^R - f_+^L$ is *antisymmetric* and the charge current contributions above and below the common electrochemical potential cancel. For example, if $T^R < T^L$ the left “hot” electrode has a larger (smaller) occupation probability for electrons with energy $\omega > \mu$ ($\omega < \mu$) than the right cold electrode. Consequently, the particle current flowing from left to right for electrons with energy $\omega > \mu$ exactly cancels the charge current for electrons flowing from the right to the left at energies $\omega < \mu$. Integrated over all frequencies this gives the zero net-charge current.

2. Pure quadrupole current

Strikingly, in contrast to charge current and spin current, the SQM current remains *nonzero* for a pure thermal bias. It comes entirely from the exchange emission part:

$$\langle \mathcal{I}_{\mathcal{Q}}^{LL} \rangle = -2\Gamma \int d\omega \Delta a^L \hat{\mathbf{J}} \odot \hat{\mathbf{J}} \neq 0, \quad (136)$$

where Γ can be pulled out of the integral since the DOS is constant at energies ω for which $a^L(\omega) \neq 0$. Since the spin-anisotropy function $a^L(\omega)$, Eq. (66), is antisymmetric as well with respect to the common electrochemical potential μ , we integrate an overall symmetric function and $\langle \mathcal{I}_{\mathcal{Q}}^{LL} \rangle$ is nonzero. This is a central result of the paper. In Fig. 21 we plot the total SQM current for a thermal bias with collinear Stoner vectors as function of the temperature difference, as given by Eq. (136). In Fig. 22 we plot the dependence on the Stoner field J^L .

The linear response³³ in the temperature bias ratio $\tau^R = (T^R - T^L)/T^R \ll 1$ varied for fixed T^L gives for the SQM current magnitude, defined here by $\langle \mathcal{I}_{\mathcal{Q}}^{LL} \rangle = -I_{\mathcal{Q}}^{LL} \hat{\mathbf{J}} \odot \hat{\mathbf{J}}$,

$$I_{\mathcal{Q}}^{LL} = \frac{\Gamma}{2} (T^L - T^R) \times \frac{T^L}{T^R} \left[1 - \left(\frac{J^L/2T^L}{\sinh(J^L/2T^L)} \right)^2 \right]. \quad (137)$$

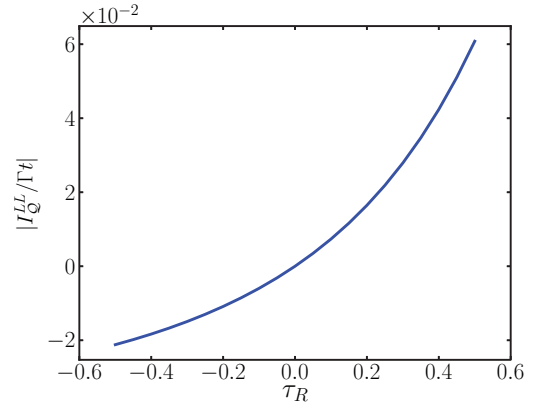


FIG. 21. (Color online) $|I_{\mathcal{Q}}^{LL}|/t$ [from Eq. (136)] with $\langle \mathcal{I}_{\mathcal{Q}}^{LL} \rangle = -I_{\mathcal{Q}}^{LL} \hat{\mathbf{J}} \odot \hat{\mathbf{J}}$ as a function of the temperature bias ratio $\tau^R = (T^R - T^L)/T^R$ for $T^L = t$, $J = 5t$, $D = 25t$, and $\Gamma = 2\pi/2500$.

For fixed different temperatures, the magnitude of the SQM current increases monotonously as a function of the Stoner splitting as shown in Fig. 22. It eventually saturates for $J^L \approx 10T^L$ at the asymptotic value of $I_{\mathcal{Q}}^{LL} \approx (\Gamma/2)\tau^R T^L$.

A crude understanding of the above results is the following. Since the magnitude of the local exchange SQM decreases with temperature [Pauli exclusion effects get washed out thermally; cf. Fig. 9 and Eq. (70)], the thermal gradient induces a “gradient in the correlations,” resulting in the SQM flow of Pauli exclusion holes from the colder to the hotter reservoir, roughly speaking.

We emphasize, however, that this should not be interpreted as a direct transfer of spin correlations between the two local SQM nodes since they first have to be converted into nonlocal spin correlations: In the language of our network picture, these are first buffered in the nonlocal intermediate node. This becomes clearer in view of the SQM conservation law (88), which reads of our device (cf. Fig. 12) after averaging $\langle \mathcal{I}_{\mathcal{Q}}^{LR} \rangle = -\langle \mathcal{I}_{\mathcal{Q}}^{LL} \rangle - \langle \mathcal{I}_{\mathcal{Q}}^{RR} \rangle$. Interchanging the role of the left and right electrode in Eq. (137), we see that the change in the

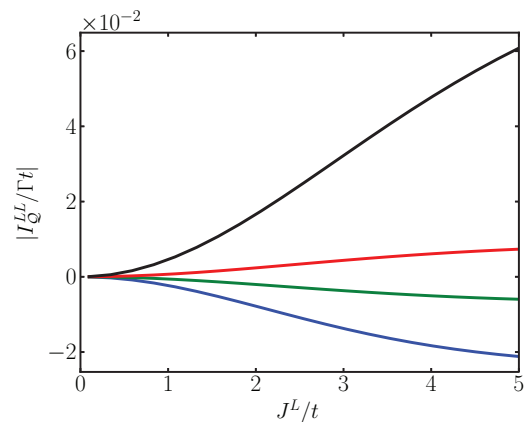


FIG. 22. (Color online) Same as Fig. 21, but now showing $|I_{\mathcal{Q}}^{LL}|/t$ as a function of Stoner splitting J^L/t for fixed thermal bias $\tau^R = (T^R - T^L)/T^R = -0.5, -0.1, 0.1, 0.5$ (from topmost to bottommost curve). The antisymmetry of the linear result Eq. (137), $I_{\mathcal{Q}}^{LL}(\tau_R) \approx I_{\mathcal{Q}}^{LL}(-\tau_R)$, breaks down in the nonlinear regime, as shown in Fig. 22 for $\tau_R = \pm 0.5$.

local spin anisotropy of the $\langle LL \rangle$ and $\langle RR \rangle$ node have opposite sign. Taking only the $O(\Delta T)$ contribution, we may replace T^L and T^R , respectively, by the average temperature in the second line of Eq. (137): We then find that there is no *net* creation of nonlocal spin correlations only to first order in the thermal bias ΔT , i.e., $\langle \mathcal{I}_{\mathcal{Q}}^{LR} \rangle = O(\Delta T^2)$.

A more rigorous explanation of the thermally driven SQM current is based on a microscopic point of view (cf. Secs. III B4 and III B5). These considerations may be useful for proposals for more complicated device setups that would allow for the detection a pure SQM current (an issue that is not covered here). The exchange SQM in Eq. (136) is quantified by the anisotropy function $a^L(\omega)$ [cf. Eq. (66) and Fig. 7], which describes the Pauli exclusion hole to which an electron at energy ω contributes. The microscopic reason why $a^L(\omega)$ changes sign was explained in detail in Sec. III B5: Basically, for $\omega < \mu$ ($\omega > \mu$) a given electron at energy ω most likely sees a parallel (antiparallel) spin at energy $\omega + J$ ($\omega - J$). Electrons with opposite energies relative to μ thus contribute with an opposite sign to the Pauli exclusion hole. Since the thermal bias transports electrons above and below the Fermi edge into opposite directions, the contributions to the local average SQM $\langle \mathcal{Q}^{LL} \rangle$ thus *add up*, explaining why Eq. (136) is finite. Notably, the thermal bias drives this flow of spin correlations between the ferromagnets without any other one-particle quantity being net transported. For example, the charge of each electron is independent of its energy and, therefore, the contributions above and below the Fermi energy cancel.

Importantly, in this case the direction of the spin-anisotropy flow can be *controlled* by the sign of the temperature gradient: For $T^L < T^R$, the SQM current magnitude $I_{\mathcal{Q}}^{LL}$ is negative; i.e., local planar spin-triplet correlations are net delocalized by the tunneling. The left local node therefore *loses* Pauli exclusion holes. This can be understood following arguments similar to that of the purely voltage-biased tunnel junction (see Sec. V B1). However, in stark contrast to pure voltage bias, the current magnitude $I_{\mathcal{Q}}^{LL}$ becomes positive if $T^R < T^L$. This physically means that net local planar spin correlations are *created* by tunneling. The reason is that electrons are injected into the left electrode *below* the Fermi energy. As these electrons obey Pauli's principle, they are *forced* to form new Pauli-exclusion holes. Furthermore, the electrons are extracted only *above* the Fermi energy and they carry away positive (axial) spin correlations (leaving a negative contribution behind). For the contrasting situation of a pure voltage bias, the energy-resolved flow direction has to be opposite: Electrons are only net injected (extracted) at energies larger (lower) than the Fermi energy.

As a conclusion, the possibility to control the spin-anisotropy flow direction by the thermal bias applied to the tunnel junction is a nontrivial result of this paper. This fact and the prediction of a pure SQM current demonstrate most clearly that triplet-spin correlations form an independent degree of freedom, which is not only stored in a system of ferromagnets, but can also be transported between them.

VI. SUMMARY AND OUTLOOK

In this paper we investigated fundamental questions about the spin anisotropy, as quantified by the SQM, which arise

when it is *considered as a transport quantity*. In the physical language of atomic and molecular magnetism, the SQM characterizes the quadratic spin anisotropy, which is usually its dominant part. It quantifies the preference of spins to be *aligned* along a specific *axis* irrespective of their *orientation* along it (up, down). We addressed three central questions related to the quantum *transport* of spin-anisotropy: (i) How can SQM be stored in and (ii) transported between two ferromagnets in a spintronic circuit and (iii) how can one define an *SQM current tensor operator* and derive SQM continuity equations and SQM-current conservation laws; how does the nonequilibrium steady-state average of the SQM current relate to the spin current?

Our work was motivated by studies^{14–16} that indicated that the physical picture of the transport of *spin degrees of freedom* through magnetic nanostructures needs to be extended. A refinement of this picture, resulting from this paper, is as follows. Electrons are charged particles with an intrinsic spin-dipole moment and vanishing higher spin moments. Therefore, the motion of an *isolated* electron is associated with a charge and spin currents only. However, in a multielectron system the electron becomes correlated with other electrons. Moving this electron therefore implies a change of correlations. In particular, the transfer of spin-triplet correlations between different subsystems is quantified by the spin-quadrupole current. This complements the results of prior studies,^{14–16} which demonstrated that these tensor-valued currents lead to an accumulation of SQM. The latter couples to the accumulation of spin and charge and their measurable currents. In this paper we ignored the complications of this accumulation, as well as interaction and nonequilibrium effects that appear in nanoscale spintronic devices. We exclusively focused on the description of transport of SQM between macro- and mesoscopic circuit elements.

Answering question (i), we found that macroscopic ferromagnets, the basic elements of spintronic devices, store a macroscopic SQM, which is generated by their internal Stoner field. This *direct* spin anisotropy is of easy-axis type and scales *quadratically* with the number of half-filled, spin-polarized orbitals N_s . This follows the classical intuition that orientation of spins also implies their alignment. However, for mesoscopic systems, an additional *quantum exchange* contribution to the SQM becomes relevant,¹⁶ which scales linearly with N_s . It quantifies the effect of Pauli-exclusion holes that exist in the triplet *two-particle* spin correlations, expressing the simple fact that electrons in the same orbital do not form a triplet spin state. This Pauli-forbidden spin anisotropy is of the easy-plane type, countering therefore the direct easy-axis anisotropy.

Importantly, the effect of the Pauli exclusion holes is cumulative; i.e., their contributions always add up and cannot cancel each other. This is in stark contrast to the average spin-dipole moment, for which contributions from electrons with opposite spin orientation can cancel each other. This shows that the average SQM is a degree of freedom *independent* of one-particle quantities such as average charge and spin.

To answer question (ii) we developed a spin-multipole transport theory with an associated network picture. For spin-dipole moment, each ferromagnet is represented by a

node of the network storing spin-dipole moment. However, due to its two-particle nature in electronic systems, SQM is also stored as nonlocal correlations between spins from different spin-polarized subsystems. The network picture of SQM therefore incorporates also *nonlocal SQM nodes*. As a consequence, the SQM network differs from the physical layout of the system of ferromagnets, both in the number of nodes and in their connectivity. For the *two-terminal* spin valve that we studied in this paper, this network thus consists of *three* SQM nodes. This network theory applies also to spin valves with embedded quantum dots.²²

Based on this microscopic picture, we inferred the proper definition of the *spin-quadrupole current tensor operators*, answering question (iii). By a continuity equation, the SQM currents generate the change of the local anisotropy due to quantum transport processes. They furthermore obey a current conservation law expressing the conservation of SQM in the tunneling. For the two-terminal spin valve it reads $\mathcal{I}_Q^{LL} + \mathcal{I}_Q^{RR} + \mathcal{I}_Q^{LR} = 0$.

Finally, we found by explicit calculation that the nonequilibrium steady-state average of *all* these SQM currents is nonzero, even for this elementary spintronic setup, and analyzed these in detail. Similar to the average SQM, these average SQM currents have a decomposition into classical and quantum *two-particle* contributions, similar to the average SQM itself. The *direct-SQM current* is implied by a nonzero average spin and *spin current*. It reflects the classical intuition that “orientation implies alignment.” In addition to this, we found a quantum *exchange-SQM current*, which is profoundly different from spin currents.

In analogy to the spin, we also distinguished dissipative and coherent contributions to the SQM: The spin precession responsible for the spin-torque term in the spin current—lifting the spin out of the plane of the Stoner vectors—has a counterpart in the SQM current. These spin-torque SQM terms similarly result from coherent fluctuations by virtual tunneling into a ferromagnet (i.e., spin-dependent scattering) which probe the spin dependence of the entire band structure. This effect is also responsible for the exchange field³⁴ in quantum dot spin valves. The different bias-voltage dependence of the dissipative and coherent terms allows for electric control of both the magnitude and the *orientation* of the spin-anisotropy current *tensor*.

Furthermore, for noncollinear ferromagnets, the spin-anisotropy current was found to be a *biaxial* tensor. Its three distinct principal values and axes reflect the lowered symmetry of a noncollinear setup, which is not revealed by the spin current, which is just a *vector*. We showed that this dependence on the Stoner vectors allows for substantial magnetic tuning of the SQM current tensor orientation. The possibility of *injecting biaxial anisotropy* into, e.g., molecular magnets is of interest since the intrinsic, spin-orbit generated anisotropy of this type is associated with quantum-spin tunneling effects.³¹

The striking central result of this paper, as announced by its title, is a pure SQM current whenever the spin current vanishes by net cancellation of one-particle contributions. This spin-anisotropy flow is driven by a gradient of Pauli exclusion holes in the triplet spin-spin correlations, that is, a true quantum two-particle current. We illustrated this

general result for a temperature-biased junction connecting two antiparallel ferromagnets with a flat-band DOS. In this case, a pure SQM current generates a *uniaxial, easy plane* anisotropy, i.e., a negative anisotropy that counteracts an easy axis anisotropy. It may be of interest to inject such a SQM current into a single-molecule magnet considered as a memory cell in order to temporarily switch off its easy-axis anisotropy barrier in order to put it into “writing” mode. This also relates to the recently studied tunnel-induced renormalization of the intrinsic anisotropy of molecular magnets in contact with spin-polarized electrodes.^{16,35,36} One may even envisage the utilization of SQM as a resource, as an alternative to conventional spintronics, i.e., utilize the storage, transport, manipulation, and readout of spin anisotropy without transporting or affecting spin polarization. The possibility of pure SQM currents pointed out in this paper indicates that this is, in principle, conceivable and warrants further study. Altogether, the above indicates that the theory of a generalized “spin-multipoletronics,” is a real possibility, if not a necessity when spintronics moves to the nanoscale.

ACKNOWLEDGMENTS

We acknowledge G. E. W. Bauer, M. Büttiker, D. P. DiVincenzo, J. König, P. Mavropoulos, M. Misiorny, R. Saptsov, and J. Splettstösser for useful discussions.

APPENDIX A: STORAGE OF SPIN-QUADRUPOLE MOMENT

In this appendix we give the calculation of the local average SQM stored in a ferromagnet; cf. Sec. III B3. We present three derivations, each of which unveils different physical and technical aspects used in the main part. The first, most straightforward approach is given in Appendix A 1. It shows how the Pauli exclusion hole arises in Eq. (A6), which provides the key to the physical interpretation of exchange SQM. Second, we give a technically more sophisticated derivation in Appendix A 2, which will be helpful to understand all steps of our transport calculations. It expresses the Pauli exclusion hole in a coordinate-free form in Eq. (A17). Third, we present in Appendix A 3 a derivation that makes explicit the spin-triplet content of the correlations by vector coupling of the spins of electron pairs. Finally, we discuss the spin-anisotropy function and derive a closed expression for the exchange SQM in the flat-band approximation (cf. Sec. II D). Throughout the appendix we focus on understanding the exchange contributions to the SQM, which we showed in the absence of tunneling to appear only locally for ($r = r'$); cf. Sec. III B3. We therefore only consider one electrode r with one band n and subsequently drop these indices in all expressions below, e.g., $c_{rnk\sigma} \rightarrow c_{k\sigma}$, when convenient.

1. Exchange SQM and the Pauli principle

We furthermore take a coordinate system for which $\mathbf{e}_z = \hat{\mathbf{J}}$ and quantize the spin along this vector. The calculation of the average local SQM starts from the operator Eq. (53) in the main text. We insert the second-quantized form (40) of the spin operator and anticommute $c_{k_1\sigma_1}^\dagger$ twice to the

left:

$$\mathcal{Q} = \sum_{\{k_i, \sigma'_i, \sigma_i\}} \mathbf{s}_{\sigma'_2, \sigma_2} \odot \mathbf{s}_{\sigma'_1, \sigma_1} c_{k_2, \sigma'_2}^\dagger c_{k_2, \sigma_2}^\dagger c_{k_1, \sigma'_1} c_{k_1, \sigma_1} \quad (\text{A1})$$

$$= \sum_{\{k_i, \sigma'_i, \sigma_i\}} \mathbf{s}_{\sigma'_2, \sigma_2} \odot \mathbf{s}_{\sigma'_1, \sigma_1} c_{k_1, \sigma'_1}^\dagger c_{k_2, \sigma'_2}^\dagger c_{k_2, \sigma_2} c_{k_1, \sigma_1}. \quad (\text{A2})$$

This generates a term $\delta_{k_2 k_1} \delta_{\sigma_2 \sigma'_1} c_{k_2, \sigma'_1}^\dagger c_{k_1, \sigma_1}$, which we omitted because it vanishes after performing the sum over the spin indices by virtue of $\mathbf{s} \odot \mathbf{s} = 0$: for all σ'_2, σ_1

$$\sum_{\sigma_2, \sigma'_1} \mathbf{s}_{\sigma'_2, \sigma_2} \odot \mathbf{s}_{\sigma'_1, \sigma_1} \delta_{\sigma_2 \sigma'_1} = \langle \sigma'_2 | \mathbf{s} \odot \mathbf{s} | \sigma_1 \rangle = 0. \quad (\text{A3})$$

Computing the average of Eq. (A2) using Wick's theorem $\langle c_{k', \sigma'}^\dagger c_{k, \sigma} \rangle = \delta_{k'k} \delta_{\sigma\sigma'} f_+(\varepsilon_{k\sigma})$ in the standard way with $f_+(\omega)$ denoting the Fermi function,

$$\langle c_{k_1, \sigma'_1}^\dagger c_{k_2, \sigma'_2}^\dagger c_{k_2, \sigma_2} c_{k_1, \sigma_1} \rangle = \langle c_{k_1, \sigma'_1}^\dagger c_{k_1, \sigma_1} \rangle \langle c_{k_2, \sigma'_2}^\dagger c_{k_2, \sigma_2} \rangle - \langle c_{k_1, \sigma'_1}^\dagger c_{k_2, \sigma_2} \rangle \langle c_{k_2, \sigma'_2}^\dagger c_{k_1, \sigma_1} \rangle, \quad (\text{A4})$$

yields a direct part and an exchange part:

$$\langle \mathcal{Q} \rangle = \sum_{k_2, k_1, \sigma_2, \sigma_1} f_+(\varepsilon_{k_2, \sigma_2}) f_+(\varepsilon_{k_1, \sigma_1}) \times (\mathbf{s}_{\sigma_1, \sigma_2} \odot \mathbf{s}_{\sigma_2, \sigma_1} - \delta_{k_2 k_1} \mathbf{s}_{\sigma_2, \sigma_2} \odot \mathbf{s}_{\sigma_1, \sigma_1}) \quad (\text{A5})$$

$$= \frac{1}{4} \sum_{k_2, k_1} (1 - \delta_{k_2 k_1}) \times \sum_{\sigma_2, \sigma_1} \sigma_1 \sigma_2 f_+(\varepsilon_{k_2, \sigma_2}) f_+(\varepsilon_{k_1, \sigma_1}) \mathbf{e}_z \odot \mathbf{e}_z. \quad (\text{A6})$$

Here we used the result

$$\mathbf{s}_{\sigma_1, \sigma_1} \odot \mathbf{s}_{\sigma_2, \sigma_2} = \mathbf{s}_{\sigma_1, \sigma_2} \odot \mathbf{s}_{\sigma_2, \sigma_1} = \frac{\sigma_1 \sigma_2}{4} \mathbf{e}_z \odot \mathbf{e}_z. \quad (\text{A7})$$

Clearly, $\mathbf{s}_{\sigma_1, \sigma_1} \odot \mathbf{s}_{\sigma_2, \sigma_2} = \sigma_1 \sigma_2 \frac{1}{4} \mathbf{e}_z \odot \mathbf{e}_z$, whereas for $\sigma_1 = -\sigma_2$ we have $\mathbf{s}_{\sigma_1, \sigma_2} \odot \mathbf{s}_{\sigma_2, \sigma_1} = \frac{1}{2} (\mathbf{e}_x - i \sigma_1 \mathbf{e}_y) \odot \frac{1}{2} (\mathbf{e}_x + i \sigma_1 \mathbf{e}_y) = \frac{1}{4} (\mathbf{e}_x \odot \mathbf{e}_x + \mathbf{e}_y \odot \mathbf{e}_y) = -\frac{1}{4} \mathbf{e}_z \odot \mathbf{e}_z$. The last step follows from $\sum_i \mathbf{e}_i \odot \mathbf{e}_i = 0$, which is just the traceless, symmetric part of the unit tensor by the coordinate-space completeness relation $\sum_i \mathbf{e}_i \mathbf{e}_i = \mathcal{I}$.

With the two-particle operator (A2) in the standard second-quantized form [see also Eq. (A21) below] the contributions to the average $\langle \mathcal{Q} \rangle$ can be discussed as scattering processes, treating \mathcal{Q} as if it were an interaction (although it is tensor valued). In Fig. 23 we represent the contributions to the average SQM (A5) by Feynman diagrams for scattering processes

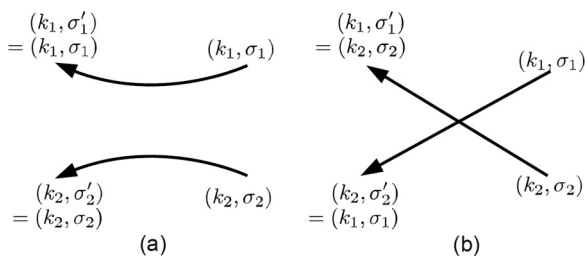


FIG. 23. Feynman diagrams for calculating the (a) direct and (b) exchange contribution to the average SQM.

between an initial pair of states (1,2) to a final pair of states (1',2').

The momenta in the final states are the same as for the initial states, $k_i = k'_i$, since the SQM operator does not act on the orbital part of the wave function [cf. Eq. (A22)]. Two different scattering processes are permitted: The first one is a direct scattering, for which the electron in initial state i ends up in state i' , restricting the spin indices to $\sigma_i = \sigma'_i$ (while already $k_i = k'_i$). These direct scattering contributions, multiplied with their tensor-valued amplitudes $\mathbf{s}_{\sigma_1, \sigma_2} \odot \mathbf{s}_{\sigma_2, \sigma_1}$ in Eq. (A5) add up to the direct SQM. This contribution to the spin anisotropy is thus generated by two electrons (labeled by their states 1 and 2) as if they were *distinguishable*, i.e., by treating the two-particle scattering classically.

The second type of scattering process, in which the particles are *exchanged*, accounts for the fact that electrons are *indistinguishable*. This is possible only if the momenta are the *same*, $k_1 = k_2$, and, furthermore, the spins are exchanged, $\sigma'_1 = \sigma_2$ and $\sigma'_2 = \sigma_1$. This exchange contribution to the average SQM entirely cancels the direct contribution for equal $k_1 = k_2$, correcting for the treatment of electrons as distinguishable particles. In other words, the exchange SQM accounts for Pauli “holes” in the triplet spin-spin correlation tensor. The Pauli principle thus counters the direct classical contribution to the spin anisotropy.

Indistinguishability becomes important if we consider pairs of electrons from the same k mode. Due to Pauli's principle, their wave function must have a symmetric orbital part and an antisymmetric spin part; that is, they form a spin singlet with zero SQM (i.e., triplet correlations are forbidden). This is analogous to the direct and exchange contributions to the average Coulomb interaction with respect to Slater determinants (e.g., in Hartree-Fock theory). In that case, nearby electrons with parallel spins repel each other due to the exchange potential. We mention that, as expected from this analogy, thermal fluctuations suppress the effect of the Pauli principle on SQM as well; cf. Eq. (A34) below.

2. Spin-trace technique

We now reformulate the above calculation in a way that is used in the transport calculations (cf. Appendix E 4): The result [Eq. (A17)] then assumes the coordinate-free form presented in Sec. III B 3,

$$\langle \mathcal{Q}^{rr} \rangle_{\text{ex}} = \sum_{k\sigma\sigma'\tau\tau'} (\mathbf{s}_{\sigma\sigma'}^r \odot \mathbf{s}_{\tau\tau'}^r) \delta_{\sigma\tau'} \delta_{\sigma'\tau} f_+(\varepsilon_{k\sigma}^r) f_-(\varepsilon_{k\sigma'}^r). \quad (\text{A8})$$

Here we reintroduced the electrode index. To recast this into *covariant* expression, we first introduce the two-particle density of states (16),

$$v_{\sigma\sigma'}^r(\omega, \omega') = \sum_k \delta(\omega - \varepsilon_{k\sigma}^r) \delta(\omega' - \varepsilon_{k\sigma'}^r), \quad (\text{A9})$$

and rewrite Eq. (A8) in terms of frequency integrals,

$$\langle \mathcal{Q}^{rr} \rangle_{\text{ex}} = \sum_{k\sigma\sigma'\tau\tau'} \int d\omega d\omega' (\mathbf{s}_{\sigma\sigma'}^r \odot \mathbf{s}_{\tau\tau'}^r) \times \delta_{\sigma\tau'} \delta_{\sigma'\tau} v_{\sigma\sigma'}^r(\omega, \omega') f_+(\omega) f_-(\omega'). \quad (\text{A10})$$

The 2DOS $v_{\sigma\sigma'}^r(\omega)$ can be expressed as a matrix element in spin space by

$$v_{\sigma\sigma'}^r(\omega, \omega') \delta_{\sigma\tau'} \delta_{\sigma'\tau} = 2 \sum_{\mu_1, \mu_2} r \langle \tau' | \check{r}_{\mu_1} | \sigma \rangle_r \mathcal{A}_{\mu_1 \mu_2}^r(\omega, \omega')_r \langle \sigma' | \check{r}_{\mu_2} | \tau \rangle_r. \quad (\text{A11})$$

Here we used the four-component operator $\check{\mathbf{r}}$ with $\check{r}_0 = \mathbb{1}/\sqrt{2}$ and $\check{r}_i = \sqrt{2}s_i$ for $i = x, y, z$. The four-dimensional matrix $\mathcal{A}_{\mu_1 \mu_2}^r$ incorporates all relevant 2DOS information. It decomposes into a scalar, two vectors, and a tensor in coordinate space:

$$\mathcal{A}_{00}^r = \frac{1}{4} \sum_{\sigma\sigma'} v_{\sigma\sigma'}^r(\omega, \omega'), \quad (\text{A12})$$

$$\mathcal{A}_{i0}^r = \frac{1}{4} \sum_{\sigma\sigma'} \sigma v_{\sigma\sigma'}^r(\omega, \omega') \hat{J}_i^r, \quad (\text{A13})$$

$$\mathcal{A}_{0j}^r = \frac{1}{4} \sum_{\sigma\sigma'} \sigma' v_{\sigma\sigma'}^r(\omega, \omega') \hat{J}_j^r, \quad (\text{A14})$$

$$\mathcal{A}_{ij}^r = \frac{1}{4} \sum_{\sigma\sigma'} \sigma \sigma' v_{\sigma\sigma'}^r(\omega, \omega') \hat{J}_i^r \hat{J}_j^r. \quad (\text{A15})$$

Inserting Eq. (A11) into Eq. (A10) and recasting the sum over the spin indices as a trace in spin space yields

$$\langle \mathcal{Q}^r \rangle_{\text{ex}} = \int d\omega d\omega' f_+^r(\omega) f_-^r(\omega') \times 2 \sum_{\mu_1 \mu_2} \mathcal{A}_{\mu_1 \mu_2}^r(\omega, \omega') \text{Tr}[\check{r}_{\mu_1} \mathbf{s} \odot \check{r}_{\mu_2} \mathbf{s}] \quad (\text{A16})$$

$$= \int d\omega d\omega' \frac{1}{4} \sum_{\sigma\sigma'} \sigma \sigma' v_{\sigma\sigma'}^r(\omega, \omega') \times f_+^r(\omega) f_-^r(\omega') \hat{\mathbf{J}}^r \odot \hat{\mathbf{J}}^r. \quad (\text{A17})$$

This recovers the results [Eqs. (64)–(67)] obtained in the main text from Eq. (A6). The explicit calculation in the last step is now reduced to using spin- $\frac{1}{2}$ operator algebra $s_i s_j = \frac{1}{4} \delta_{ij} \mathbb{1} + \frac{1}{2} \sum_k i \varepsilon_{ijk} s_k$ and $\mathbf{s} \odot \mathbf{s} = 0$, i.e., without using matrix elements. These steps are analogous to the evaluation of the diagrammatic expressions for the SQM current in Appendix D 4.

3. SQM and triplet spin correlations

Finally, we express the SQM tensor operator \mathcal{Q} in the second-quantized form. This allows one to perform a vector coupling of the pairs of the involved spins, thereby making explicit that only triplet correlations are “measured” by $\langle \mathcal{Q} \rangle$, something that did not become clear in the above calculations. This is merely important for the physical understanding, but seems to bring no advantage for calculations. The many-body quadrupole operator is a sum over quadrupole operators of pairs of particles, the latter labeled by $a, b = 1, 2, 3, \dots$,

$$\mathcal{Q} = \sum_{a < b} \mathcal{Q}^{ab}, \quad (\text{A18})$$

with Cartesian components $i, j = x, y, z$:

$$\mathcal{Q}_{ij}^{ab} = 2 \left(\frac{1}{2} (s_i^a s_j^b + s_j^a s_i^b) - \frac{1}{3} \delta_{ij} \sum_k s_k^a s_k^b \right). \quad (\text{A19})$$

Here we inserted the total spin operator $\mathbf{S} = \sum_a \mathbf{s}^a$ into Eq. (1) and used the result $\mathcal{Q}^{aa} = 0$ (“a single electron has no anisotropy”; cf. Sec. II A). The SQM from pair (ab) can also be expressed by coupling the two spins to $\mathbf{S}^{ab} = \mathbf{s}^a + \mathbf{s}^b$,

$$\mathcal{Q}_{ij}^{ab} = \frac{1}{2} (S_i^{ab} S_j^{ab} + S_j^{ab} S_i^{ab}) - \frac{1}{3} \delta_{ij} (\mathbf{S}^{ab})^2, \quad (\text{A20})$$

using $s_i^a s_j^a = \frac{1}{4} \delta_{ij} + i \frac{1}{2} \sum_k \varepsilon_{ijk} s_k^a$. Note the factor 2 in Eq. (A19). The general second quantization prescription immediately gives

$$\mathcal{Q} = \sum_{\{k_i \sigma_i\}} \frac{1}{2} \langle k_2' \sigma_2' k_1' \sigma_1' | \mathcal{Q}^{12} | k_2 \sigma_2 k_1 \sigma_1 \rangle \times c_{k_1' \sigma_1'}^\dagger c_{k_2' \sigma_2'}^\dagger c_{k_2 \sigma_2} c_{k_1 \sigma_1}. \quad (\text{A21})$$

We now make explicit use the particular property of the matrix elements of the pair SQM \mathcal{Q}^{12} . First, we note that \mathcal{Q}^{12} acts only on the spin of the electrons,

$$\langle k_2' \sigma_2' k_1' \sigma_1' | \mathcal{Q}^{12} | k_2 \sigma_2 k_1 \sigma_1 \rangle = \delta_{k_2' k_2} \delta_{k_1' k_1} \langle \sigma_2' \sigma_1' | \mathcal{Q}^{12} | \sigma_2 \sigma_1 \rangle. \quad (\text{A22})$$

If we inserted this into Eq. (A21) we would recover Eq. (A2). Instead of this, we now introduce a singlet-triplet basis for each pair of considered spins σ_1 and σ_2 above:

$$|S\rangle = \frac{1}{\sqrt{2}} \sum_{\sigma} \sigma |\sigma \bar{\sigma}\rangle, \quad (\text{A23})$$

$$|T0\rangle = \frac{1}{\sqrt{2}} \sum_{\sigma} |\sigma \bar{\sigma}\rangle, \quad (\text{A24})$$

$$|Tm\rangle = |mm\rangle, \quad m = \pm, \quad (\text{A25})$$

where $\bar{\sigma} = -\sigma$. The crucial point is that \mathcal{Q}^{12} only has matrix elements in the triplet sector. This follows from the fact that \mathcal{Q}^{12} is symmetric under exchange of the spins; i.e., $[P, \mathcal{Q}^{12}] = 0$, where P is the exchange operator of particle 1 and 2. Therefore, \mathcal{Q}^{12} is block diagonal with respect to the eigenspaces of P , which are here the singlet and triplet states satisfying $P|S\rangle = -|S\rangle$ and $P|Tm\rangle = +|Tm\rangle$. Thus, $\langle S | \mathcal{Q}^{12} | Tm \rangle = \langle Tm | \mathcal{Q}^{12} | S \rangle = 0$. Moreover, the diagonal singlet block is zero, $\langle S | \mathcal{Q}^{12} | S \rangle = 0$ by Eq. (A20), with $a = 1, b = 2$, and $\mathcal{Q}^{12}|S\rangle = 0$, completing the proof. As a result,

$$\langle \sigma_2' \sigma_1' | \mathcal{Q}^{12} | \sigma_2 \sigma_1 \rangle = \sum_{mm'} \langle \sigma_2' \sigma_1' | Tm \rangle \langle Tm | \mathcal{Q}^{12} | Tm' \rangle \langle Tm' | \sigma_2 \sigma_1 \rangle. \quad (\text{A26})$$

Inserting Eq. (A26) into Eq. (A21), we obtain the central result of the appendix,

$$\mathcal{Q} = \sum_{mm'} \frac{1}{2} \langle Tm' | \mathcal{Q}^{12} | Tm \rangle \sum_{\{k_i\}} E_{k_2 k_1}^{m' \dagger} E_{k_2 k_1}^m, \quad (\text{A27})$$

with two-particle operators that explicitly generate *only triplet pairs*:

$$E_{k_2 k_1}^m = \sum_{\sigma_2 \sigma_1} \langle T m | \sigma_2 \sigma_1 \rangle c_{k_2 \sigma_2} c_{k_1 \sigma_1} \quad (\text{A28})$$

$$= \begin{cases} c_{k_2 m} c_{k_1 m}, & m = \pm 1, \\ \frac{1}{\sqrt{2}} \sum_{\sigma} c_{k_2 \sigma} c_{k_1 \bar{\sigma}}, & m = 0. \end{cases} \quad (\text{A29})$$

Considered as an interaction, \mathcal{Q} thus only scatters triplet correlated pairs of electrons. Due to the restrictions on the spins in these operators $E_{k_2 k_1}^m$, the averages are

$$\begin{aligned} & \langle E_{k_2 k_1}^{m'} E_{k_2 k_1}^m \rangle \\ &= \delta_{mm'} \times \begin{cases} f(\varepsilon_{k_2 m}) f(\varepsilon_{k_1 m}) (1 - \delta_{k_2 k_1}), & m = \pm 1, \\ \frac{1}{2} \sum_{\sigma} f(\varepsilon_{k_2 \sigma}) f(\varepsilon_{k_1 \bar{\sigma}}) (1 - \delta_{k_2 k_1}), & m = 0, \end{cases} \end{aligned} \quad (\text{A30})$$

with the tensor-valued matrix elements $\langle T + | \mathcal{Q}^{12} | T + \rangle = \langle T - | \mathcal{Q}^{12} | T - \rangle = -\langle T 0 | \mathcal{Q}^{12} | T 0 \rangle / 2 = \frac{1}{2} \mathbf{e}_z \odot \mathbf{e}_z$ given by Eqs. (2) and (3) in the main text. These relations follow from the fact that \mathcal{Q}^{12} is traceless in the Hilbert space, $\sum_{m=0,\pm 1} \langle T m | \mathcal{Q}^{12} | T m \rangle = 0$ and that the $m = \pm$ states have the identical spin anisotropy. We recover Eq. (A6):

$$\begin{aligned} \langle \mathcal{Q} \rangle &= \frac{1}{4} \mathbf{e}_z \odot \mathbf{e}_z \sum_{k_2 k_1} (1 - \delta_{k_2 k_1}) \\ &\times \left[\sum_{m=\pm} f_+(\varepsilon_{k_2 m}) f_+(\varepsilon_{k_1 m}) - \sum_{\sigma=\pm} f_+(\varepsilon_{k_2 \sigma}) f_+(\varepsilon_{k_1 \bar{\sigma}}) \right]. \end{aligned} \quad (\text{A31})$$

This derivation, however, shows explicitly that the $m = \pm 1$ terms contribute the same, uniaxial anisotropy tensor $\langle T \pm | \mathcal{Q}^{12} | T \pm \rangle$, whereas the $m = 0$ term contributes an easy-plane anisotropy tensor $\langle T 0 | \mathcal{Q}^{12} | T 0 \rangle = -2 \langle T + | \mathcal{Q}^{12} | T + \rangle$. Moreover, the Pauli-exclusion hole factor $1 - \delta_{k_2 k_1}$ is immediately explicit. Thus, $\langle \mathcal{Q} \rangle$ can be calculated by first accounting for triplet correlations between spins of pairs of electrons in all possible orbitals, including the same orbital,

$$\begin{aligned} \langle \mathcal{Q} \rangle_{\text{dir}} &= \frac{1}{4} \sum_{k_2 k_1 \sigma_2 \sigma_1} \sigma_2 f(\varepsilon_{k_2 \sigma_2}) \sigma_1 f(\varepsilon_{k_1 \sigma_1}) \mathbf{e}_z \odot \mathbf{e}_z \\ &= \langle \mathbf{S} \rangle \odot \langle \mathbf{S} \rangle, \end{aligned} \quad (\text{A32})$$

giving Eq. (57), and then subsequently canceling the latter violation of the Pauli principle by the exchange term,

$$\langle \mathcal{Q} \rangle_{\text{ex}} = -q_{\text{ex}} \mathbf{e}_z \odot \mathbf{e}_z, \quad (\text{A33})$$

with the positive exchange magnitude,

$$q_{\text{ex}} = \frac{1}{4} \sum_k [f_+(\varepsilon_{k\uparrow}) - f_+(\varepsilon_{k\downarrow})]^2. \quad (\text{A34})$$

We obtain Eq. (62) from the main text. Finally, we show that the two-particle DOS $\nu_{\sigma\sigma'}$ can be decomposed explicitly into *triplet* DOS components: Converting the sums in Eq. (A34) to integrals we obtain

$$q_{\text{ex}} = \int d\omega d\omega' f_+(\omega) f_+(\omega') \sum_{\sigma\sigma'} \sigma\sigma' \nu_{\sigma\sigma'}(\omega, \omega'). \quad (\text{A35})$$

The only relevant combination of the 2DOS in the above expression can be recast as

$$\sum_{\sigma\sigma'} \sigma\sigma' \nu_{\sigma\sigma'} = \nu_{T+} + \nu_{T-} - \sqrt{2} \nu_{T0}, \quad (\text{A36})$$

with the triplet exchange 2DOS function ($m = \pm$)

$$\nu_{Tm}(\omega, \omega') := \nu_{mm}(\omega, \omega'), \quad (\text{A37})$$

$$\nu_{T0}(\omega, \omega') := \frac{1}{\sqrt{2}} \sum_{\sigma} \nu_{\sigma\bar{\sigma}}(\omega, \omega'). \quad (\text{A38})$$

This gives a precise decomposition into triplet spin correlations that contribute to $\langle \mathcal{Q} \rangle_{\text{ex}}$.

4. Spin-anisotropy function

Finally, we further substantiate the physical interpretation of the anisotropy function, which plays a key role in the main text. The basic idea of ‘‘quadrupolarization’’ of two triplet-correlated electrons is simply to ‘‘count’’ whether the spins are parallel ($\uparrow\uparrow$ or $\downarrow\downarrow$, counted as $+$) or antiparallel ($\uparrow\downarrow$ or $\downarrow\uparrow$, counted as $-$). In both cases their individual orientations, i.e., their *dipolarization* \uparrow or \downarrow , is ignored. Equation (A35) precisely expresses this notion for the exchange SQM. It is instructive to start from the k -sum representation (A34) and to write it as

$$q_{\text{ex}} = \sum_{k\sigma} f_+(\varepsilon_{k\sigma}) a_{k\sigma}. \quad (\text{A39})$$

Here, *given* that an electron with spin σ occupies orbital k , we ‘‘count’’ by

$$a_{k\sigma} = \sum_{\sigma'} \frac{\sigma\sigma'}{4} f(\varepsilon_{k\sigma'}), \quad (\text{A40})$$

the average quadrupolarization contribution from electrons in that same orbital k : Parallel spin $\sigma' = \sigma$ gives $+f_+(\varepsilon_{k\sigma})$; antiparallel $\sigma' = \bar{\sigma}$ gives $-f(\varepsilon_{k\bar{\sigma}})$.³⁷ Converting the sum to an integral, we obtain Eq. (64) of the main text:

$$q_{\text{ex}} = \int d\omega f_+(\omega) \bar{\nu}(\omega) a(\omega). \quad (\text{A41})$$

The anisotropy function $a(\omega) = \sum_{\sigma} a_{\sigma}(\omega)$ has two contributions:

$$\bar{\nu}(\omega) a_{\sigma}(\omega) := \sum_k a_{k\sigma} \delta(\omega - \varepsilon_{k\sigma}). \quad (\text{A42})$$

The quantity $\bar{\nu}(\omega) a_{\sigma}(\omega)$ is the exchange quadrupolarization of a spin σ electron at energy ω . One should note that the function $a_{k\sigma}$, defined by Eq. (A40), does not only depend on the energy $\varepsilon_{k\sigma}$, but also on the energy $\varepsilon_{k\bar{\sigma}}$. Since $\varepsilon_{k\bar{\sigma}}$ is not necessarily an implicit function of $\varepsilon_{k\sigma}$ for arbitrary band structures, one can, in general, reformulate Eq. (A42) only in terms of the 2DOS (16),

$$\bar{\nu}(\omega) a_{\sigma}(\omega) = \int d\omega' f_+(\omega') \sum_{\sigma'} \frac{\sigma\sigma'}{4} \nu_{\sigma\sigma'}(\omega, \omega'), \quad (\text{A43})$$

resulting in Eq. (67) of the main text.

However, for the Stoner model, which we discuss from hereon, the simple relation $\varepsilon_{k\bar{\sigma}} = \varepsilon_{k\sigma} - \sigma J/2$ can be exploited

to express $a_{k\sigma}$ as a function of $\varepsilon_{k\sigma}$ only. We therefore obtain the simpler result,

$$\bar{v}(\omega)a_\sigma(\omega) = v_\sigma(\omega)[f_+(\omega) - f_+(\omega + \sigma J)], \quad (\text{A44})$$

which only depends on the 1DOS v_σ . This unfortunately hides the underlying two-particle nature of the exchange SQM, but aids the interpretation of the total spin-anisotropy function: Equation (A44) shows that the contribution $a_\uparrow(\omega)$ from up-spins is positive and comes from the range of energies $\mu - J < \omega < \mu$, whereas the contribution $a_\downarrow(\omega)$ from down-spins is negative and comes from energies $\mu < \omega < \mu + J$ (both up to thermal smearing). Adding both contributions yields for the full spin-anisotropy function after some manipulations,

$$a(\omega) = \frac{1}{4}[2f_+(\omega) - f_+(\omega + J) - f_+(\omega - J)] + \frac{1}{4}n(\omega)[f_+(\omega + J) - f_+(\omega - J)]. \quad (\text{A45})$$

Here it should be noted that $n(\omega)$ is not independent of J but is a function of it through Eqs. (13), (15), and (18).³⁸ The combinations of Fermi functions are nonzero only for energies $|\omega - J| \lesssim T$.

It was pointed out in Sec. VC for a purely thermally biased tunnel junction that the finite SQM current that remains whenever the spin current vanishes arises entirely from the exchange SQM, i.e., from the *antisymmetric part* of the spin-anisotropy function $a(\omega)$ relative to μ . Generally, when assuming a weakly energy-dependent average DOS $\bar{v}(\omega)$ in the range $|\omega - J| \lesssim T$, the first term Eq. (A45) always gives rise to such a term. The second term, in which the spin-polarization $n(\omega)$ is multiplied by a symmetric function relative to μ , can cancel this function only if $n(\omega)$ is strongly antisymmetric [i.e., $n(\omega) = \pm 1$ for $\omega \gtrless 0$, up to thermal smearing]. If we further specialize to the approximation of a flat band symmetric about μ (cf. Sec. IID), this second term is exactly zero because the spin polarization vanishes in the window $[\omega - J, \omega + J]$ up to thermal smearing. Only the first line of Eq. (A45) remains and gives a thermally induced pure SQM current as discussed in Sec. VC: Substituting $x = (\omega - \mu)/T$, Eq. (A41) can be rewritten as

$$q_{\text{ex}} = \frac{\bar{v}T}{4} \int dx f(x)[2f(x) - f(x - j) - f(x + j)], \quad (\text{A46})$$

where $f(x) = [e^x + 1]^{-1}$ and $j = J/T$. As $a(\omega)$ is nonzero in an energy window $2J$ centered at μ , which is far away from the band edges, we can replace the 1DOS with its constant value \bar{v} and extend the limits integration to $\pm\infty$. Using the identity $f(x) = 1 - f(-x)$ and the result

$$\int dx f(x)f[-(x - y)] = \begin{cases} 1, & y = 0, \\ yb(y), & \text{else,} \end{cases} \quad (\text{A47})$$

where $b(x) = [e^x - 1]^{-1}$ is the Bose function, and taking the limit $y \rightarrow 0$, we obtain Eq. (70) of the main text:

$$q_{\text{ex}} = \frac{\bar{v}}{4}[-2 + jb(j) + (-j)b(-j)] \quad (\text{A48})$$

$$= \frac{\bar{v}}{2} \left[\frac{j}{2} \coth\left(\frac{j}{2}\right) - 1 \right]. \quad (\text{A49})$$

APPENDIX B: SYMMETRIC AND TRACELESS TENSORS

In this appendix, we collect some relevant results on symmetric, traceless tensors. We first show how a particular type of such tensors, constructed from two real vectors \mathbf{a} and \mathbf{b} ,

$$\mathcal{A} = \mathbf{a} \odot \mathbf{b} = \frac{1}{2}(\mathbf{ab} + \mathbf{ba}) - \frac{1}{3}(\mathbf{a} \cdot \mathbf{b})\mathcal{I}, \quad (\text{B1})$$

can be diagonalized using dyadic calculus,³⁹ i.e., without introducing a coordinate system. The tensor \mathcal{A} can be expressed in terms of its principal values λ_μ and normalized vectors $\hat{\mathbf{v}}_\mu$ that define the principal axes as

$$\mathcal{A} = \sum_{\mu=0,\pm} \lambda_\mu \hat{\mathbf{v}}_\mu \hat{\mathbf{v}}_\mu^T. \quad (\text{B2})$$

The results [Eqs. (123)–(132)] of the main text can then be obtained from Eq. (115) by setting $\mathbf{a} = \hat{\mathbf{J}}^L$ and $\mathbf{b} = E^L \hat{\mathbf{J}}^L + A^L \hat{\mathbf{J}}^R + T^L (\hat{\mathbf{J}}^L \times \hat{\mathbf{J}}^R)$. To diagonalize (B1), we have to distinguish two cases.

Case (i) $\mathbf{a} \nparallel \mathbf{b}$: eigenvalues

$$\lambda_\mu = -\frac{1}{3}(\mathbf{a} \cdot \mathbf{b}) + \frac{1}{2}\delta_{\mu,\pm}[(\mathbf{a} \cdot \mathbf{b}) + \mu ab], \quad (\text{B3})$$

where $\mu = 0, \pm$, and normalized eigenvectors

$$\hat{\mathbf{v}}_0 = \frac{1}{|\mathbf{a} \times \mathbf{b}|}(\mathbf{a} \times \mathbf{b}), \quad (\text{B4})$$

$$\hat{\mathbf{v}}_\pm = \frac{1}{2ab[ab \pm (\mathbf{a} \cdot \mathbf{b})]}[ab \pm ba] \quad (\text{B5})$$

with $a = |\mathbf{a}|, b = |\mathbf{b}|$.

Case (ii) $\mathbf{a} \parallel \mathbf{b}$, i.e., $\mathbf{b} = \alpha\mathbf{a}$: eigenvalues for $\mu = 0, \pm$

$$\lambda_\mu = (\delta_{\mu,+} - \frac{1}{3})\alpha a^2, \quad (\text{B6})$$

and $\hat{\mathbf{v}}_+ = \mathbf{a}/a$ and $\hat{\mathbf{v}}_0, \hat{\mathbf{v}}_-$ are any two orthonormal vectors that span the plane perpendicular to $\hat{\mathbf{v}}_+$.

To prove case (i), we first note that one principal axis is obviously $\mathbf{v}_0 = \mathbf{a} \times \mathbf{b} \neq 0$:

$$\mathcal{A} \cdot \mathbf{v}_0 = \left[\frac{1}{2}(\mathbf{ab} + \mathbf{ba}) - \frac{1}{3}(\mathbf{a} \cdot \mathbf{b})\mathcal{I} \right] \cdot (\mathbf{a} \times \mathbf{b}) \quad (\text{B7})$$

$$= -\frac{1}{3}(\mathbf{a} \cdot \mathbf{v})\mathbf{v}_0 = \lambda_0 \mathbf{v}_0. \quad (\text{B8})$$

In order to derive the the remaining principal values, we need to set up the characteristic equation

$$0 = \det(\mathcal{A} - \lambda\mathcal{I}) \quad (\text{B9})$$

$$= \det(\mathcal{A}) - \lambda \text{spm}(\mathcal{A}) + \lambda^2 \text{tr}(\mathcal{A}) - \lambda^3, \quad (\text{B10})$$

where the coefficients are given by the trace, the sum of principal minors, and the determinant of \mathcal{A} , respectively:

$$\text{tr}(\mathcal{A}) = \sum_i \mathcal{A}_{ii}, \quad (\text{B11})$$

$$\text{spm}(\mathcal{A}) = \frac{1}{2} \text{tr}(\mathcal{A}_\times^\times \mathcal{A}), \quad (\text{B12})$$

$$\det(\mathcal{A}) = \frac{1}{6} (\mathcal{A}_\times^\times \mathcal{A}) : \mathcal{A}. \quad (\text{B13})$$

Here we used the shorthand notations $(\mathcal{A}_\times^\times \mathcal{A})_{i_1 i_2} = \sum_{j_1, j_2, k_1, k_2} \varepsilon_{i_1 j_1 k_1} \varepsilon_{i_2 j_2 k_2} \mathcal{A}_{j_1 j_2} \mathcal{A}_{k_1 k_2} \varepsilon_{j_2 k_2 i_2}$ and $\mathcal{B} : \mathcal{A} = \sum_{i,j} \mathcal{B}_{ij} \mathcal{A}_{ij}$. Equations (B11)–(B13) are the (only) three rotational invariants, i.e., they are invariant under transformations $\mathcal{A} \rightarrow \mathcal{R} \cdot \mathcal{A} \cdot \mathcal{R}^T$, where \mathcal{R} is a rotation matrix: $\mathcal{R} \cdot \mathcal{R}^T = \mathcal{R}^T \cdot \mathcal{R} = \mathcal{I}$. Inserting Eq. (B1) we

obtain

$$\text{tr}(\mathcal{A}) = (\mathbf{a} \cdot \mathbf{b}), \quad (\text{B14})$$

$$\text{spm}(\mathcal{A}) = -\frac{1}{3}(\mathbf{a} \cdot \mathbf{b})^2 - \frac{1}{4}(\mathbf{a} \times \mathbf{b})^2, \quad (\text{B15})$$

$$\det(\mathcal{A}) = \frac{2}{27}(\mathbf{a} \cdot \mathbf{b})^3 + \frac{1}{12}(\mathbf{a} \cdot \mathbf{b})(\mathbf{a} \times \mathbf{b})^2. \quad (\text{B16})$$

Inserting these into Eq. (B10), one finds that λ_0 , given by (B3) with $\mu = 0$, is indeed a principal value of \mathcal{A} . By polynomial division we obtain a quadratic equation for the remaining principal values λ_{\pm} , which is solved by Eq. (B3) with $\mu = \pm$. The general solution of $(\mathcal{A} - \lambda_{\pm}\mathcal{I}) \cdot \mathbf{v}_{\pm} = 0$ is given by³⁹

$$\mathbf{v}_{\pm} = \mathbf{c} \cdot [(\mathcal{A} - \lambda_{\pm}\mathcal{I})_{\times}(\mathcal{A} - \lambda_{\pm}\mathcal{I})] \quad (\text{B17})$$

$$= -\frac{1}{2}\mathbf{c} \cdot [(\mathbf{a} \times \mathbf{b})(\mathbf{a} \times \mathbf{b}) + (2q_{\pm}(\mathbf{a} \cdot \mathbf{b}) - q_{\pm}^2)\mathcal{I} - q_{\pm}(\mathbf{ab} + \mathbf{ba})], \quad (\text{B18})$$

where $q_{\pm} = (\mathbf{a} \cdot \mathbf{b}) \pm |\mathbf{a}||\mathbf{b}|$. Here \mathbf{c} is a vector such that $\mathbf{v}_{\pm} \neq 0$ and either $\mathbf{c} = \mathbf{a}$ or $\mathbf{c} = \mathbf{b}$ fulfills this condition, yielding the result (B5) after normalization.

For case (ii) we have $\mathcal{A} = \mathbf{a} \odot \alpha \mathbf{a} = \alpha(\mathbf{a}\mathbf{a} - a^2\mathcal{I}/3)$. Since $\mathbf{a} \times \mathbf{b} = 0$, the above results cannot be applied. The vector \mathbf{a} obviously defines a principal axis since $\mathcal{A} \cdot \mathbf{a} = +\frac{2}{3}\alpha a^2 \mathbf{a}$, and for any vector \mathbf{a}_{\perp} in the plane perpendicular to \mathbf{a} we have $\mathcal{A} \cdot \mathbf{a}_{\perp} = -\frac{1}{3}\alpha a^2 \mathbf{a}_{\perp}$. This confirms the principal values (B6), completing the proof.

APPENDIX C: ROTATION OF THE SQM BY SQM CURRENTS

In this appendix we show that a SQM tensor \mathcal{Q} is rotated if it does not commute with the SQM current tensor $\mathcal{I}_{\mathcal{Q}}$ as pointed out in Sec. VB3. More formally, $[\mathcal{Q}, \mathcal{I}_{\mathcal{Q}}]_{-} = 0$ implies that both tensors have collinear principal axes. We outline the analogous situation for the spin vector: It is geometrically clear that the spin \mathbf{S} does not rotate, that is, $\mathbf{S} = S(t)\mathbf{e}_3$ in some time-independent basis if and only if the spin current vector $\mathbf{I}_{\mathbf{S}} = \dot{\mathbf{S}}$ is collinear to \mathbf{S} at all times.

We now outline a proof of this statement, which can be extended to the SQM. Assume \mathbf{S} does not rotate; then $\mathbf{S} = S(t)\mathbf{e}_3$ in some time independent basis \mathbf{e}_i . Then $\dot{\mathbf{S}} = \dot{S}(t)\mathbf{e}_3 = \mathbf{I}_{\mathbf{S}}$. Thus, $\mathbf{I}_{\mathbf{S}} \cdot \mathbf{S} = \pm|\mathbf{S}||\mathbf{I}_{\mathbf{S}}| \cdot \mathbf{e}_3 = \pm|\mathbf{S}||\mathbf{I}_{\mathbf{S}}|$. Conversely, assume $\mathbf{S} \cdot \mathbf{I}_{\mathbf{S}} = \pm|\mathbf{S}||\mathbf{I}_{\mathbf{S}}|$, i.e., $\mathbf{S} = S(t)\mathbf{e}_3(t)$ and $\mathbf{I}_{\mathbf{S}} = I_{\mathbf{S}}(t)\mathbf{e}_3(t)$, but for some time-dependent $\mathbf{e}_3(t)$. One can derive a contradiction from the latter assumption. First, we have $\dot{\mathbf{S}} = \dot{S}(t)\mathbf{e}_3(t) + S(t)\dot{\mathbf{e}}_3(t) = \mathbf{I}_{\mathbf{S}} = I_{\mathbf{S}}(t)\mathbf{e}_3(t)$. By assumption, the normalization is preserved; that is, $\frac{d}{dt}(\mathbf{e}_3 \cdot \mathbf{e}_3) = 2\mathbf{e}_3 \cdot \dot{\mathbf{e}}_3 = 0$. Thus, if $\dot{\mathbf{e}}_3 \perp \mathbf{e}_3$, we have $\dot{S}(t) = I_{\mathbf{S}}(t)$ and either $S(t) = 0$ (which implies a trivial spin) or $\dot{\mathbf{e}}_3 = 0$, contradicting our assumption. This completes the proof.

We now prove a similar statement for the SQM tensor \mathcal{Q} and its current $\mathcal{I}_{\mathcal{Q}} = \dot{\mathcal{Q}}$,

$$\mathcal{Q} \text{ has fixed principal axes} \Leftrightarrow [\mathcal{Q}, \mathcal{I}_{\mathcal{Q}}]_{-} = 0. \quad (\text{C1})$$

Assume $\mathcal{Q} = \sum_i Q_i(t)\mathbf{e}_i\mathbf{e}_i^T$ has a time-independent basis, i.e., only the principal values $Q_i(t)$ change but the principal axes \mathbf{e}_i do not rotate. Thus, $\dot{\mathcal{Q}} = \sum_i \dot{Q}_i(t)\mathbf{e}_i\mathbf{e}_i^T = \mathcal{I}_{\mathcal{Q}} = \sum_{ij} I_{ij}(t)\mathbf{e}_i\mathbf{e}_j^T$, implying $I_{ij}(t) = \delta_{ij}\dot{Q}_i(t)$ and consequently $[\mathcal{Q}, \mathcal{I}_{\mathcal{Q}}]_{-} = 0$. Now assume the converse, i.e., $\mathcal{I}_{\mathcal{Q}}$ and \mathcal{Q} commute. Since both are real, symmetric tensors, they can be

diagonalized and since they commute they have common principal axes: $\mathcal{Q} = \sum_i Q_i(t)\mathbf{e}_i(t)\mathbf{e}_i^T(t)$ and $\mathcal{I}_{\mathcal{Q}} = \sum_i I_i(t)\mathbf{e}_i(t)\mathbf{e}_i^T(t)$. We next derive a contradiction from the assumption $\dot{\mathbf{e}}_i(t) \neq 0$. We first find $\dot{\mathcal{Q}} = \sum_i [\dot{Q}_i\mathbf{e}_i\mathbf{e}_i^T + Q_i(\dot{\mathbf{e}}_i\mathbf{e}_i^T + \mathbf{e}_i\dot{\mathbf{e}}_i^T)] = \mathcal{I}_{\mathcal{Q}}$ and note that $\dot{\mathbf{e}}_i\mathbf{e}_i^T$ is independent of $\mathbf{e}_k\mathbf{e}_k^T$ for all k because $\dot{\mathbf{e}}_i \perp \mathbf{e}_k$. Thus, we have $I_i = \dot{Q}_i$ and either $Q_i = 0$ for all i or $\dot{\mathbf{e}}_i\mathbf{e}_i^T + \mathbf{e}_i\dot{\mathbf{e}}_i^T = 0$, which would imply $\dot{\mathbf{e}}_i = 0$. Thus, \mathbf{e}_i is time independent and the proof is complete.

APPENDIX D: CHARGE, SPIN, AND SPIN-QUADRUPOLE CURRENT IN $O(\Gamma)$

In this section, we apply the general diagrammatic technique developed in Appendix E, accounting only for contributions up to first order in the tunneling rate Γ assuming spin-conserving tunneling. For the charge current and spin current, the construction as described in Appendix E7 gives two contributing diagrams, depicted in Fig. 24(a).

In first order, there is only one irreducible contraction possible. Furthermore, the H.c. indices η are fixed by the observable vertex. However, there are two possibilities to choose the charge indices χ for the tunneling double vertex. The total sign of the diagram equals χ since we have (i) a factor -1 due to one crossing, (ii) a factor $\bar{\chi}$ due to the early and late vertices, and (iii) a factor $+$ since there are no intermediate vertices. This results in

$$\begin{aligned} \langle I_{R_{\mu}}^L \rangle &= 2\text{Im} \left[\int d\omega_1 d\omega_{1'} \frac{1}{i0 - \omega_{1'} + \omega_1} \right. \\ &\times \sum_{\rho_1 \rho_{1'} \tau_1 \tau_{1'}} \sum_{\chi} \chi (F_{\chi}^L)_{\rho_1}(\omega_1) (F_{\bar{\chi}}^R)_{\rho_{1'}}(\omega_{1'}) (\check{t}_{\tau_1} \check{t}_{\tau_2}) \\ &\left. \times \text{tr}(\check{r}_{\rho_{1'}} \check{r}_{\tau_2} \check{r}_{\rho_1} r_{\mu} \check{r}_{\tau_1}) \right], \quad (\text{D1}) \end{aligned}$$

where $(F_i)_{\rho_i} = \bar{v}^{r_i}(\omega_i) f_{\bar{\chi}_i}^{r_i}(\omega_i) \sqrt{2}[\delta_{\rho_i,0} + (1 - \delta_{\rho_i,0})n^r \hat{J}_{\rho_i}^r]$. Note that r_{μ} is associated with the current vertex and therefore has no ‘‘check.’’ For our case, the tunneling is spin-independent so that $\check{t}_{\tau} = \sqrt{2}t\delta_{\tau,0}$. We use furthermore $\check{r}_0 = r_0/\sqrt{2} = \mathbb{1}/\sqrt{2}$, $\check{r}_i = \sqrt{2}r_i = \sqrt{2}s_i$ for $i = 1, 2, 3$ and

$$\begin{aligned} \text{tr}(\check{r}_{\rho_{1'}} \check{r}_{\rho_1} \check{r}_{\mu}) &= \frac{1}{\sqrt{2}}\delta_{\mu 0}\delta_{\rho_1 \rho_{1'}} + \frac{1}{\sqrt{2}}\bar{\delta}_{\mu,0}(\delta_{\rho_1 0}\delta_{\rho_{1'} \mu} + \delta_{\rho_{1'} 0}\delta_{\rho_1 \mu} + i\varepsilon_{\rho_{1'} \rho_1 \mu}). \quad (\text{D2}) \end{aligned}$$

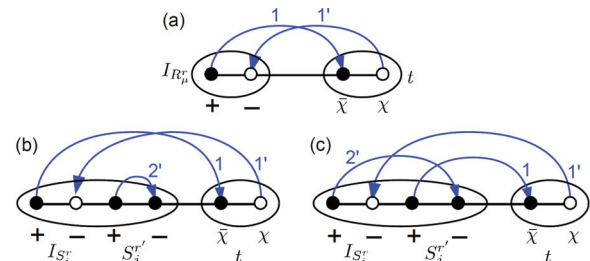


FIG. 24. (Color online) Diagrams representing $O(\Gamma)$ contributions to (a) charge current and spin current, (b) direct SQM current, and (c) exchange-SQM current.

We obtain the charge current (89) given in the main text,

$$\begin{aligned} \langle I_N^L \rangle &= 2\text{Im} \left\{ \int_{11'} \frac{1}{\pi} \Gamma_{11'}^{LR} (-\Delta_{11'}) (1 + \mathbf{n}_1^L \cdot \mathbf{n}_{1'}^R) \right. \\ &\quad \times \left. \left[P \frac{1}{\omega_1 - \omega_{1'}} - i\pi \delta(\omega_1 - \omega_{1'}) \right] \right\} \\ &= 2 \int_{11'} \Gamma_1 \Delta_1 (1 + \mathbf{n}_1^L \cdot \mathbf{n}_{1'}^R), \end{aligned} \quad (\text{D3})$$

and for the spin current we obtain Eq. (90) of the main text,

$$\begin{aligned} \langle I_{S_i}^L \rangle &= 2\text{Im} \left\{ \int_{11'} \Gamma_{11'}^{LR} (-\Delta_{11'}) \right. \\ &\quad \times \left[P \frac{1}{\omega_1 - \omega_{1'}} - i\pi \delta(\omega_1 - \omega_{1'}) \right] \\ &\quad \times \left. \frac{1}{2} [\mathbf{n}_1^L + \mathbf{n}_{1'}^R + i(-\mathbf{n}_1^L \times \mathbf{n}_{1'}^R)] \right\} \\ &= \int_1 \Gamma_1 \left[\Delta_1 (\mathbf{n}_1^L + \mathbf{n}_{1'}^R) + \frac{\mathbf{n}_1^L}{\bar{v}_1^R} \times \beta_1^R + \beta_1^L \times \frac{\mathbf{n}_{1'}^R}{\bar{v}_1^L} \right]. \end{aligned} \quad (\text{D5})$$

Here we introduced the short-hand notations $\Gamma_1 = \Gamma_{11'}^{LR}$, $n_1^r = n^r(\omega_1)$ and furthermore

$$\Gamma_{11'}^{LR} = \Gamma_{11'}^{RL} = 2\pi |t|^2 \bar{v}^L(\omega_1) \bar{v}^R(\omega_{1'}), \quad (\text{D6})$$

$$\Delta_{11'} = f_+^R(\omega_{1'}) - f_+^L(\omega_1), \quad (\text{D7})$$

$$\beta^r(\varepsilon) = - \int d\omega P \frac{f_+^r(\omega) \bar{v}^r(\omega) n^r(\omega)}{\omega - \varepsilon}. \quad (\text{D8})$$

Here $P(\frac{1}{z}) = \text{Re}(\frac{1}{z+i0})$ denotes the principal value.

The calculation of the SQM current in $\text{O}(\Gamma)$ for spin-independent tunneling proceeds in a similar way. However, due to its two-particle nature, there are two pairs of diagrams with different contraction topologies, which make up the direct [Fig. 24(b)] and the exchange contribution [Fig. 24(c)] to the SQM current, respectively. Each pair differs with respect to charge indices.

On the level of diagrams, one immediately sees that the expressions involving the spin operator and the spin current operator factorize for the direct contribution since the contraction labeled with $2'$ in Fig. 24(b) does not cross any other lines. This corresponds to the product of the expectation value of two operators. Therefore, without any further calculation, we obtain

$$\langle \mathcal{I}_{\mathcal{Q}}^{LL} \rangle_{\text{dir}} = 2 \langle \mathbf{I}_S^L \rangle \odot \langle \mathbf{S}^L \rangle, \quad (\text{D9})$$

where $\langle \mathbf{I}_S^L \rangle$ is the previously calculated spin current (D5). The evaluation of the exchange contribution is more complicated because the $2'$ contraction does cross other lines. Applying the diagram rules from Appendix E 8, we obtain

$$\begin{aligned} \langle \mathcal{I}_{\mathcal{Q}}^{LL} \rangle_{\text{ex}} &= 2 \cdot 2 \sum_{\chi} \bar{\chi} \text{Im} \int d\omega_1 d\omega_{1'} d\omega_2 \\ &\quad \times \frac{2t^2 f_-^L(\omega_2) f_{\chi}^L(\omega_1) (F_{\bar{\chi}}^R)_{\rho_{1'}}(\omega_{1'})}{i0 + \omega_1 - \omega_{1'}} \\ &\quad \times \mathcal{A}_{\mu\nu}^L \text{tr}(\check{r}_{\mu} \mathbf{s} \odot \check{r}_{\nu} \mathbf{s}_{\rho_{1'}}), \end{aligned} \quad (\text{D10})$$

where the 2DOS (16) enters through the matrix $\mathcal{A}_{\mu\nu}^L$ given by Eqs. (A12)–(A15). The first factor 2 comes from Hermitian conjugation symmetry; the second factor of 2 is due to the product rule when applying the derivative to the SQM operator, which is quadratic in spin [cf. Eq. (85)]; and the third one in the second line is associated with the SQM current vertex (see Appendix E 8). The sign factor is obtained as follows: The number of crossings is even and the intermediate spin vertex has $\eta_e = +$, giving no sign, but from the early and late vertex, we obtain a sign factor $\bar{\chi}$. It remains to calculate the spin trace by employing the anticommutation relations of spin- $\frac{1}{2}$ operator algebra and the identity $\mathbf{s} \odot \mathbf{s} = 0$ [cf. Eq. (51)]:

$$\begin{aligned} \langle \mathcal{I}_{\mathcal{Q}}^{LL} \rangle_{\text{ex}} &= 2 \int_{1,2'} f_+^L(\omega_2) \Gamma_1^{LR} \Delta_1 \\ &\quad \times \left[\frac{(\mathcal{A}_{12'}^L)_{0i} n_1^R \mathbf{e}_i \odot \hat{\mathbf{J}}^R + (\mathcal{A}_{12'}^L)_{ij} \mathbf{e}_i \odot \mathbf{e}_j}{\bar{v}_1^L} \right] \\ &\quad + 2 \int_{1,1',2'} f_+^L(\omega_2) \Gamma_{11'}^{LR} \Delta_{11'} P \frac{1}{\omega_1 - \omega_{1'}} \\ &\quad \times \left[\frac{(\mathcal{A}_{12'}^L)_{ij} n_{1'}^R \mathbf{e}_i \odot (\mathbf{e}_j \times \hat{\mathbf{J}}^R)}{\bar{v}_1^L} \right] \end{aligned} \quad (\text{D11})$$

$$\begin{aligned} &= -2 \int_1 \Gamma_1^{LR} \Delta_1 [\tilde{a}_1^L n_1^R \hat{\mathbf{J}}^L \odot \hat{\mathbf{J}}^R + a_1^L \hat{\mathbf{J}}^L \odot \hat{\mathbf{J}}^L] \\ &\quad - 2 \int_{1,1'} \Gamma_{11'}^{LR} \Delta_{11'} P \frac{1}{\omega_1 - \omega_{1'}} \\ &\quad \times [a_1^L n_{1'}^R \hat{\mathbf{J}}^L \odot (\hat{\mathbf{J}}^L \times \hat{\mathbf{J}}^R)]. \end{aligned} \quad (\text{D12})$$

Restoring all indices explicitly, we obtain Eq. (91), the main result of the paper. Moreover, we identified the spin-anisotropy functions (104) and (66):

$$a^L(\omega) = \int d\omega' f_+^L(\omega') \sum_{\sigma\sigma'} \frac{\sigma\sigma'}{4} \frac{v_{\sigma\sigma'}^L(\omega, \omega')}{\bar{v}^L(\omega)}, \quad (\text{D13})$$

$$\tilde{a}^L(\omega) = \int d\omega' f_+^L(\omega') \sum_{\sigma\sigma'} \frac{\sigma'}{4} \frac{v_{\sigma\sigma'}^L(\omega, \omega')}{\bar{v}^L(\omega)}. \quad (\text{D14})$$

APPENDIX E: COVARIANT REAL TIME DIAGRAMMATICS

In this appendix, we give a self-contained derivation of the technique used for calculating the charge, spin-dipole and SQM currents. Using this technique the actual calculation becomes very compact and is presented in Appendix D. The interest in presenting the derivation here lies in three factors. (i) The real-time technique is more general and can be applied to more complex systems containing strongly interacting localized systems. Therefore, it is not often applied to noninteracting systems since other approaches are available in that case. However, for the calculation of multiparticle averages, its practical rules of calculation prove to be very convenient. Therefore, it is of interest to point out how the technique simplifies when applied to noninteracting problems. (ii) We reformulate the real-time technique here such that one can deal more efficiently with any nontrivial spin dependencies. In a forthcoming work we show that this generalizes to the more complex cases.²² (iii) Finally, it is also of great help to have these simpler calculations, formulated in the same way,

for comparison to the more complex ones (for which other approaches do not work anymore).²²

After reviewing the compact Liouville space notation^{40–42} in Appendix E 1, we indicate how the general real-time approach simplifies and show that the calculation of operator expectation values in the long-time limit and to any order in the tunnel-coupling $\Gamma = 2\pi v^L v^R |t|^2$ amounts to evaluation of irreducible diagrams in a perturbation expansion (Appendix E 3). The central technical achievement of this paper is a *covariant* formulation of these diagram rules for the charge, spin-dipole, and SQM current: The expressions they produce are manifestly invariant under the change of the coordinate system and of the spin-quantization axis (cf. Secs. III B 1 and III B). They are thus coordinate-free both in real space and in Hilbert/Liouville space. This reformulation is crucial to keep the calculation of the nonequilibrium steady-state average of the SQM tractable. The required steps are

- (1) separation of spin and energy dependence in the diagrammatic expressions, recasting the spin part as traces over Pauli operators (Appendix E 4);
- (2) collection of all sign factors (Appendix E 5);
- (3) halving the number of diagrams by exploiting their complex conjugation symmetry (Appendix E 6);
- (4) identification of observable-specific diagram rules for charge, spin-dipole (Appendix E 7); and finally
- (5) spin-quadrupole current (Appendix E 8).

To our knowledge, steps (1), (3) and (5) have not been conveniently integrated into the real-time diagrammatic technique so far. We note that the technique formulated is more general than the problem of interest in two ways: It applies to (i) arbitrary orders of the tunnel coupling and (ii) models with spin-dependent tunnel amplitudes.

1. Compact notation in Liouville space

The calculation is formulated entirely in Liouville space, the space of linear operators acting on a Hilbert space of a quantum mechanical system. The linear transformations of operators, the elements of Liouville space, are called superoperators. Although our notation follows Ref. 40 and recent developments reported in Ref. 42, we have made some further convenient modifications which warrant some discussion.

Similar to any usual operator, any superoperator can be expressed in terms of *field superoperators*, which we define following⁴²

$$J_{1\cdot} = (-\chi_1 \eta_1)^{\mathcal{N}} \begin{cases} c_{r_1 \eta_1 n_1 k_1 \sigma_1} \cdot, & \chi_1 \eta_1 = -, \\ \cdot c_{r_1 \eta_1 n_1 k_1 \sigma_1}, & \chi_1 \eta_1 = +. \end{cases} \quad (\text{E1})$$

Here the “ \cdot ” denotes the operator argument of the superoperator, and $\mathcal{N} = [N, \cdot]$ is the particle number superoperator. The subscript “1” is an abbreviation for all indices,

$$1 = (\chi_1, \eta_1, r_1, n_1, k_1, \sigma_1). \quad (\text{E2})$$

Here η_1 is the Hermitian conjugation index, which determines whether the field operator is a creation operator ($c_{\eta_1=-} = c^\dagger$) or an annihilation operator ($c_{\eta_1=+} = c$) of an electron in electrode r_1 in band n_1 in mode k_1 with spin σ_1 . This notation uses the charge index χ_1 , which distinguishes whether physically the total superparticle number is increased ($\chi_1 = +$) or decreased

($\chi_1 = -$) by the action of J_1 [note η_1 does not have such physical meaning: an annihilation (creation) operator acting from the right *increases* (*decreases*) the superparticle number]. We prefer this physically more meaningful charge index χ instead of the commonly used Keldysh index $p = -\chi \eta$.

The time evolution of the density operator in Appendix E 3 is generated by the Liouvillian superoperator $L = L_0 + L_T$ describing the internal evolutions, $L_0 = [H_0, \cdot]$, and the one due to tunneling, $L_T = [H_T, \cdot]$. Using Eq. (E1), we obtain

$$L_0 = \delta_{\chi_1, +} \varepsilon_1 J_1 J_{\bar{1}}, \quad (\text{E3})$$

with $\varepsilon_1 = \varepsilon_{n_1 k_1 \sigma_1}^{r_1}$ and

$$L_T = T_{11'} J_1 J_{1'}, \quad (\text{E4})$$

where

$$T_{11'} = \bar{\chi}_{1'} \delta_{\eta_1 \bar{\eta}_{1'}} \delta_{\chi_1 \bar{\chi}_{1'}} \delta_{r_1 L} \delta_{r_{1'} R} [T_{\sigma_1 \sigma_{1'}}^{LR}]^{\eta_{1'}}. \quad (\text{E5})$$

Here we extended the use the Hermitian-conjugation index η as *superscript* to indicate complex conjugation, i.e., $[T_{\sigma_1 \sigma_{1'}}^{LR}]^+ := T_{\sigma_1 \sigma_{1'}}^{LR}$ and $[T_{\sigma_1 \sigma_{1'}}^{LR}]^- := T_{\sigma_1 \sigma_{1'}}^{LR*}$. In Eqs. (E3) and (E4) we implicitly sum over all indices contained Eq. (E2).

Our main interest is to deal efficiently with the dependence of expressions on the choice of the spin-quantization axis. However, for noncollinear spin-polarized systems, there exists no specific choice for the spin-quantization axis that simplifies the calculations considerably. The best strategy is therefore to completely remove a reference to the spin quantization axis in all expressions. We start with the tunneling Liouvillian, for which we allow for any type of symmetry-breaking tunneling processes, for example, due to a magnetic impurity in the barrier. The most general tunneling amplitudes reads

$$T_{\sigma\sigma'}^{LR} = {}_L \langle \sigma | \check{\mathbf{t}} \cdot \check{\mathbf{r}} | \sigma' \rangle_R, \quad (\text{E6})$$

where $\check{\mathbf{r}} \cdot \check{\mathbf{t}} = \sum_{\mu=0}^3 \check{r}_\mu \check{t}_\mu$. Here $\check{\mathbf{r}}$ is a four-component vector of operators $\check{r}_0 = \mathbb{1}/\sqrt{2}$ and $\check{r}_i = \sqrt{2} s_i$ for $i = x, y, z$ forming a basis for the Liouville space formed by operators acting on the spin- $\frac{1}{2}$ Hilbert space. The basis is orthonormal with respect to the scalar product $(A, B) = \text{tr}(A^\dagger B)$. The tunneling is completely specified by a four-component vector $\check{\mathbf{t}}$: If L_T is spin-conserving, as assumed in the main part of the paper, the spatial components of $\check{t}_\mu = \delta_{\mu,0} \sqrt{2} t$ must be zero [and Eq. (E6) reduces to Eq. (11) of Sec. II]. Spin-nonconserving tunneling processes are thus introduced by any further nonzero components $\check{t}_i = t_i/\sqrt{2}$ for $i = x, y, z$. Note that the spin-dependence through the bra and ket in Eq. (E6) merely reflects the choice of (different, arbitrary) quantization axes for the field operators in the reservoirs connected by the tunneling: Clearly it should cancel out of the final answer. Written in the form (E6), the tunneling Liouvillian is explicitly covariant: Changing either of these quantization axes merely changes the meaning of the dummy indices σ, σ' . There is also no explicit dependence on the coordinate system either, since $\check{\mathbf{t}} \cdot \check{\mathbf{r}}$ is a coordinate-free expression.

2. Wick's theorem for superoperators

For the perturbative calculation of expectation values in Appendix E 3, we use Wick's theorem for the field superoperators

as defined in Eq. (E1), which reads as⁴³

$$\langle J_n \cdots J_1 \rangle = \text{tr}(J_n \cdots J_1 \rho_0) = \sum_{\text{contr.}} (-1)^{N_p} \prod_{i < j} \gamma_{ji}, \quad (\text{E7})$$

with the grand canonical distribution

$$\rho_0 = \prod_r \frac{1}{Z^r} e^{-(H_0^r - \mu N^r)/T^r}, \quad (\text{E8})$$

the partition function $Z^r = \text{tr}_r(e^{-(H_0^r - \mu N^r)/T^r})$, and the contraction function

$$\gamma_{11'} = (-\chi_{1'} \eta_{1'}) \delta_{1\bar{1}'} |_{\text{excl. } \chi} f_{1'}. \quad (\text{E9})$$

Here $f_1 = f[\bar{\chi}_1(\varepsilon_{k_1\sigma_1}^{r_1} - \mu^{r_1})/T^{r_1}]$ with the Fermi function $f(x) = 1/(e^x + 1)$. In Eq. (E9), $\delta_{1\bar{1}'} |_{\text{excl. } \chi}$ denotes a Kronecker symbol for all indices 1 and $\bar{1}'$ except for the charge indices χ . In agreement with physical intuition, the charge index $\chi_{1'}$ at the beginning of the process determines the type of distribution function appearing: $\chi_{1'} = +(-)$ corresponds to a particle (hole).⁴⁴ In Eq. (E7), we sum as usual over all possible pair contractions and N_p is the signature of the permutation that is needed to disentangle all pairs of contracted superoperators while keeping the order of the contracted operators within a pair. The easy form of Eq. (E7) relies on the fact that the field superoperators obey anticommutation relations,

$$[J_1, J_{1'}]_+ = (-\chi_1 \eta_{1'}) \delta_{1\bar{1}'}, \quad (\text{E10})$$

with $\delta_{1\bar{1}'} = \delta_{r_1 r_{1'}} \delta_{k_1 k_{1'}} \delta_{n_1 n_{1'}} \delta_{\sigma_1 \sigma_{1'}} \delta_{\chi_1 \chi_{1'}} \delta_{\eta_1 \eta_{1'}}$ with the conjugate multi-index:

$$\bar{1} = (-\chi_1, -\eta_1, r_1, n_1, k_1, \sigma_1). \quad (\text{E11})$$

The inclusion of the *fermion-parity* superoperator $(-\chi_1 \eta_1)^{N}$ in Eq. (E1) is crucial for the validity of Eq. (E10) from which Eq. (E7) basically follows, as pointed out by Saptsov *et al.*⁴²

3. Perturbative calculation of expectation values

The expectation value of an observable A is given by

$$\langle A \rangle(t) = \text{Tr}(A \rho^{\text{tot}}(t)), \quad (\text{E12})$$

where $\rho^{\text{tot}}(t) = e^{-iL(t-t_0)} \rho_0$ is the time-dependent density operator of the total system and $L = L_0 + L_T$ is the Liouvillian. We are interested in the long-time limit of Eq. (E12), which by virtue of the final value theorem,

$$A := \lim_{t \rightarrow \infty} \text{tr}(A \rho(t)) = (-i) \lim_{z \rightarrow i0} z \langle A \rangle(z), \quad (\text{E13})$$

follows from the Laplace transform $\langle A \rangle(z) = \int_{t_0}^{\infty} dt e^{izt} \langle A \rangle(t)$ of $\langle A \rangle(t)$ with $\text{Im}(z) > 0$. We obtain

$$\langle A \rangle(z) = \text{Tr} \left(A \frac{i}{z - L_0 - L_T} \rho_0 \right). \quad (\text{E14})$$

The trace can be evaluated if we rewrite the resolvent $(z - L_0 - L_T)^{-1}$ in terms of a power series in L_T , apply Wick's theorem, collect diagrams irreducibly contracted to the A operator into a self-energy kernel $\Sigma_A^{\text{irr}}(z)$, and re-sum the series

$$\langle A \rangle(z) = \Sigma_A^{\text{irr}}(z). \quad (\text{E15})$$

To compare this simple result to the usual situation considered in the real-time approach, we assume for a moment that the

leads are tunnel-coupled to an *interacting* system with a few degrees of freedom. Since only the noninteracting leads can be integrated out by applying Wick's theorem, the objective is to derive an exact effective theory for the reduced density operator of the system $\rho = \text{Tr}_{\text{res}} \rho^{\text{tot}}$. By merely replacing $\text{Tr}(A \dots) \rightarrow \text{Tr}_{\text{res}}(\dots)$, one may take the same steps as above to express the Laplace transform of the reduced density matrix as

$$\rho(z) = \text{Tr}_{\text{res}} \left(\frac{i}{z - L_0 - L_T} \rho_0 \right) \quad (\text{E16})$$

$$= \frac{i}{z - L - \Sigma(z)} \rho(t_0), \quad (\text{E17})$$

where $\Sigma(z)$ is the (reducible) self-energy. Equation (E16) is used as a starting point for a diagrammatic perturbation theory in the coupling L_T . In our case, we have simply no “reduced system”, i.e., $L = \Sigma(z) = 0$ and $\rho(z) = i/z$ for $\rho(t_0) = \text{Tr}_{\text{res}} \rho^{\text{tot}}(t_0) = 1$ when we take the trace over leads.

Most of the steps that follow up can be generalized to the case where there is a nontrivial system coupled to the reservoirs,²² making the following analysis of interest.

The left action of A , considered as a superoperator, can be expressed in terms of field superoperators, i.e.,

$$A \cdot = A_{a_1, \dots, a_m a_{1'}, \dots, a_{m'}} J_{a_1} \cdots J_{a_m} J_{a_{1'}} \cdots J_{a_{m'}}, \quad (\text{E18})$$

where we assume $r_{a_i} = L$ and $r_{a_{i'}} = R$, which can always be achieved by a rearrangement of the field superoperators by virtue of the anticommutation relation (E10). Using $L_T = T_{11'} J_1 J_{1'}$ and $L_0 J_1 = J_1(L_0 - x_1)$ with $x_1 = \eta_1 \varepsilon_1$, we can shift all field superoperators to the left. Since ρ_0 is an eigenstate of the internal Liouvillian, that is, $L_0 \rho_0 = 0$, we can pull ρ_0 also to the left, setting all L_0 to zero in the resolvents and finally apply Wick's theorem Eq. (E7). We obtain for the n th-order contribution to the Laplace transform:

$$\begin{aligned} \Sigma_A^{\text{irr}}(z)|_n &= \sum_{\text{contr.}, \{k\}} A_{a_1, \dots, a_m a_{1'}, \dots, a_{m'}} T_{n n'} \cdots T_{1 1'} \\ &\times \prod_{k=1}^n \frac{1}{z + X_k} (-1)^{N_p} \prod_{i < j} \gamma_{ji}. \end{aligned} \quad (\text{E19})$$

The sum includes all possible pair contractions and all indices $\{k\} = \{a_1, \dots, a_{m'}, n, n', \dots, 1, 1'\}$. The frequencies in the propagators read

$$X_i = \sum_{j < i} (\eta_j \varepsilon_j + \eta_{j'} \varepsilon_{j'}). \quad (\text{E20})$$

We represent the expressions contributing to Eq. (E19) by diagrams as follows: Each tunneling amplitude $T_{ii'}$ is associated with a double vertex (two dots) on a line. The line represents the free propagation of the system, directed from right (earlier times) to left (later times), so that the order of the vertices naturally corresponds to the order of the field operators in the expression Eq. (E19). The leftmost element is a $2m$ vertex with $2m$ dots, which represents the m particle observable A . As usual,⁴⁰ contractions are depicted by lines *above* the propagator line connecting two associated dots i and j . Furthermore, the electrode indices of the dots are fixed: All i indices belong to $r = L$ (solid dots in Fig. 25), whence all i' indices belong to $r = R$ (open dots in Fig. 25).

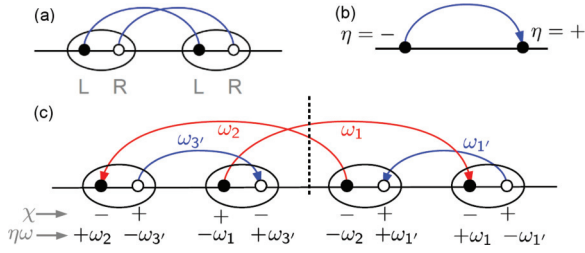


FIG. 25. (Color online) Examples for Liouville space diagrams: (a) two contracted tunneling Liouvillians, (b) Hermitian conjugation indices expressed by directions of arrows, (c) reading off the propagator for a certain segment (for the segment indicated by the vertical dashed line, we obtain $X_2 = \omega_1 - \omega_2$). Charge indices χ are denoted by + or - below the propagator line, the factors $\eta\omega$ appearing in Eq. (E20) are shown for the sake of completeness.

The factor X_i of the i th propagator segment can be readily read off from the diagrams as illustrated in Fig. 25: First, all energies associated with contractions that connect dots that lie on the same side of this segment do not contribute to X_i [cf. Fig. 25(c), blue contractions]. For “later” dots this is clear as they are always excluded in the sum of definition (E20). For “earlier” dots the respective energy occurs twice in the sum with opposite sign η_i [enforced to the contraction (E9)]. Thus, only the contraction lines that intersect a vertical line drawn at the i th propagator segment contribute to X_i [red contractions in Fig. 25(c)]. To determine X_i completely, we need to know the H.c. indices η_i , which we depict by arrows attached to the contraction lines: If a vertex has $\eta_i = +(-)$, the arrow points towards (away from) this vertex [see Fig. 25(b)].

Finally, we indicate the charge index $\chi = \pm$ of every dot in the diagram by a sign below the propagator line [see Fig. 25(c)]. Note that charge indices χ of a double vertex must be opposite by Eq. (E5). Our diagrams therefore represent the algebraic expression associated with both a fixed contraction structure and *fixed* (η, χ) indices. The latter is a distinction to the Liouville space diagrams used, e.g. in Ref. 40: Here distinct combinations of (η, χ) represent *distinct* diagrams. Hence, the n th-order contribution $\langle A \rangle_n$ to the expectation value of A is represented by a set of diagrams covering all allowed combinations contractions *and* all combinations for (η, χ) 's.

For the ensuing discussion, we first ignore any sign factors in $\langle A \rangle_n(z)$, for example, due to the contraction functions. This discussion and the question of which diagrams are allowed are most conveniently postponed to the very end of our derivations.

4. Energy-spin separation

We now arrive at the crucial part of the derivation of *covariant* diagram rules: the separation of the spin-dependent and energy-dependent parts in $\Sigma_A^{\text{tr}}(i0)$ and recasting the former as a trace in spin space similar to Appendix A 2. For the sake of simplicity, we first replace the observable vertex with a tunneling vertex and discuss modifications afterwards.

In Eq. (E19), we have three different spin-dependent factors: (i) the energies $\varepsilon_i = \varepsilon_{n_i k_i \sigma_i}^{r_i}$, (ii) the contractions $\gamma_{ij} \propto \delta_{\sigma_i \sigma_j}$, and (iii) the tunneling amplitudes $t_{\sigma \sigma'}$.

(i) + (ii) Any pair of contracted indices, say i and j occur in Eq. (E19) with a sum of the form

$$\sum_{n_i, k_i} \delta_{\sigma_i \sigma_j} g(\varepsilon_{n_i k_i \sigma_i}^{r_i}), \quad (\text{E21})$$

where g is some function of $\varepsilon_{n_i k_i \sigma_i}^{r_i} = \varepsilon_{n_j k_j \sigma_j}^{r_j}$. We can get rid of the spin dependence of the energies by introducing the spin-dependent DOS, proceeding analogous to the derivation of Eq. (45). Equation (E21) then equals

$$\int d\omega_i \bar{v}^{r_i}(\omega_i) g(\omega_i) [\langle \sigma_j | \check{\mathbf{r}} \cdot \check{\mathbf{n}}^{r_i}(\omega_i) | \sigma_i \rangle_{r_i}]^{\bar{\eta}_i}. \quad (\text{E22})$$

The scalar product now involves a new 4-vector with $\check{\mathbf{n}}(\omega) = \sqrt{2}(1, n^r(\omega) \hat{\mathbf{J}}^r)$. Furthermore, we artificially introduced the complex conjugation by $\bar{\eta}$ even though the matrix elements ${}_r \langle \sigma | \check{\mathbf{r}} \cdot \check{\mathbf{n}}^r(\omega) | \sigma' \rangle_r$ are real. This will become advantageous for later manipulations. We therefore simply replace ε_i with ω_i in Eq. (E19) and the sum over the index i now abbreviates also an integration over ω_i instead of a summation over n_i, k_i .

(iii) The spin-dependence of the tunneling amplitudes can be rewritten as a matrix element in spin space, too:

$$[T_{\sigma \sigma'}^{LR}]^{\eta'} = [{}_L \langle \sigma | \check{\mathbf{t}} \cdot \check{\mathbf{r}} | \sigma' \rangle_R]^{\eta'}. \quad (\text{E23})$$

We next separate the frequency-dependent parts (propagators, Fermi functions, $\check{\mathbf{t}}$ and $\check{\mathbf{n}}$ vectors) and the spin-dependent matrix elements, which leads to

$$A|_n = \sum_{\{\kappa, \rho, \omega_i\}} (\text{signs})(\text{prop.}) \left[\cdots \check{t}_{\kappa_i} \cdots \frac{(F_i)_{\rho_i}}{\pi} \cdots \right] \times \sum_{\{\sigma\}} (\cdots (\check{r}_{\kappa_i})_{\sigma_i \sigma_i'}^{\eta_i'} \cdots (\check{r}_{\rho_i})_{\sigma_k \sigma_k'}^{\bar{\eta}_k'} \cdots). \quad (\text{E24})$$

The sum over the κ_i 's and ρ_i 's indicates the scalar products of the respective 4-vectors with the matrix elements $(\check{r}_{\mu})_{\sigma_i \sigma_i'}$ of the charge-spin operator \check{r}_{μ} . For simplicity, we do not indicate here the quantization axis for the basis states used to express these matrix elements since we see below that this choice drops out. We moreover introduced the abbreviation

$$(F_i)_{\rho_i} = \bar{v}^{r_i}(\omega_i) \check{n}_{\rho_i}^{r_i}(\omega_i) f_{\bar{\chi}_i}^{r_i}(\omega_i). \quad (\text{E25})$$

Interestingly, the sum over the spin indices factorizes into sums over the spin indices of vertices that are connected in the diagrams in a *loop* (when formally considering contraction lines to be connected at each double vertex [cf. Fig. 25(c)], which consists of a single loop). The contribution of each loop can be evaluated independently as follows: We start at an arbitrary dot and follow the directed contraction line. For every loop element we encounter (vertex, contraction), we put charge-spin operators in a sequence from the right to the left into a trace. For example, starting at the dot labeled $1'$ in Fig. 25(c), we obtain the expression $\text{tr}(\check{r}_{\kappa_1'} \check{r}_{\rho_1} \check{r}_{\kappa_3'} \check{r}_{\rho_3'} \check{r}_{\kappa_4'} \check{r}_{\rho_2'} \check{r}_{\kappa_2'} \check{r}_{\rho_1'})$. Thus, Eq. (E24) becomes

$$A|_n \sim (\text{signs}) \int_{\{\omega_i\}} (\text{propagators}) \times \prod_{\text{loops}} \text{tr}[\cdots (\check{\mathbf{t}} \cdot \check{\mathbf{r}}) \cdots (\mathbf{F}_i \cdot \check{\mathbf{r}}) \cdots], \quad (\text{E26})$$

where we moved the frequency-dependent 4-vectors \mathbf{t} and \mathbf{F}_i into the spin traces and restored the scalar products.

The rest of this section is dedicated to prove this simple rule. We therefore start from the sequence of matrix elements $\check{r}_{\sigma\sigma'}$, obtained by writing them down from the right to the left in the order in which we encounter them when following a directed loop. We have to prove that pairs of the same spin indices are next to each other when we change all Hermitian conjugation indices of the matrix elements in to in Eq. (E24) to + (except for the left- and rightmost one), so that the expression can be recast as a trace. We suppress the μ indices for convenience and we let σ_{prec} denote a spin index of the preceding element we have already run through and σ_{succ} refers to a spin index of the succeeding loop element. We have to insert the following factors.

(i) For each contraction, put a factor $\check{r}_{\sigma_{\text{late}}\sigma_{\text{early}}}^{\eta_{\text{early}}}$ where η_{early} is the H.c. index of the earlier vertex involved. We first note that the H.c. index η_i of the vertex i at which we start to follow a contraction line has always $\eta_i = -$ (the arrow points away from the vertex). We have to distinguish two cases: (ia) If we start at the early vertex (e.g., contraction 1' in Fig. 11), we have $\eta_{\text{early}} = -$ and thus $\check{r}_{\sigma_{\text{late}}\sigma_{\text{early}}}^{\eta_{\text{early}}} = \check{r}_{\sigma_{\text{succ}}\sigma_{\text{prec}}}^+$; in case (ib) we start at the late vertex [e.g., contraction 1 in Fig. 25(c)], so $\eta_{\text{early}} = +$ and thus $\check{r}_{\sigma_{\text{late}}\sigma_{\text{early}}}^{\eta_{\text{early}}} = \check{r}_{\sigma_{\text{prec}}\sigma_{\text{succ}}}^- = \check{r}_{\sigma_{\text{succ}}\sigma_{\text{prec}}}^+$, using the Hermiticity of the Pauli matrices.

(ii) For each double vertex, we put a factor $\check{r}_{\sigma_{\text{late}}\sigma_{\text{early}}}^{\eta_{\text{early}}}$. Again, there are two cases: (a) If $\eta_{\text{early}} = +$, we arrive at the earlier vertex, so we have $\check{r}_{\sigma_{\text{late}}\sigma_{\text{early}}}^{\eta_{\text{early}}} = \check{r}_{\sigma_{\text{succ}}\sigma_{\text{prec}}}^+$ [e.g., later double vertex in Fig. 25(c)]; (b) if $\eta_{\text{early}} = -$ [e.g., earlier vertex in Fig. 25(c)], we arrive at the later vertex, so we have $\check{r}_{\sigma_{\text{left}}\sigma_{\text{right}}}^{\eta_{\text{early}}} = \check{r}_{\sigma_{\text{prec}}\sigma_{\text{succ}}}^- = \check{r}_{\sigma_{\text{succ}}\sigma_{\text{prec}}}^+$. These considerations prove the simple rule

$$\sum_{\{\sigma_i, \sigma_{i'}\}} \check{r}_{\sigma_n \sigma_{n'}}^+ \cdots \check{r}_{\sigma_1 \sigma_{1'}}^+ \check{r}_{\sigma_1 \sigma_n}^+ = \text{tr}(\check{r} \cdots \check{r}). \quad (\text{E27})$$

Here we used that the matrix elements of adjacent Pauli operators are taken for spin states with respect to the *same* quantization axis; i.e., we can combine $\sum_{\sigma_{i'}} \check{r}_{\sigma_1 \sigma_{i'}}^+ \check{r}_{\sigma_{i'} \sigma_n}^+ = r_1 \langle \sigma_1 | \hat{r} | \sigma_{i'} \rangle_{r_1'} \langle \sigma_{i'} | \hat{r} | \sigma_n \rangle_{r_n} = r_1 \langle \sigma_1 | \hat{r} \hat{r} | \sigma_n \rangle_{r_n}$ and so on.

5. Sign factors

Having tackled the most tedious part, the spin and energy dependence, it remains to collect all sign factors of an expression from its representing diagram, yielding

$$\text{signs} = (-1)^{\#\text{cr.}} \prod_{\text{early+late vertices}} \chi_e \prod_{\text{intermediate vertices}} \eta_e. \quad (\text{E28})$$

Here $\#\text{cr.}$ is the number of crossing contraction lines and “e” always refers to the earlier vertex of each double vertex. The meaning of early/intermediate/late vertices is depicted in Fig. 26 and explained in the proof of Eq. (E28).

To prove Eq. (E28), we first note that there are three origins for signs: (i) an overall permutation factor $(-1)^{N_p}$ from Wick’s theorem (E7), (ii) a factor $(-\chi_{\text{early}} \eta_{\text{early}})$ for every contraction [see Eq. (E9)], and (iii) a factor $(-\chi_{\text{early}})$ for every double vertex [see Eq. (E5)]. The sign from (i) is readily obtained from the number of crossing contraction lines in the diagrams, giving the first factor of Eq. (E28). The signs due to (ii) and (iii) can be determined together: First of all, the minus signs

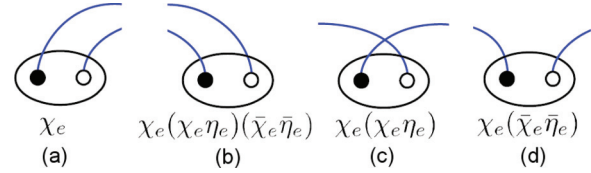


FIG. 26. (Color online) Different types of vertices: late (double) vertex (a), early (double) vertex (b), and intermediate double vertices (c), (d). The corresponding sign factors are denoted below the vertex. Note that χ_e, η_e refer to the earlier vertex of the double vertex and *not* to being earlier in the contractions.

can be omitted since the number of contractions and double vertices is always even. For the further procedure, it is helpful to distinguish three types of vertices sketched in Fig. 26: (a) “late (double) vertices”, where both vertices are the later ones in their contractions. Then no signs due to contractions have to be considered and only the charge index of the earlier vertex occurs. We furthermore have (b) “early (double) vertices” where both vertices are the earlier ones in their contractions. The signs due to *both* contractions cancel each other since charge and H.c. indices of both vertices in any double vertex are opposite. Thus, the sign for this type of vertex is again given by the earlier charge index. Finally, there are (c) “intermediate (double) vertices,” where one of the vertices is earlier and the other one is later in its contraction. The sign factor is in this case the H.c. index η_{early} of the earlier vertex of the double vertex.

6. Hermitian conjugated partner diagrams

Since any observable must have a real expectation value, the imaginary parts of all diagrams have to cancel each other. In fact, diagrams come in complex conjugates pairs, which are obtained from each other by inverting the H.c. indices, or, diagrammatically speaking, by inverting all arrow directions. Therefore, it is sufficient to take only *one* diagram as a *representative* of both. We therefore obtain schematically instead of Eq. (E26)

$$A|_n \sim 2\text{Re}(\text{signs}) \int_{\{\omega_i\}} (\text{propagators}) \times \prod_{\text{oriented loops}} \text{tr}[\cdots (\check{\mathbf{t}} \cdot \check{\mathbf{r}}) \cdots (\mathbf{F}_i \cdot \check{\mathbf{r}}) \cdots]. \quad (\text{E29})$$

We next explicitly show how the complex-conjugation symmetry arises in our formulation of real-time diagrammatics. Inverting all H.c. indices, $\eta_i \rightarrow \bar{\eta}_i$, involves the following modifications.

(i) The sign factor is negated. All charge indices may be kept fixed except for those of the current vertex [see Eq. (E33)]. This involves an additional minus sign from the early and late double vertices. The sign due to the intermediate vertices does not change since their number $\#\text{IV}$ of this type of vertices is always even. Reverting all $\eta_e \rightarrow \bar{\eta}_e$ therefore results in an additional factor $(-1)^{\#\text{IV}} = 1$ compared to the original sign factor.

(ii) The order of the Pauli operators in the spin trace is inverted, yielding the complex conjugate of the original trace

expression,

$$\text{tr}(\check{r}_1 \cdots \check{r}_n) \rightarrow \text{tr}(\check{r}_n \cdots \check{r}_1) = \text{tr}(\check{r}_1 \cdots \check{r}_n)^*, \quad (\text{E30})$$

where we used $\check{r}_1^\dagger = \check{r}_1$ and $(\check{r}_n^\dagger \cdots \check{r}_1^\dagger) = (\check{r}_1 \cdots \check{r}_n)^\dagger$.

(iii) The propagators are mapped onto their negative Hermitian conjugate since $X_i \rightarrow -X_i$:

$$\frac{1}{i0 + X_i} \rightarrow \frac{1}{i0 + (-X_i)} = -\left(\frac{1}{i0 + X_i}\right)^*. \quad (\text{E31})$$

As the number of propagators is odd, we obtain an additional minus sign.

Since all remaining factors are real [cf. Eq. (E26)] and have no further η dependence, we conclude that the mapping $\eta_i \rightarrow \bar{\eta}_i$ results in the *positive* complex conjugate contribution of the initial expression. Adding both these partner diagrams gives two times the real part of one of the two diagrams, proving Eq. (E29).

7. Covariant diagram rules for charge current and spin current

We first describe the modifications of the covariant diagram rules required for the charge current and spin current, which can be treated simultaneously as outlined in Sec. IV A. The expressions for the current operator read [see Eq. (80)]

$$I_{R'_\mu} = \sum_{nn'kk'\sigma\sigma'} (-ir_\mu T)_{\sigma\sigma'}^{r\bar{r}} c_{rnk\sigma}^\dagger c_{\bar{r}n'k'\sigma'} - \text{H.c.}, \quad (\text{E32})$$

with $(rT)_{\sigma\sigma'} = \sum_\tau r_{\sigma\tau} T_{\tau\sigma'}^{r\bar{r}}$. The structure of the current is very similar to the tunneling Hamiltonian with the simple replacement $T_{\sigma\sigma'}^{r\bar{r}} \rightarrow (-ir_\mu T)_{\sigma\sigma'}^{r\bar{r}}$. Introducing a superoperator for the left action $\mathcal{I}_{R'_\mu} \cdot = I_{R'_\mu} \cdot$, we may therefore treat the corresponding current vertices similar to the tunneling Liouvillian by making the replacement

$$\bar{\chi}_{1'} [{}_L \langle \sigma_1 | \check{\mathbf{t}} \cdot \check{\mathbf{r}} | \sigma_{1'} \rangle_R]^{n_{1'}} \rightarrow \delta_{\bar{\chi}_{1'} \eta_{1'}, +} [(-i)_L \langle \sigma_1 | i_{R'_\mu} | \sigma_{1'} \rangle_R]^{n_{1'}}, \quad (\text{E33})$$

with $i_{R'_\mu}$ given by Eq. (E36) below. The restriction $\delta_{\bar{\chi}_{1'} \eta_{1'}, +}$ is due to the fact that all field operators in $\mathcal{I}_{R'_\mu}$ act from the left, whereas the tunneling Liouvillian as a commutator also possesses a part that acts from the right. Consequently, we have accounted for the following modifications.

- (i) Insert $i_{R'_\mu}$ instead of $(\check{\mathbf{t}} \cdot \check{\mathbf{r}})$ into the spin traces.
- (ii) Set $\eta_{1'} = \bar{\chi}_{1'} = +$. The first equality follows from the factor $\delta_{\bar{\chi}_{1'} \eta_{1'}, +}$ in Eq. (E33) and the second from the freedom to chose one representative of the complex conjugated diagrams, which we fix by an explicit choice for $\eta_{1'}$. Note that the ‘‘missing’’ factor $\bar{\chi}_{1'} = +$ in the second line of Eq. (E33) does give any further modifications for this choice.
- (iii) Replace $\text{Re}(\cdots) \rightarrow \text{Im}(\cdots)$ in Eq. (E29), which is due to the additional factor $(-i)^{\eta_{1'} = +} = -i$ in Eq. (E33).

We now present a systematic way to draw all diagrams and read off the respective n th-order contributions to the expectation value $I_{R'_\mu} |n\rangle$, schematically given by

$$I_{R'_\mu} |n\rangle \sim \sum_{\substack{\text{irr. contr.} \\ \{\chi, \eta\}}} 2\text{Im} \left\{ (\text{signs}) \int_{\{\omega_i\}} \left(\cdots \frac{1}{i0 + X_i} \cdots \right) \right. \\ \left. \times \prod_{\text{loops}} \text{tr}[\cdots (\check{\mathbf{t}} \cdot \check{\mathbf{r}}) \cdots (\mathbf{F}_i \cdot \check{\mathbf{r}}) \cdots] \right\}. \quad (\text{E34})$$

The first sum in Eq. (E34) adds up all possible diagrams, whereas the residual term corresponds to an individual diagram. All allowed diagrams contributing to $I_{R'_\mu} |n\rangle$ are obtained by the following drawing instructions [an easy example is given in Fig. 25(c)].

1. *Propagator and vertices.* For the n th-order contribution, put $2n$ double vertices on a propagator line. The later (earlier) vertex of each double vertex refers to the left (right) electrode. Mark the latest vertex with the symbol $I_{R'_\mu}$, designating this one to be the observable vertex. *Symbols:* A horizontal line represents the propagator line; double dots encircled by a line depict the double vertices; solid (open) dots refer to the left (right) electrode, respectively.

2. *Contractions.* Construct all possible irreducible contractions. Solid (open) vertices are only permitted to be contracted with solid (open) vertices. *Symbols:* Contractions are depicted as solid lines above the propagator; attach an ‘‘ i ’’, denoting the Liouville index of the *earlier* dot in each contraction.

3. *Hermitian conjugation indices.* Construct all possibilities for the choice of the H.c. indices, obeying the following rules. (i) The H. c. indices of each double vertex have to be opposite, (ii) the earlier H.c. index of the observable vertex is $+$, and (iii) the H.c. indices have to alternate in each loop. *Symbols:* Arrow pointing to (away from) a dot is associated with $\eta = +$ ($\eta = -$).

4. *Charge indices.* Construct all possible charge index arrangements, restricted by (i) the charge indices of a double vertex have to be opposite, (ii) the charge indices of the observable vertex have to be opposite to the H.c. indices. *Symbols:* $+$, $-$ below the vertex.

Translating diagrams into algebraic expressions, schematically indicated in Eq. (E34), proceeds as follows.

1. *Propagators.* For each propagator segment following a *tunneling* vertex write down a factor

$$\frac{1}{i0 + X} \quad \text{with} \quad X = \sum (\omega_{\text{early}} - \omega_{\text{late}}). \quad (\text{E35})$$

The sum in X involves all frequencies associated with contractions that cross over that segment from the left to the right (earlier frequency) or from the right to the left (later frequency), respectively.

2. *Loopwise evaluation of spin traces.* Start at any point and follow the loop in the direction of the arrow. Insert from the right to the left into a trace in spin space the following terms when encountering

- (i) a tunneling vertex, $\check{\mathbf{t}} \cdot \check{\mathbf{r}}$;
- (ii) an observable vertex,

$$i_{R'_\mu} = \begin{cases} -(\check{\mathbf{t}} \cdot \check{\mathbf{r}}) r_\mu, & r = R, \\ +r_\mu (\check{\mathbf{t}} \cdot \check{\mathbf{r}}), & r = L; \end{cases} \quad (\text{E36})$$

(iii) a contraction, $\mathbf{F}_i \cdot \check{\mathbf{r}}$ where i refers to the earlier dot, $(F_i)_{\rho_i} = \bar{v}^{r_i}(\omega_i) f_{\bar{\chi}_i}^{r_i}(\omega_i) \check{n}_{\rho_i}^{r_i}(\omega_i)$, and

$$\check{n}_\rho^r = \sqrt{2} \begin{cases} 1, & \rho = 0, \\ n^r \hat{J}_\rho^r, & \rho = 1, 2, 3. \end{cases} \quad (\text{E37})$$

Repeat this for all other loops in the diagram.

3. Signs. Put a factor

$$(-1)^{\#\text{cr.}} \prod_{\text{early+late vertices}} \chi_e \prod_{\text{intermediate vertices}} \eta_e,$$

where $\#\text{cr.}$ is the number of crossings of contractions, the subscript “ e ” refers to the earlier dot of a vertex. For the meanings of late, early, and intermediate double vertices see Fig. 26.

4. *Complete expectation value.* Multiply all expressions obtained from steps 1, 2, and 3 and integrate over all frequencies $\{\omega_i\}$, where i refers to the indices associated with the contractions. Take $2\text{Im}(\dots)$ of this expression and sum up the contributions of all valid diagrams.

8. Covariant diagram rules for spin-quadrupole current

The calculation of the expectation value of the SQM current requires some modifications compared to that of the charge and spin-dipole currents. The reason is that the spin-quadrupole current operator for node $\langle rr' \rangle$, i.e., $\mathcal{I}_{\mathcal{Q}}^{rr'} = i[H_T, \mathcal{Q}^{rr'}]$, is a dyadic of two vector operators:

$$\mathcal{I}_{\mathcal{Q}}^{rr'} = \frac{1}{2}[g^{rr'} \mathbf{I}_{\mathcal{S}'} \odot \mathbf{S}^{r'} + (r \leftrightarrow r') + \text{H.c.}]. \quad (\text{E38})$$

We remind the reader of the factor $g^{rr'} = 2$ if $r \neq r'$ and $g^{rr} = 1$. Crudely speaking, the diagrams for the spin-quadrupole current have the same structure as for the spin current, but include an additional spin vertex. However, the spin operator has to be treated differently from the tunneling or current vertices (E32) as it contains only *one* sum over the k modes [see Eq. (40)] instead of two. We discuss this point later in detail.

We restrict ourselves in the following to spin-independent tunneling. If and only if this is the case, we may replace $\mathbf{I}_{\mathcal{S}}^{\bar{r}}$ with $2\mathbf{I}_{\mathcal{S}}^{\bar{r}}$, where

$$\mathbf{I}_{\mathcal{S}}^{\bar{r}} = \sum_{k,k',\sigma,\sigma'} [-i_r \langle \sigma | \mathbf{i}_{\mathcal{S}'} | \sigma' \rangle_{\bar{r}}] c_{rk\sigma}^\dagger c_{\bar{r}k'\sigma'}, \quad (\text{E39})$$

with $\bar{r} = R, L$ for $r = L, R$ and $\mathbf{i}_{\mathcal{S}'}^{\bar{r}}$ defined in Eq. (E36) for $\mu = x, y, z$. Note that $\mathbf{I}_{\mathcal{S}}^{\bar{r}}$ only accounts for the contribution to the spin current for electrode r due to tunneling from subsystem \bar{r} to r , but not for tunneling from r to \bar{r} . Using Eq. (E38), the expectation value of the spin-quadrupole current is then given by

$$\langle \mathcal{I}_{\mathcal{Q}}^{rr'} \rangle = 2g^{rr'} \text{Re}[\text{tr}(\mathbf{I}_{\mathcal{S}}^{\bar{r}} \odot \mathbf{S}^{r'}) \rho(t)] + (r \leftrightarrow r'). \quad (\text{E40})$$

In the following, we discuss the modifications that are necessary to calculate Eq. (E40) starting from the spin current. First of all, $\mathcal{I}_{\mathcal{Q}}^{rr'}$ contains four field operators so that the associated observable vertex is a quadruple vertex instead of a double vertex. This is sketched in Fig. 27: The later two vertices refer to the spin current operator (whose dots refer to *two* electrodes) and the earlier vertices refer to the spin

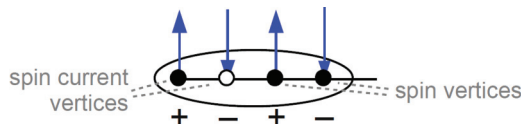


FIG. 27. (Color online) SQM current vertex for $r = L$, see text.

operator (whose dots refer to only *one* electrode). As all field operators act from the left, all charge indices are opposite to the H.c. indices. The action of the spin operator can be expressed by

$$S_j \sim \delta_{\eta_{l'}, +} \delta_{-\eta_{l'} \chi_{l'}, +} \delta_{\chi_{l'}, \bar{\chi}_{l'}} \delta_{\eta_{l'}, \bar{\eta}_{l'}} \delta_{k_l k_{l'}} (s_j^r)_{\sigma_l \sigma_{l'}} J_1 J_{1'}. \quad (\text{E41})$$

This fixes $\eta_{\text{early}} = \bar{\chi}_{\text{early}} = +$.

The technical challenge for implementing the spin-quadrupole current vertex is the single k summation in the spin operator. If we contract the two dots within the spin operator this is no problem since the contraction also sets the k indices to be the same anyway. However, if the two dots are contracted with other vertices, their k 's are not independent, so we cannot introduce the one-particle DOS for both contractions individually (denoted by 1 and 1' in the following). Instead, we obtain an expression of the form

$$\sum_{\tau_1 \tau_{1'}} \sum_{k_1} \delta_{\sigma_1 \tau_1} \delta_{\sigma_{1'} \tau_{1'}} g(\varepsilon_{n_1 k_1 \tau_1}^{r'}, \varepsilon_{n_1 k_1 \tau_{1'}}^{r'})_{r'} \langle \sigma_1 | \mathbf{s} | \sigma_{1'} \rangle_{r'}, \quad (\text{E42})$$

where g is some function and the Cartesian index j refers to the spin operator. We may treat this expression similar to the calculation of the exchange contribution to the SQM in equilibrium (see Sec. IIC) by introducing the two-particle density of states $\nu_{\sigma_1 \sigma_{1'}}^r(\omega_1, \omega_{1'})$ (16) and expressing the latter by Eq. (A11). Then the term in (E42) equals

$$\int_{\{\omega_1, \omega_{1'}\}} g(\omega_1, \omega_{1'}) 2\mathcal{A}_{\mu\nu}^{r'} \langle \sigma_1 | \check{r}_\mu \mathbf{s} \check{r}_\nu | \sigma_{1'} \rangle_{r'}, \quad (\text{E43})$$

where the 2DOS (16) enters through the matrix $\mathcal{A}_{\mu\nu}^r$ given by Eqs. (A12)–(A15). Consequently, the frequency and energy part of the diagrams can be treated without modification as explained in Appendix E4. Furthermore, the signs can be treated without modifications as well as we can simply omit the factor $\bar{\chi}_{l'} = +$ in Eq. (E41). In contrast, the spin part is altered: We now insert for the spin vertex and the two associated contractions the factor $\sqrt{2} \mathcal{A}_{\mu\nu}^r \check{r}_\mu s_j \check{r}_\nu$ into the spin trace.

Finally, we mention that the symmetrization in $r \leftrightarrow r'$ and multiplying with $g^{rr'}$ in Eq. (E40) is equivalent to multiplying with a factor of 2 and symmetrizing in $r \leftrightarrow r'$ only for $r \neq r'$.

We now summarize the modifications of the diagram rules for the SQM current compared to the spin current. We first state the drawing rules.

1. *Propagator and vertices.* The observable vertex consists of four vertices, the later two depicting $\mathbf{I}_{\mathcal{S}'}^{\bar{r}}$ and the earlier two depicting $\mathbf{S}^{r'}$.

2. *Contractions.* No changes.

3. *Indices.* The H.c. indices of the observable vertex are fixed to $(-, +, -, +)$ and the charge indices are opposite to this.

The changes in the rules for translation into algebraic expressions are as follows.

1. *Propagators.* No changes.

2. *Evaluation of loops.* If the vertices associated with $\mathbf{S}^{r'}$ in Eq. (E40) are (a) contracted with each other, then insert $\mathbf{F}_+^{r'}(\omega_{1'}) \cdot \check{r} \mathbf{s}$. If they are (b) contracted with other vertices, then insert $2t^2 f_{\bar{\chi}_1}^{r_1}(\omega_1) f_{\bar{\chi}_1}^{r_{1'}}(\omega_{1'}) \mathcal{A}_{\mu\nu}^{r'} \check{r}_\mu \mathbf{s} \check{r}_\nu$.

This accounts for both dots of the spin double vertex and their contractions. Here 1 (1') refers to the earlier indices of the contractions of the later (earlier) dot in the spin double vertex.

3. *Signs.* For the evaluation of the signs, treat the SQM current vertex as two double vertices.

4. *Complete expectation value.* Multiply with a factor of 2 and retain the symmetric and traceless parts of the tensor-valued result $\sim \mathbf{i}_S \otimes \mathbf{s}$. If $r \neq r'$, symmetrize the result in $r \leftrightarrow r'$.

- ¹M. Julliere, *Phys. Lett. A* **54**, 225 (1975).
- ²J. C. Slonczewski, *Phys. Rev. B* **39**, 6995 (1989).
- ³R. M. Potok, J. A. Folk, C. M. Marcus, and V. Umansky, *Phys. Rev. Lett.* **89**, 266602 (2002).
- ⁴M. Braun, J. König, and J. Martinek, *Superlattices Microstruct.* **37**, 333 (2005).
- ⁵G. Schmidt, *J. Phys. D: Appl. Phys.* **38**, R107 (2005).
- ⁶L. I. Glazman and M. É. Raïkh, *Pis'ma Zh. Eksp. Teor. Fiz.* **47**, 378 (1988) [*JETP Lett.* **47**, 452 (1988)].
- ⁷D. Goldhaber-Gordon, H. Shtrikman, D. Mahalu, D. Abusch-Magder, U. Meirav, and M. A. Kastner, *Nature (London)* **391**, 156 (1998).
- ⁸K. Ono, D. G. Austing, Y. Tokura, and S. Tarucha, *Science* **297**, 1313 (2002).
- ⁹D. Weinmann, W. Häusler, W. Pfaff, B. Kramer, and U. Weiss, *Eur. Phys. Lett.* **26**, 467 (1994).
- ¹⁰Y. Chye, M. E. White, E. Johnston-Halperin, B. D. Gerardot, D. D. Awschalom, and P. M. Petroff, *Phys. Rev. B* **66**, 201301(R) (2002).
- ¹¹M. Braun, J. König, and J. Martinek, *Phys. Rev. B* **70**, 195345 (2004).
- ¹²R. S. D. Gatteschi and J. Villain, *Molecular Nanomagnets* (Oxford University Press, Oxford, 2006).
- ¹³H. Brune and P. Gambardella, *Surf. Sci.* **603**, 1812 (2009).
- ¹⁴B. Sothmann and J. König, *Phys. Rev. B* **82**, 245319 (2010).
- ¹⁵M. M. E. Baumgärtel, M. Hell, S. Das, and M. R. Wegewijs, *Phys. Rev. Lett.* **107**, 087202 (2011).
- ¹⁶M. Misiorny, M. Hell, and M. R. Wegewijs, *Nature Phys.* (2013), doi: 10.1038/NPHYS2766.
- ¹⁷M. Misiorny, I. Weymann, and J. Barnaś, *Phys. Rev. B* **86**, 245415 (2012).
- ¹⁸W. N. Cottingham and D. A. Greenwood, *An Introduction to Nuclear Physics* (Cambridge University Press, Cambridge, UK, 2001), Vol. 1.
- ¹⁹The exchange term is only by chance proportional to $\langle S_x^2 + S_y^2 \rangle$ at zero temperature. At finite temperatures, this does not hold anymore, showing that both terms are physically quite distinct.
- ²⁰Here, one has to treat the spin vector as a stochastic variable when averaging over the grand-canonical ensemble. Spearman's rank correlation coefficient C_{AB} for two random variables A, B is defined by $C(A, B) = \langle (A - \langle A \rangle)(B - \langle B \rangle) \rangle$. Equation (60) is a linear combination of the $C(S_i^r, S_j^{r'})$ for different components of the spin operator so that only triplet correlations are extracted. However, if all $C(S_i^r, S_j^{r'}) = 0$, this implies $\langle \mathcal{Q}^{rr'} \rangle_{\text{ex}} = 0$.
- ²¹For $\hat{\mathbf{J}} = \mathbf{e}_z$ we get $\langle \mathcal{Q} \rangle_{\text{ex}} = -q_{\text{ex}} \mathbf{e}_z \odot \mathbf{e}_z = -q_{\text{ex}} [\frac{2}{3} \mathbf{e}_z \mathbf{e}_z - \frac{1}{3} (\mathbf{e}_x \mathbf{e}_x + \mathbf{e}_y \mathbf{e}_y)]$; that is, $\langle \mathcal{Q}_{zz} \rangle_{\text{ex}} = -\frac{2}{3} q_{\text{ex}} = -\frac{2}{3} \frac{N_x}{4} = -\frac{1}{3} \langle S_z \rangle_{T=0}$, in agreement with Eq. (31).
- ²²M. Hell and M. R. Wegewijs (unpublished).
- ²³ $[S_i^r, I_j^{r'}] \neq 0$ can be explicitly shown by inserting the expressions for the spin operator (25) and the spin current operator (80), respectively, and applying the anticommutation relations of the field operators.
- ²⁴Although the restrictions on the network connectivity derives from the bilinearity of the tunneling Hamiltonian (9), this does not mean that SQM cannot be exchanged directly between local nodes: When calculating the *averages*, including coherent processes of higher order in the bilinear coupling, this is indeed found to occur; see Ref. 22.
- ²⁵The current contribution of electrons at energy ω is changed by the factor $[1 + \cos(\theta)n^L(\omega)n^R(\omega)]$, i.e., when *both* spin-polarizations are nonzero. For parallel Stoner vectors the fraction of electrons with spin σ in electrode r with energy ω is changed from $1/2$ to $[1 + \sigma n^r(\omega)]/2$ as compared to the nonmagnetic case. These electrons can only access a fraction $[1 + \sigma n^{\bar{r}}(\omega)]/2$ of the states in the other electrode \bar{r} instead of $1/2$ as in the nonmagnetic case. The reason for this is conservation of spin by the tunneling [cf. Eq. (11)], so all states with opposite spin in the other electrode are forbidden final states. In total, this changes the current by a factor $\sum_{\sigma} (1 + \sigma n^r)(1 + \sigma n^{\bar{r}})/2 = 1 + n^L n^R > 1$. In the case of noncollinear Stoner vectors electrons can access both spin channels of the other electrode due to nonzero spin-overlap factors in Eq. (11), giving an overall additional reduction factor $\cos(\theta)$.
- ²⁶In contrast, charge current and spin current are finite in the thermodynamic limit by themselves and *not* per electron. This has the same reason as for the averages—the average spin *per electron*—but only the average SQM per electron *pair* have a finite limit; cf. discussion of the exchange SQM (59).
- ²⁷We also have to account for the situation in which the role of the first and the second copy are interchanged, respectively; however, when summing over all contributions this gives the same result as in the first case. This yields the additional factor of 2 in the SQM current.
- ²⁸The analogy between SQM and spin torque becomes explicit when rewriting $T_S^L = \int d\omega \Gamma (\frac{\alpha^R}{\bar{v}^R} f_+^L - \frac{\beta^R}{\bar{v}^R}) n^L$ by interchanging $\omega \leftrightarrow \omega'$ in the first term contributing to the double integral (98). Then T_{ex}^L is obtained from T_S^L by replacing the spin-polarization by the quadrupolarization function, $n^L \rightarrow a^L$.
- ²⁹Equation (121) holds for $V^* < J$, i.e., $J < D/\pi$, which is valid for the flat-band approximation (cf. Sec. IID). Otherwise, Eq. (119) is already limited by $|J|$.
- ³⁰If $\theta \neq 0, \pi$, the SQM current could only be uniaxial if $A_{\mathbf{Q}}^L = 0$ and $T_{\mathbf{Q}}^L = 0$ is fulfilled at the same time [otherwise the I_{λ} are clearly angle dependent according to Eqs. (127) and (128)]. This is in general not expected as the SQM torque senses the band structure over a wide energy range.
- ³¹D. Gatteschi and R. Sessoli, *Angew. Chem., Int. Ed.* **42**, 268 (2003).
- ³²Assuming $N_s \gtrsim 10$, we neglect the exchange SQM torque since $T_S^L \sim T_{\text{ex}}^L$ [cf. Eqs. (117) and (120)].
- ³³Equation (137) is obtained by substituting $x = (\omega - \mu^L)/T^L$ in Eq. (136) and expanding the bias function $\Delta(\omega) \approx -f'(x)x\tau^R$ with $f(x) = (e^x + 1)^{-1}$. This gives $I_{\mathbf{Q}}^{LL} \approx \frac{\tau}{2} T^L \tau^R \int dx f'(x)x[2f(x) - \sum_{\sigma} f(x + \sigma j)]$ to which we apply Eq. (A47) from Appendix A 4.
- ³⁴J. König and J. Martinek, *Phys. Rev. Lett.* **90**, 166602 (2003).

- ³⁵M. Misiorny, I. Weymann, and J. Barnaś, *Phys. Rev. Lett.* **106**, 126602 (2011).
- ³⁶F. May, M. R. Wegewijs, and W. Hofstetter, *Beilstein J. Nanotechnol.* **2**, 693 (2011).
- ³⁷Note that these two electrons are treated here *as if* they could occupy the same k mode, which is, of course, forbidden by the Pauli principle. As explained in Appendix A 1, this only corrects for the mistake that is made when the direct SQM is calculated by treating all electrons as distinguishable objects, that is, when ignoring Pauli principle.
- ³⁸In particular, one cannot set $n(\omega) = 0$ for all ω without setting $J = 0$, since these are equivalent for the Stoner dispersion considered.
- ³⁹I. V. Lindell, *Methods for Electromagnetic Field Analysis*, IEEE Series on Electromagnetic Wave Theory (Wiley, IEEE Press, Washington, DC, 1996).
- ⁴⁰H. Schoeller, *Eur. Phys. J. Special Topics* **168**, 179 (2009).
- ⁴¹M. Leijnse and M. R. Wegewijs, *Phys. Rev. B* **78**, 235424 (2008).
- ⁴²R. B. Saptsov and M. R. Wegewijs, *Phys. Rev. B* **86**, 235432 (2012).
- ⁴³R. B. Saptsov, private notes (2010).
- ⁴⁴Please note that the sign of Fermi function in Eq. (E9) is determined by $\bar{\chi}_{I'}$ instead of $\chi_{I'}$ as in usual real-time diagrammatics. There the charge index refers to the process taking place on the quantum dot (e. g., electron tunneling in) and not to the process happening in the electrodes (e. g., tunneling out).